NAA-SR-10307
COPY

PIQUA NUCLEAR POWER FACILITY OPERATIONS ANALYSIS PROGRAM PROGRESS REPORT NO. 4 (JANUARY 1, 1964 – JUNE 30, 1964)

AEC Research and Development Report

ATOMICS INTERNATIONAL
A DIVISION OF NORTH AMERICAN AVIATION, INC.

Price $4.00
Available from the Office of Technical Services
Department of Commerce
Washington 25, D. C.

NAA-SR-10307
REACTOR TECHNOLOGY
110 PAGES

PIQUA NUCLEAR POWER FACILITY OPERATIONS ANALYSIS PROGRAM PROGRESS REPORT NO. 4

(JANUARY 1, 1964 – JUNE 30, 1964)

By

H.S. COLE
D.F. HAUSKNECHT
O.G. JENKINS, JR.
D.E. LEW
H. MANDEL
E.N. PEARSON
H.J. RUBINSTEIN
R.R. STIENS
O. TESZLER
D. TONDI

ATOMICS INTERNATIONAL

A DIVISION OF NORTH AMERICAN AVIATION, INC.
P.O. BOX 309 CANOGA PARK, CALIFORNIA

CONTRACT: AT(11-1)-GEN-8
ISSUED: DECEMBER 15, 1964

DISTRIBUTION

This report has been distributed according to the category "Reactor Technology" as given in "Standard Distribution Lists for Unclassified Scientific and Technical Reports" TID-4500 (34th Ed.), September 1, 1964. A total of 900 copies was printed.

CONTENTS

CONTENTS (CONT.)

TABLES

TABLES (CONT)

FIGURES

FIGURES (CONT)

I. REVIEW OF OPERATIONS

The Piqua Nuclear Power Facility (PNPF) achieved criticality in June 1963; fuel loading was completed in July 1963 and low power testing carried out through October 1963. Initial power operation took place early in November 1963. Full power was first attained on January 27, 1964. After achieving full power, the reactor operated steadily until the first scheduled shutdown on May 21, 1964 for fuel shuffling, maintenance and a required containment building leak test. As of that date the PNPF had generated 77.7 million kwh of heat (i. e., in excess of 21 million kwh of electricity gross), and contributed approximately 40% of the energy generated by the City of Piqua (Table I).

TABLE I

PNPF OPERATING HISTORY

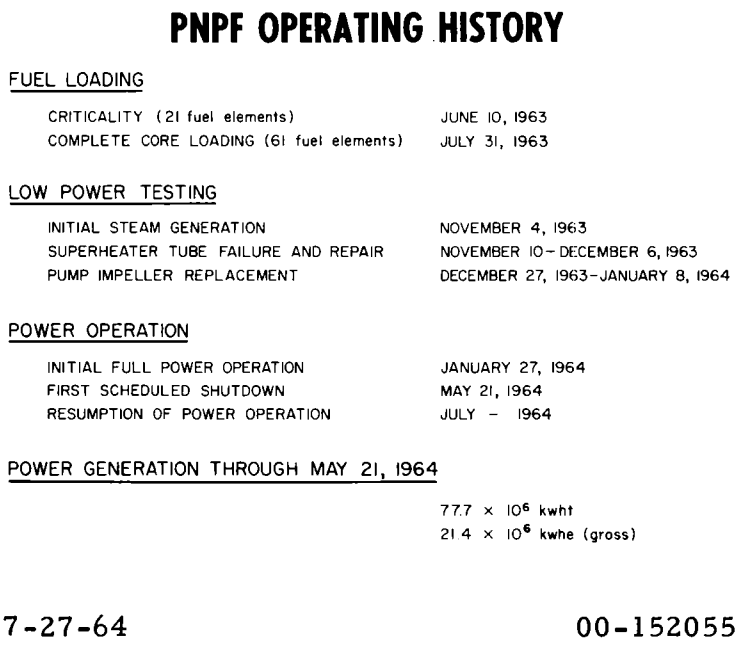

The general performance of the plant as a power producer has been excellent. The first power run, initiated in January 1964 continued for 59 days of uninterrupted operation. Since the start of power operation (January 27, 1964) the PNPF produced steam for 2548 hr out of 2706 available hr for a 94.2% cumulative availability. During the month of February 1964 the availability was 100%. The plant has been following the load requirements of the City with a high

power demand in the daytime and a low demand at night and over the weekends. The consequential load swinging has resulted in a monthly average capacity factor of 49%.

Two major problems were encountered during this operating period: (a) control rod slippage and drive coil circuit failure; and (b) control rod position indicator drift. These items did not cause any major shutdown, and were repaired during the planned shutdown initiated on May 21.

The pertinent operating statistics for the PNPF are given in Table II. Figure 1 shows the cumulative energy generation history for this report period (January 1, 1964 through June 30, 1964). Figure 2 illustrates the average daily gross electrical power generation.

TABLE II

OPERATIONS STATISTICS SUMMARY

OPERATIONS PARAMETERS	CALENDAR MONTH							
	1963 (Oct 30– Dec 31)	1964 January	February	March	April	May	June	To Date (June 30, 1964)
Thermal Power Generation (Mwh)	4,460	8,828	18,528	19,440	19,384	7,094	0	77,734
Cumulative Thermal Power Generation (Mwh)	4,460	13,288	31,816	51,256	70,640	77,734	77,734	77,734
Average Thermal Power (Mw)	-	25.3	26.6	26.4	27.1	22.6	Planned Shutdown	25.6
Availability (%)	-	94.2	100.0	97.0	97.1	74.6		94.2
Capacity Factor (%)	-	55.5	50.5	57.4	59.2	21.0		39.4

Note: Cumulative thermal power generation is calculated from October 30, 1963, while the capacity factor and availability are calculated as of January 27, 1964. The availability factor for the month of May was lowered somewhat as a result of control rod drive circuit problems. The plant capacity factor was significantly lower because of the scheduled shutdown initiated on May 21 and preceded by several days of stand-by operation.

A chronological history of pertinent occurrences at PNPF during this report period is presented in the following pages.

The reactor was shut down on December 27, 1963 for removal of the temporary orifice plate in the reactor return line, and modification of the main heat transfer pumps, by installation of lower capacity impellers. After the pumps

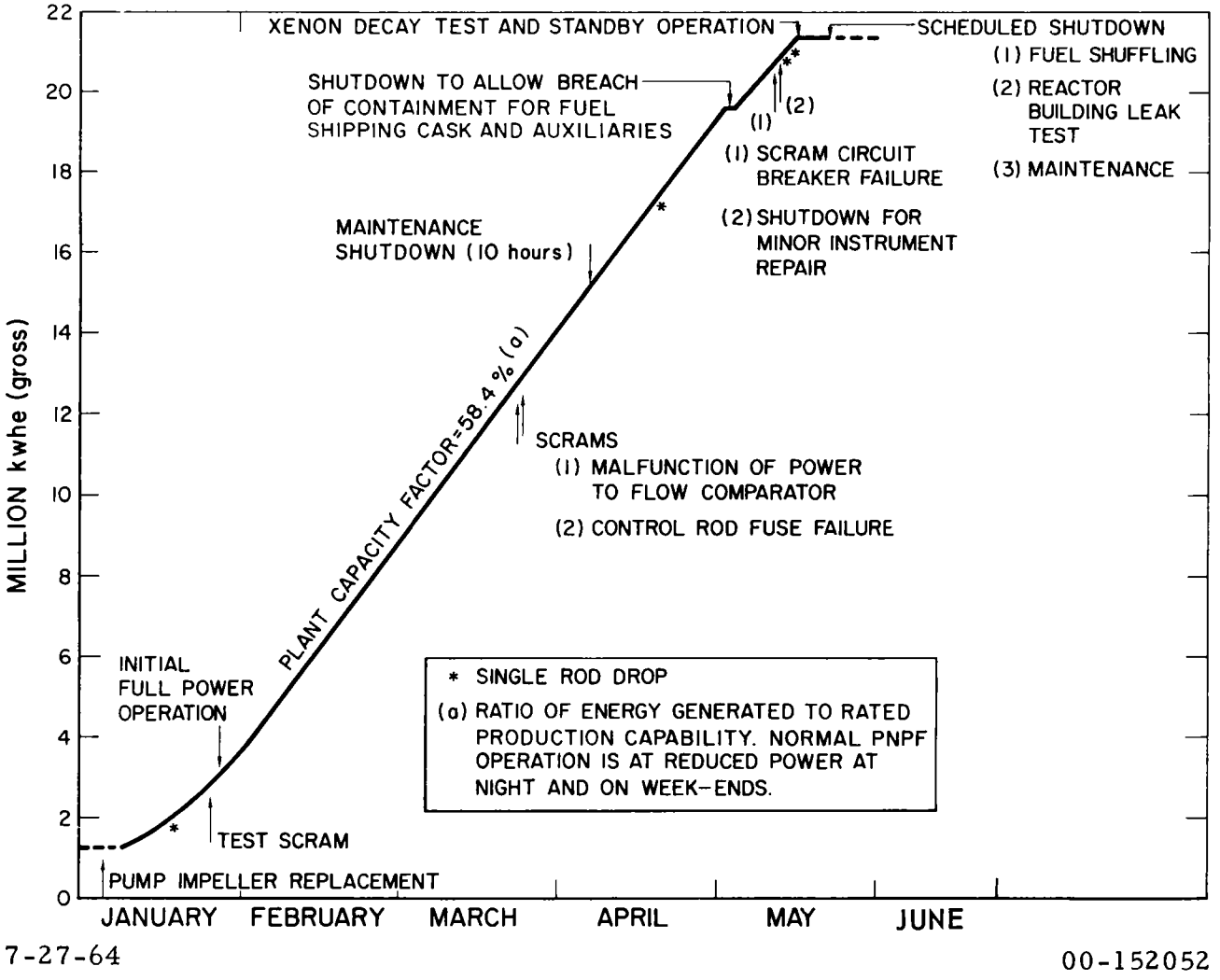

Figure 1. PNPF OPERATION
January – June 1964

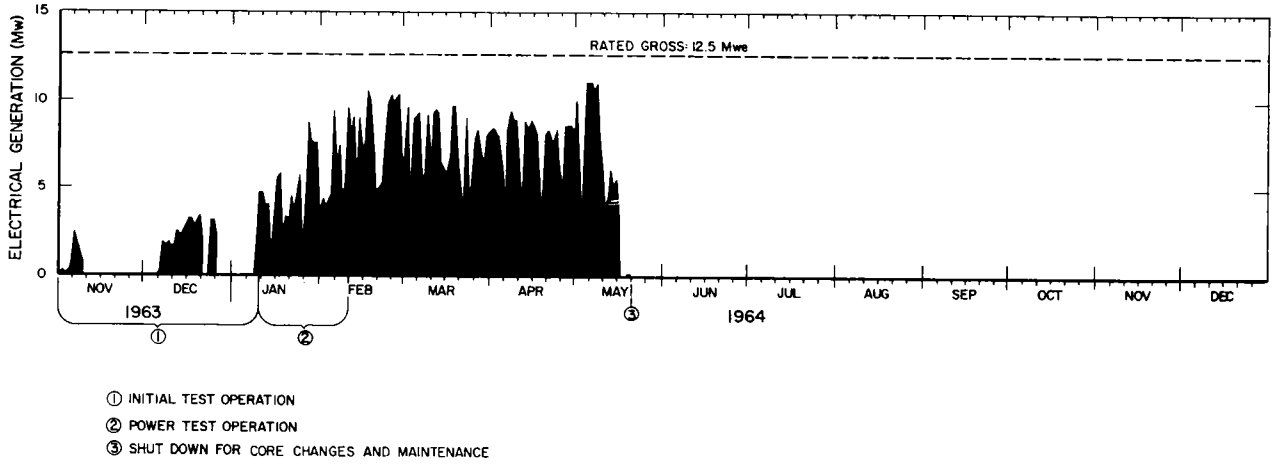

Figure 2. PIQUA NUCLEAR POWER FACILITY
Average Daily Power
Gross Megawatts (e)

were reassembled, the system was filled and pump operation was initiated. The pumps operated very quietly with no detectable vibration. Flow characteristic tests indicated that the modification had reduced maximum pump flow as was anticipated.

Critical reactor operation was resumed on January 8, and low power testing was performed. The critical rod configuration deviated less than 0.01% Δk from the predicted value. A recheck of the source-independent critical flux level was made and found to be slightly lower than it had been during the previous low power testing.

After the low power testing was completed, power was increased and system temperature was raised to operating level. Plant warmup and steam temperature to the turbine were effected without difficulty.

On January 10, reactor power was raised in steps to 25 Mwt, to test the effects of the new control rod operating pattern* on the power distribution. The new control rod pattern yielded a flatter and more symmetric power distribution. With the reactor at 25 Mwt, the power range detectors were adjusted to read power levels determined by calorimetric measurements.

A false period scram occurred on January 14. At the time of scram, reactor power level had been reduced to the startup (zero power) range to accommodate conventional plant testing. Noise from channel IV period circuitry caused the scram. Following the scram, the reactor remained shut down for about 16 hr while testing was performed to determine the optimum settings of the boiler bypass control linkage.

On January 17, while the PNPF was being operated in the load following mode at 25 Mwt, a sudden partial loss of steam from the conventional power plant to the turbine header was experienced. The resulting drop in header pressure reset the boiler organic flow and the Reactor Outlet Temperature Control (ROTC) system, causing the reactor to pick up the load and the PNPF steam generation rate to increase. The steam generation rate peaked at 100,000 lb/hr

*Rod No. 1 in, rods 3 and 6 controlling, all other rods out. Old pattern was: rod No. 1 in and rods 2, 4, and 6 controlling with all others out; or rod No. 1 in, rods 3, 5, and 7 controlling with all others out.

(with the reactor at 32 Mwt) for about 30 sec. Operations personnel immediately returned the control system to manual and reduced the steam generation rate to 70,000 lb/hr. Due to power-temperature coefficient effects, no control rod motion occurred during automatic correction for the pressure decrease at the conventional plant header. The plant control system response to this exigency was satisfactory since no operating limits were exceeded.

On January 18, the hold-circuit transformer for control rod No. 13 burned out, and the rod dropped full into the reactor. The operator immediately withdrew control rod No. 3 far enough to offset the worth of control rod No. 13, thereby preventing a reactor shutdown. The transformer was replaced, control rod No. 13 was again withdrawn to the "full out" position, and control rod No. 3 returned to its original control position. When the power level dropped initially, a gain in reactivity, due to power-temperature effects, was realized. This gain provided partial compensation for the loss effected by the control rod drop, and allowed the operator time to prevent a shutdown by withdrawing control rod No. 3.

On January 22, the PNPF was tested under one-pump operating conditions. Pump 1-B was secured and the power was increased in the manual mode, in discrete steps from 3.4 to 25 Mwt. No problems were encountered. Upon completion of the test, 1-B was returned to service.

On January 24, load-swing testing was performed to demonstrate the capability of the PNPF and the conventional plant to accommodate rapid load swings in a safe and controlled manner.

On January 25, a scram test was performed from about 80% rated power. The conventional plant was able to pick up the load before the drop in turbine steam pressure became excessive. All instrument responses appeared normal. Before re-starting the reactor, the transformers on the 13 control rod hold-coil circuits were replaced because of their inability to maintain rated voltages.

On January 27, the power level was increased to about 35 Mwt and held at this level until the conventional plant granted permission to go to 100% power. Prior to the rise to full power, an out-of-balance condition was observed in the power distribution between the east and west side of the core. This condition was attributed to unequal insertion of the two controlling rods (No. 3 and No. 6). The two controlling rods were repositioned and adjusted to balance the power distribution.

After a balance in power distribution was achieved, the power level was raised in two steps to about 45.8 Mwt and held at this level for about 5-1/2 hr. The power level was subsequently lowered because of reduced municipal load demands. Load-following operation continued between 25 and 90% power, according to municipal demands, until the end of January generating 8,820,500 kwh thermal energy.

A thorough radiation survey was made at full power operation. Results of the survey indicated the PNPF shielding to be adequate.

During February, the PNPF was operated continuously at power levels between 20 and 100% of full power, as dictated by plant load demands and testing requirements. The formal testing program for the PNPF was completed February 10, and true load-following operation was initiated at 0630 hr on February 11, 1964. Plant availability in February was 100% with a 58.5% capacity factor.

During March, the PNPF was operated in both load-following and base load modes over a range of 30 to 100% of full power for 722 hr generating 19,439,770 kwh of gross thermal energy. Significant events of March operations were as follows:

a) Burning of HB in the waste-fired boiler was carried out. Several system shutdowns and startups were made to familiarize shift personnel with system operation. Operation of the waste-fired boiler on propane was completed for a planned, sustained HB burning run in April.

b) 28,000 lb of new coolant (flaked) were loaded to the storage tanks to be melted and used for coolant make-up.

c) After 59 consecutive days of power operation, the PNPF scrammed by a spurious high power-to-flow ratio signal from the scram circuit (FPXL 101) on March 23. The indicated loss of flow was attributed to a malfunction of the steam tracing circuitry. While the reactor was down, separate steam traps were installed on the power/flow transmitters, to assure continuous steam tracing flow.

d) On March 24, while the reactor was base loaded at 16.5 Mwt, all control rods dropped into the core due to two blown fuses in the

control rod hold circuit variac circuitry. The fuses were replaced and the reactor power level was restored.

During April, the PNPF was operated in the base load or load-following modes for ~699 hr, at power levels ranging from 2% to 100% of full rated power, producing 19,383,780 kwh of thermal energy.

On April 6, the reactor was shutdown for about 10 hr for maintenance on several key items, including:

a) Installation of a new 3-element variac stack, and ammeters in the control rod hold current circuit. Variac output fuses were removed and bench checked; a 90 ampere circuit breaker was installed on the supply side of the variacs.

b) Adjustment and checking of power/flow channels A, B, and C trip points.

c) Installation of new capacitors in power/flow low flow channels A and C.

d) Repair of reactor inlet temperature recorder. This recorder had been inoperative, necessitating operation in automatic flux control rather than reactor outlet temperature control mode.

e) Repair of the organic/steam differential pressure control system.

Prior to the shutdown, the power level had been administratively limited to 75% of rated power. After the foregoing maintenance items were completed, this administrative limitation was removed and operation to 100% of rated power was permitted.

Due to core burnup, the control rod operating pattern was altered to incorporate control rod No. 1 along with previously used control rods No. 3 and 6, so that xenon override could be provided during high power operation in the early morning hours.

On April 19, power was lost on the grip coil of the control rod in No. 3 position, which was on automatic control at this time. The control rod dropped and steam production was interrupted, although the reactor was maintained critical with control rods No. 1 and No. 6. Trouble shooting disclosed that one of the parallel grip coil circuits had low resistance. The wiring was rearranged

so that the good half of the grip coil circuit was made to carry the entire load. Tests were then run to determine that the grip circuit was satisfactory; the original rod configuration was restored and power operation was resumed.

The purification system was operated for about 660 hr during April at column feed rates ranging from 940 to 960 lb/hr. During the last week in April, a 1-1/2 day shutdown was effected to enable performance checks of bottoms flow and HB flow instruments. Except for this shutdown, the purification system was operated at all times when the reactor was operated.

Intermittent waste-fired boiler operation continued throughout April.

During May the PNPF was operated for 318 hr, producing 7,094,360 kwh of thermal energy. Power levels ranged from 3 to 40.6 Mwt. On May 21, the reactor was shut down for fuel changes, maintenance, and building leak testing.

Significant events occurring during May are as follows:

a) The reactor was shut down on May 2, to permit transport of the single-element fuel shipping cask and associated equipment through the equipment access lock to the reactor building 100 ft level. Re-establishment of containment was completed on the same day; however, resolution of an apparent reactivity discrepancy delayed taking the reactor critical until the following day, May 3.

b) A scram, due to tripping of the power/flow comparator units occurred at 1100 hr on May 11. Cause of the trip was due to opening of the load side circuit breaker on the noise-free motor alternator, which in turn caused a switching transient (while transferring to raw power) on the power/flow comparators.

   The reactor was again critical and the power level at 10% by 2230 hr. At that time, a bypass switch on the leak detection system was turned to the "clear" position. Abnormal operation of the pressurizing loop followed immediately, so the reactor was shutdown. The problem, a broken wire in the plant protective system, was found and corrected.

   During the restart procedure, it was discovered that both sets of control rod No. 2 raise and hold coil circuits and half of each the grip and lower coil circuits were shorted. The restart was accomplished

with control rod No. 2 left fully inserted; startup was completed by 1300 hr on May 12.

c) On May 13, while the reactor was operating at about 17 Mwt, the remaining hold coil on rod No. 11 failed, dropping the control rod into the active core and interrupting steam production by dropping the reactor power level to about 2 Mwt. Using control rod No. 1, the reactor power was restored after about a 78 min delay in steam production. Operation continued with both control rods No. 2 and No. 11 fully inserted.

d) On May 14, the hold coil on control rod No. 9 failed, allowing control rod No. 9 to drop into the active core, resulting in about a one hour loss in steam production. As investigation showed that control rod No. 9 was still operable, it was withdrawn and normal operation was resumed.

e) An equilibrium run for xenon testing was started on May 14, and continued until May 16, when the power was reduced to zero for xenon decay measurements. The xenon decay test was terminated on May 18.

f) The PNPF reactor was operated at 3 Mwt on May 19 and 20, to act as emergency standby while the power plant personnel tested a conventional boiler. Subsequently, a series of pre-shutdown tests was started, including:

    1) In-core filter ΔP vs flow

    2) Temperature defect measurements and,

    3) Isothermal temperature calibrations.

g) The PNPF was then shut down for core changes, maintenance, and building leak testing.

h) During the shutdown, a nitrogen atmosphere was provided for the reactor and main heat transfer system as well as for the steam generator, to maintain an inert atmosphere throughout. The purification system was also operated to lower the HB concentration so that the chances of coolant deterioration would be reduced in case of accidental

exposure to air and to provide continuous control of coolant purity during the shutdown.

i) On May 25, the reactor vessel head was removed and an investigation of the control rod circuitry problems was started.

j) On Sunday, May 31, all electrical power, with the exception of the DC bus, and the emergency lighting panel was turned off to permit a modification of the automatic start circuit for the diesel generator. After potential transformer leads were transferred from the supply side of the main 480 V transformer, it was not possible to close the 480 V breaker. The leads were returned to their original condition pending further investigation of the problem.

During the 2-1/2 hr electrical outage, the nuclear instrument thimble temperatures and the biological shield temperatures were monitored continuously while the shield cooling pumps were out of service. The highest thimble temperature obtained was 95°F, and the highest biological shield temperature was 118°F at the vessel support plate.

The PNPF reactor remained shutdown during June for fuel changes and maintenance. Major events occurring at the PNPF in June were:

a) On June 3, an in-core filter was removed from core position D-9 and disassembled for examination. The maximum radiation level encountered was 1 r/hr, at the metal container tip which extends into the head of the fuel element. Radiation levels in the filter media were less than 20 mrad/hr β, γ including 5 mr/hr γ. Three sections of this filter were shipped to Atomics International headquarters (Canoga Park, California) for analysis.

b) On June 5, the evaluation element (serial No. P-1071) from core position D-9 was removed and loaded into the shipping cask. On June 7, this element was shipped via truck to the Atomics International Components Development Hot Cell at Santa Susana, California for examination as a part of the fuel examination program.

c) Physical examination of the six control rod drives showed that material collected on the upper control head of the control rod at the

pin connections was the cause of the electrical shunts affecting the position indicating circuitry. Several of the control rods had shorts at the pin connectors. The three control rod jumpers that had indicated shorts were checked and all of the shorts were found to be external to the reactor in the Conax connector. Two control rod power coil cases were found to be shorted. One of the shorts was in the power coil case lead-through and the other was a short to ground inside the power coil case. All harness and jumper wiring checked as satisfactory, thus eliminating wiring as a contributing factor to the electrical shunt problem. The electrical shunt problem was corrected by replacing the upper control heads with heads made of Lavite, a material with a high dielectric constant, and where necessary, replacing the coil cases and/or Conax connectors.

d) On June 13, the reactor building was pressurized to 5 psig with air for a building leak rate test. The leak rate was found to be less than 0.3% of the contained volume per day.

e) The purification system was shutdown early in June to permit replacement of seals on the bottoms transfer pumps P-21A and B, and to permit other maintenance and modifications to the purification, waste gas, and decay heat removal systems. These tasks were finished by June 20 and the purification system was run continuously at a throughput of about 700 lb/hr for the rest of June.

f) Repairs, including replacement of the refractory brick, on the waste fired boiler were completed in June. Operation of the boiler, using propane, was resumed on June 27.

A. NUCLEAR TESTING

1. Scram Tests

Scram tests were performed at the PNPF to determine the effects of a scram from power on a number of system parameters and to insure that no potentially hazardous conditions developed. The tests were conducted over the range from 10 Mwt to 37 Mwt (~ 80% of full power).

Reactor parameters were recorded on a high-speed oscillograph during each of the tests. The effect of the scrams on several of these properties is shown in Figures 3 and 4. The greater organic flow for the 37 Mwt test (14,000 gpm compared to 8600 gpm for the 10 Mwt tests) is reflected in the reduction in coolant transport times over those for the low power case.

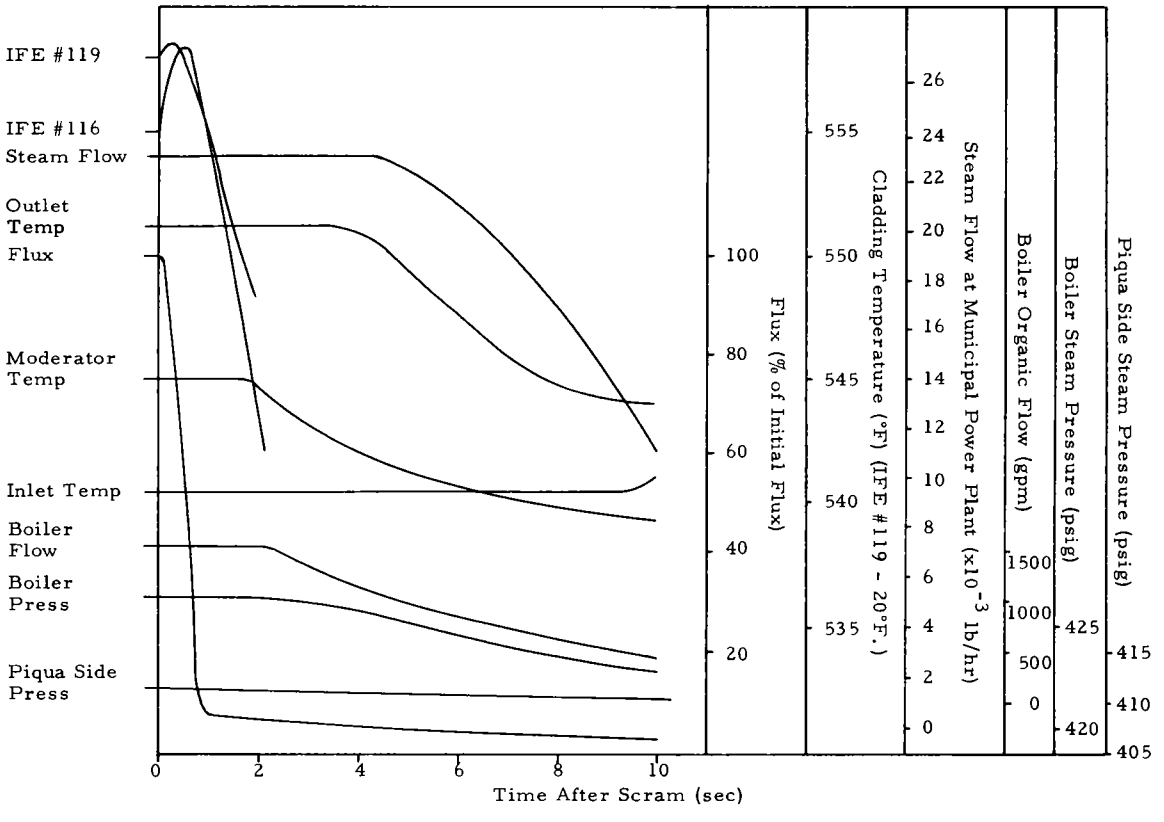

Figure 3. PNPF Parameters vs Time Following a Scram from 10 Mwt

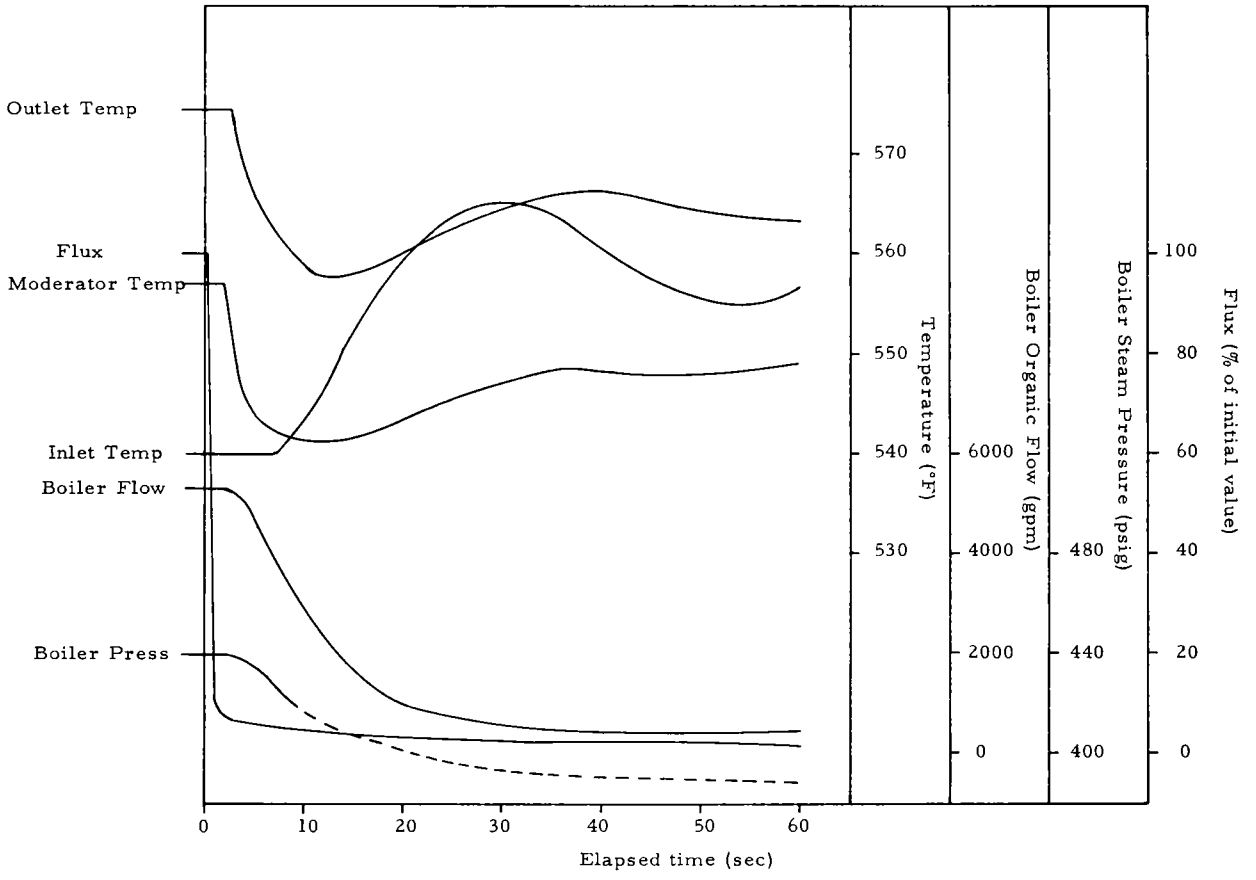

Figure 4. PNPF Parameters vs Time Following A Scram from 37 Mwt

The tests demonstrated that it is possible for the reactor to scram from large loads without causing serious problems or difficulties.

2. Power Coefficient

Measurements were made to evaluate the steady-state power coefficient over the entire power range at a number of coolant flows. The measurements consisted of changing from one equilibrium power to another by changing the boiler flow, thus providing the changes necessary to evaluate the coefficient. Control rod movement was not employed in these tests. The values obtained were normalized to an average core temperature of 550°F, which is approximately the value at full power. For this normalization, it was assumed that the power coefficient increases with temperature in the same manner as does the isothermal temperature coefficient.

Analysis of data showed the power coefficient magnitude to be independent of power level and proportional to the inverse of the reactor inlet flow. The measured values and fitted curve are given in Figure 5. At a flow of 14,000 gpm the curve gives a value of -0.0092 ± 0.0002% Δk/Mwt and a total reactivity defect at full power due to a power coefficient of 0.42% Δk.

B. REACTIVITY HISTORY

The computer program for calculating reactivity history has undergone considerable change in an attempt to successfully follow reactivity behavior at the PNPF. Early efforts were not successful because the position indicators (PnI) did not provide reliable control rod position readings. Also, data recorded from the up and down step counters associated with each control rod driver were unreliable due to the difference in length between an up and a down step. In late February, the set of integrating counters which count and arithmetically sum the number of steps of upward and downward motion for each control rod were put into service. These step counters were rezeroed daily and the number of steps necessary for rezeroing recorded.

With the improved determination of rod positions two problem areas became apparent in the calculated results. The more serious of the two was xenon worth, which masked the second difficulty, the average burnup rate. Calculation of xenon worth at Piqua was improved through trial and error, by varying the nuclear cross-sections for absorption and fission of the poison and fuel. This was done using three intervals of data which included two shutdowns and re-starts and the xenon test, all of which took place during May. By optimizing the results calculated for all three intervals of data, a set of cross-sections was chosen. The average burnup rate was then determined by comparing the rod positions at the end of the May xenon test (very low xenon concentration) with the rod positions recorded before any burnup occurred. Taking the samarium which remained in the core into account, the average burnup rate was experimentally found to be .190 cents/Mwd-MTU in contrast to .272 cents/Mwd-MTU which was the value determined from neutron diffusion theory calculations. The newly determined constants were incorporated in the computer program and the data were re-evaluated for the period of operation during which readings from the integrating step counters were reported. Figure 6 is a graph of the daily reactivity difference calculated for approximately 1830 hours. This time

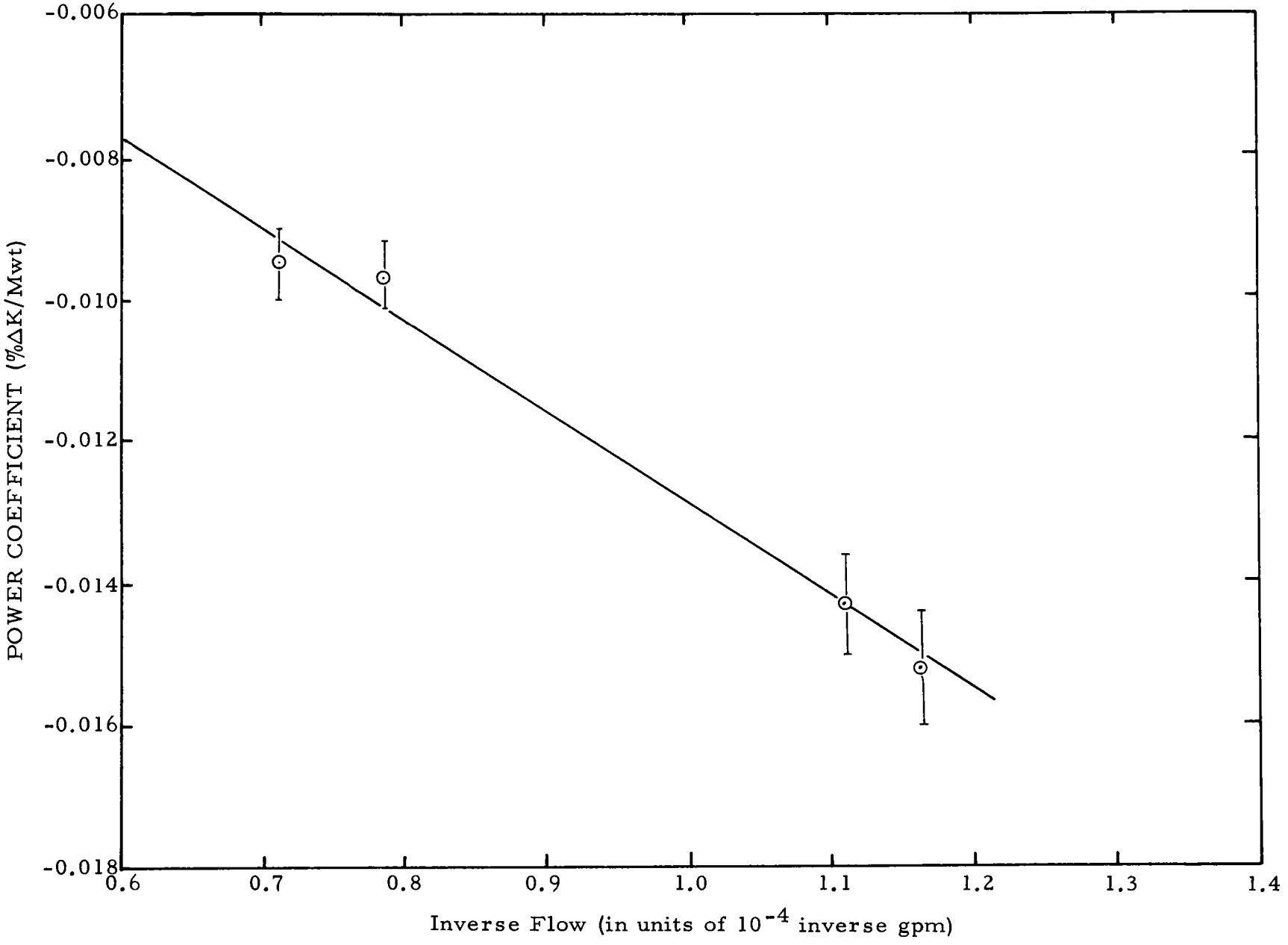

Figure 5. Power Coefficient as a Function of Inverse Flow

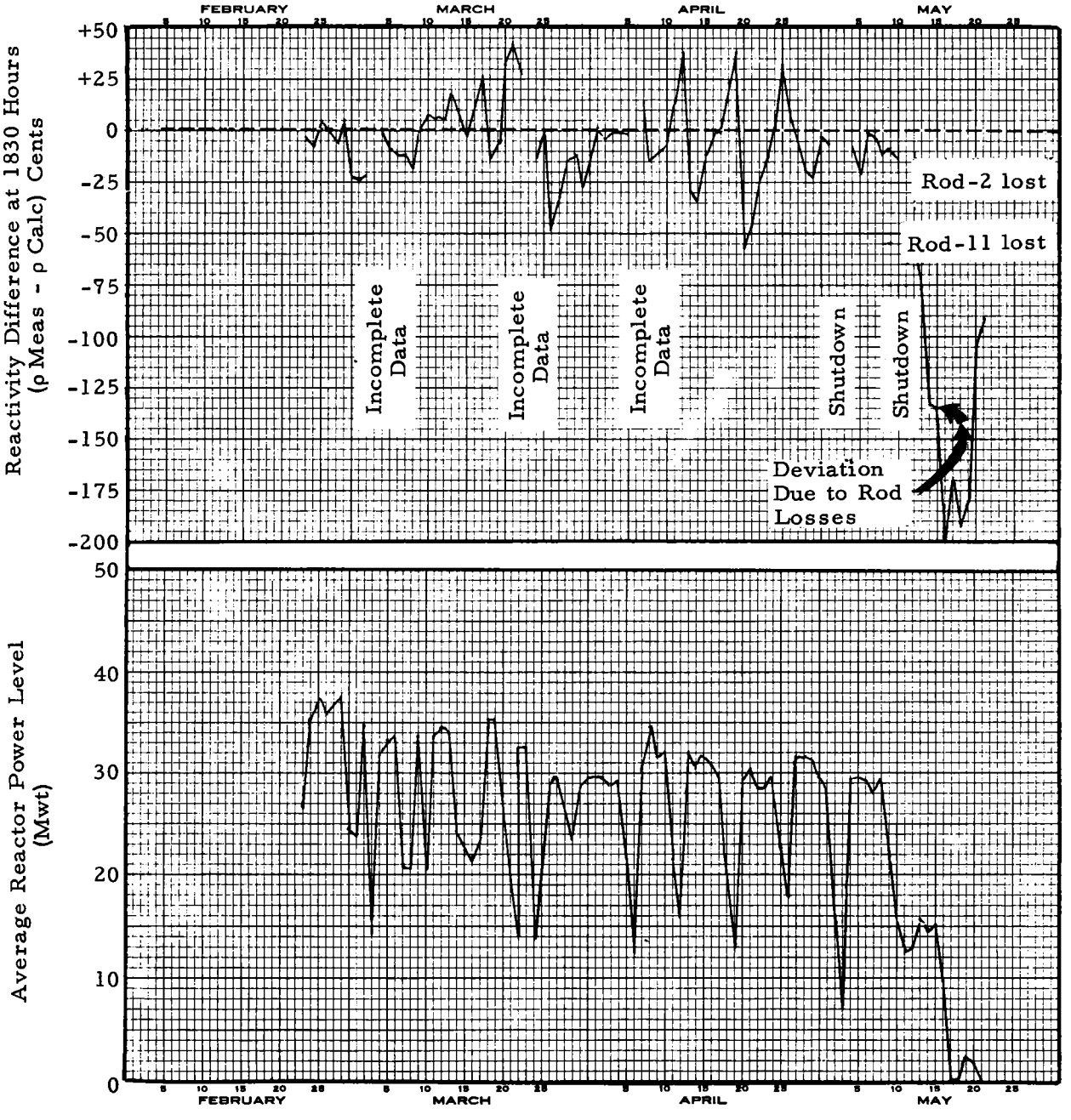

Figure 6. Summary of Reactivity History Results

of day is near the end of high power operation and, hence, changes in temperature, xenon, samarium and control rod positions are usually small at this time. Since it is the closest that the core comes to a truly steady-state condition, this period is favorable for calculation of reactivity. Any core changes not accounted for by the program should be discernible.

Figure 7 is a graph of the reactivity error caused by the difference in step length between up and down control rod movement. Since the integrating step counters for control rods No. 3 and No.6 are rezeroed each morning, the error eliminated at that time was accumulated during the previous day's operation. The graph in Figure 7 has been drawn so that datum recorded on a particular date is plotted with the preceding day's date.

Since the rate of accumulation of the error in control rod positions is not known explicitly, application of the measured error to any data points except the last one before rods No.3 and No.6 are rezeroed is not clear. However, some indication of the rate of buildup of the error through the day can be seen from the regular variation of the reactivity difference which has been observed for a large number of days of operation. A sample of this observed behavior is shown in Figure 8.

When the reactor is restarted after the two special dummy elements are removed, rod positions from the PnI are expected to be used for the reactivity history calculations. If the PnI prove to be accurate and reliable the reactivity difference calculations will improve.

C. CORE TEMPERATURE, HEAT FLUX AND POWER DISTRIBUTION

During the past six month period, the computer program for calculating peak cladding temperature, peak heat flux and relative power of each fuel element from operating data was completed and checked out. A brief outline of the analysis was previously presented* while a detailed topical report** describing the theory and application of the program has been written and published.

---

*"PNPF-OAP Progress Report No. 3 (July 1, 1963 - December 31, 1963)," NAA-SR-9473.

**D.F. Hausknecht, "Computer Calculation of Fuel Cladding Temperature, Heat Fluxes and Power Distribution in the PNPF Core," NAA-SR-TDR 8850, April 20, 1964.

In developing the computer program it was necessary to assume a particular control rod program. The rod program assumed was 130→100*, but early calculations showed that the peak cladding temperature limit (750°F) and the peak heat flux limit (127,000 Btu/ft^2-hr) would be exceeded at full power due to the presence of the two special dummy elements in core locations F-7 and F-15. Hence, the operational rod program was changed to 120→100 in order to level the neutron flux and power distribution. At the time the computer program was completed it was not practical to make the major modifications that would be required to accommodate the 120→100 rod program for the short period which remained until the two special dummies were replaced with live fuel. Hence, the relative power calculations which depend on empirical data gave accurate results during the past six months. The peak cladding temperature and peak heat flux results did not show absolute accuracy, but did imply core constancy for the period.

When the power distribution was first calculated for full power operation, it was established that the radial power distribution was symmetrical with no steep gradients anywhere in the core. The elements found to be generating the highest relative powers were as follows:

Core Position	Relative Power
D-13	1.55
E-12	1.74
G-10	1.67
H-11	1.59

A representative sample of the power contour maps is shown in Figure 9. The relative power calculations which were performed at least once per week, showed no significant variation from the results shown in Figure 9.

When the reactor is restarted after the special dummy elements are replaced with live fuel and the control rod program becomes 130→100, calculation of the maximum cladding temperature and heat flux is expected to yield accurate

*Control rod patterns are specified by three numbers which indicate how many rods are inserted in each ring of rods. For example, the pattern designated 130 has the central rod, three alternate inner ring rods and no outer ring rods inserted.

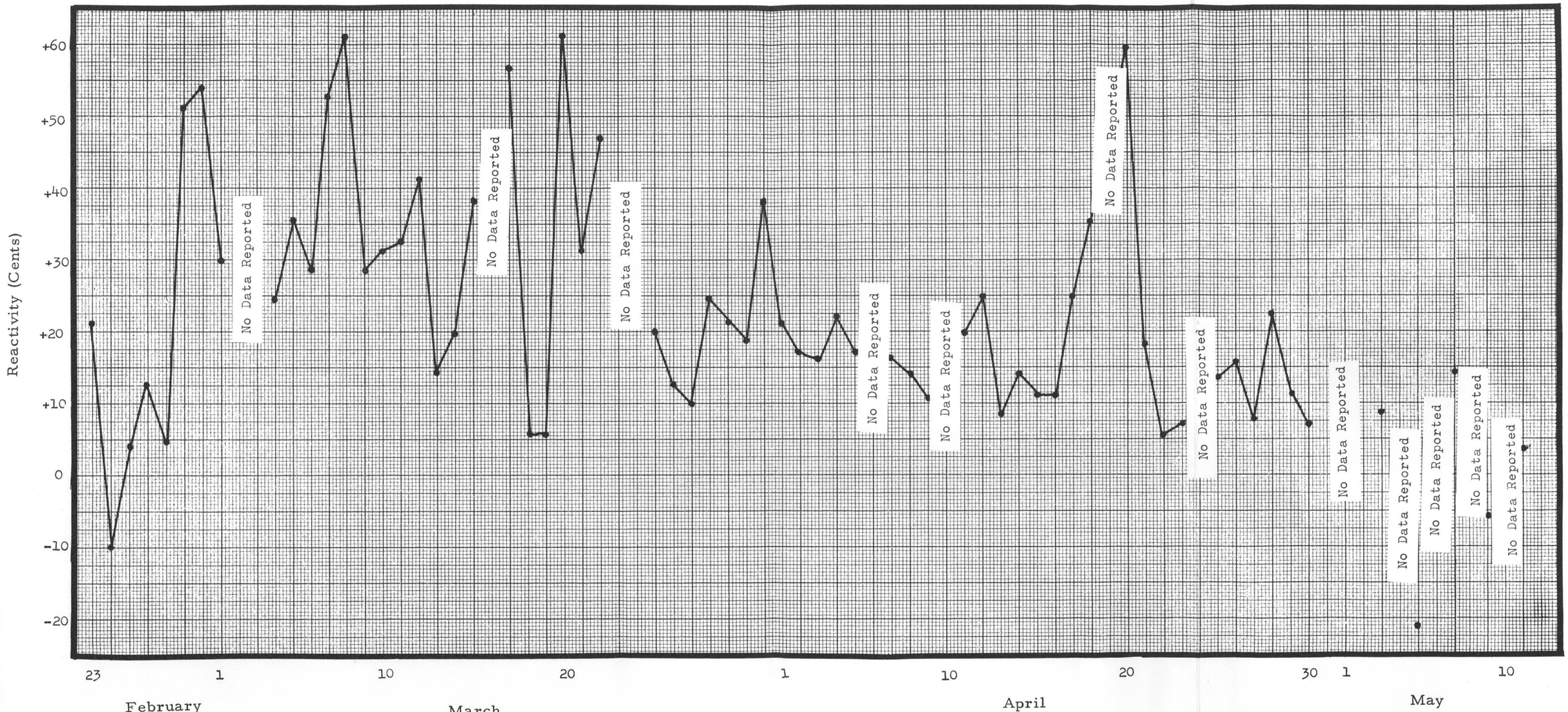

Figure 7. Measured Step Counter Corrections for Control Rods No. 3 and No. 6

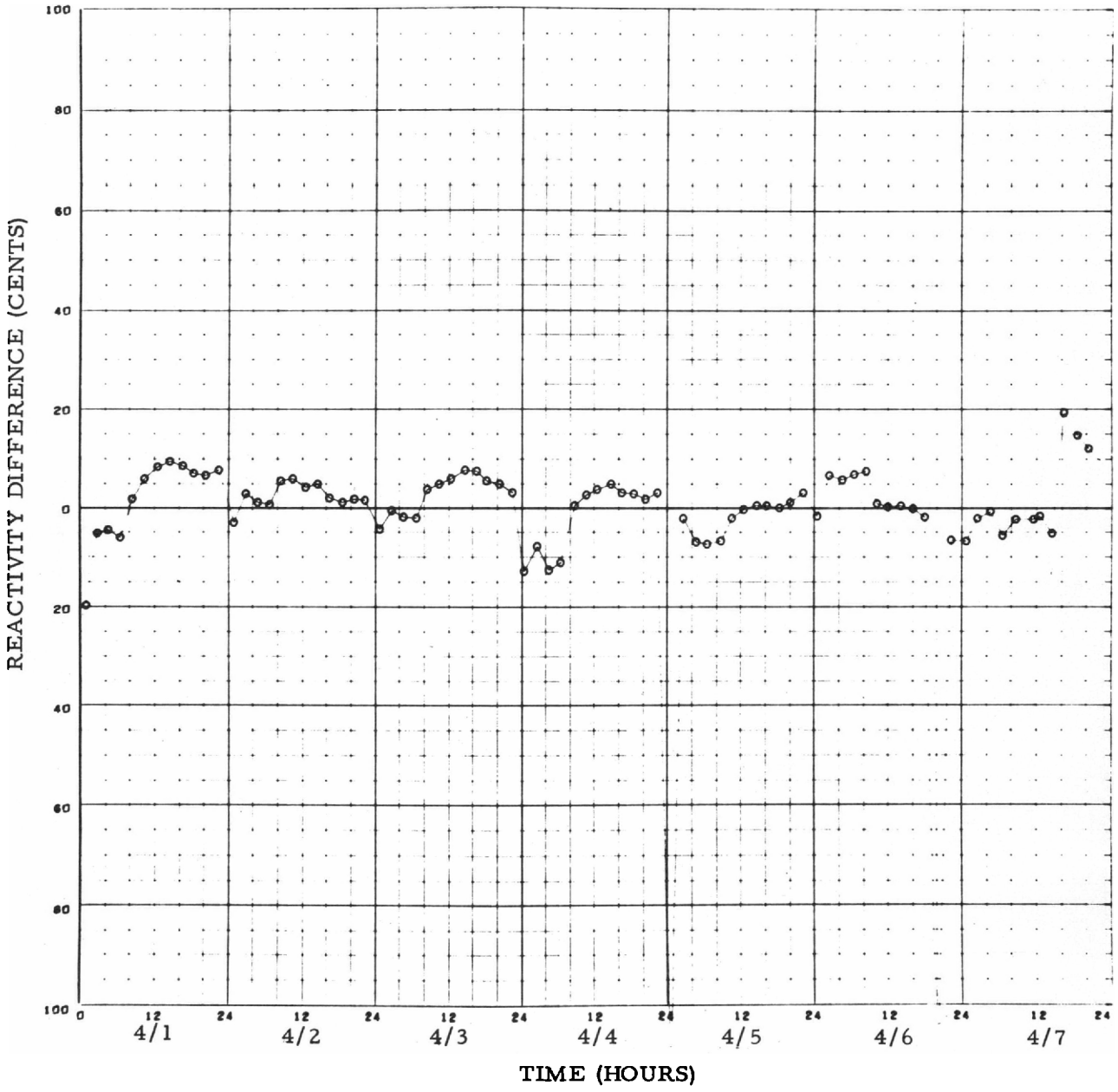

Figure 8. Sample of Results Showing Regular Daily Variation

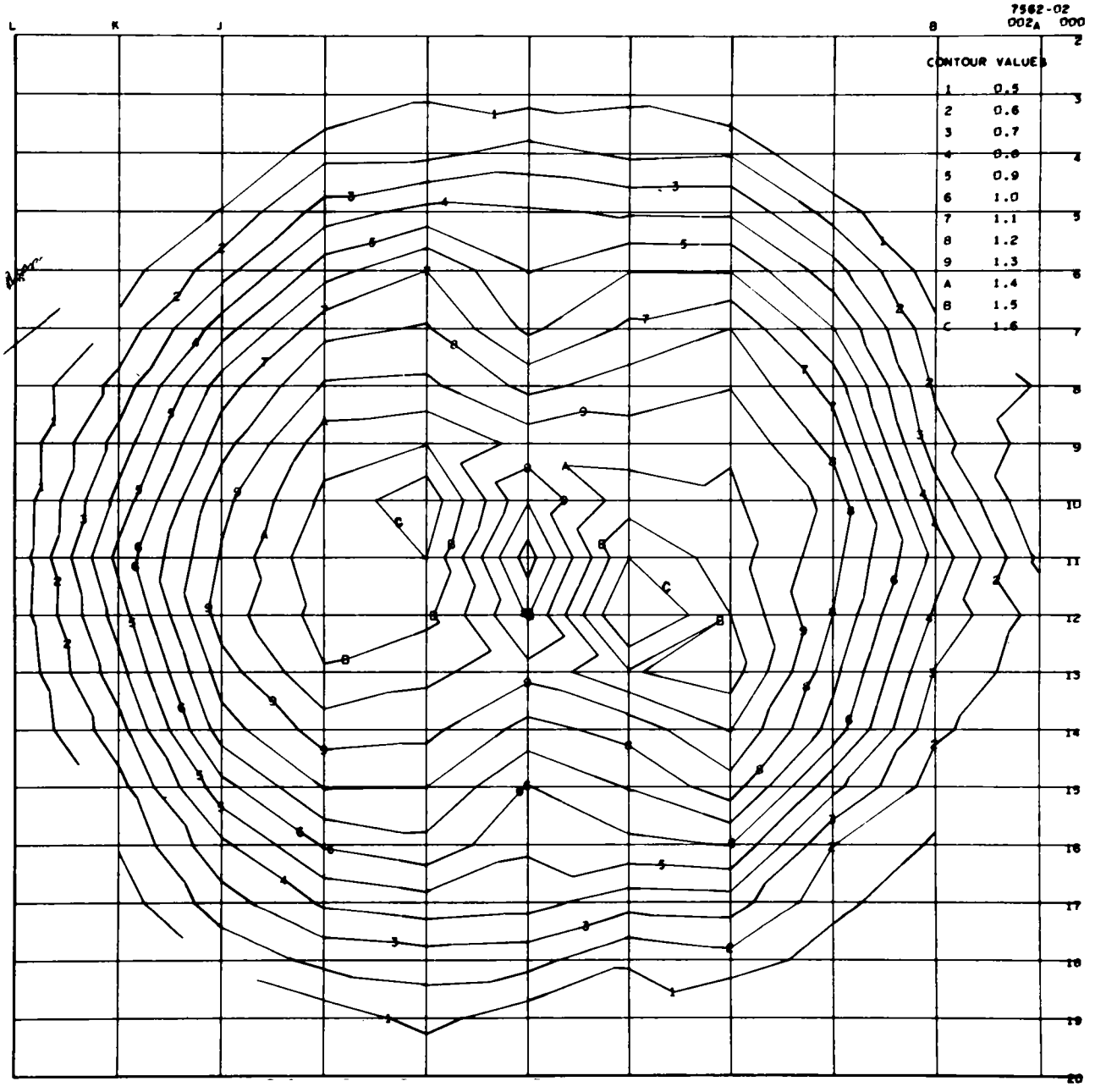

Date – May 3, 1964; Time 1230; Power 37.4 Mwt;
Control Rods 3 and 6 are 65 Percent Withdrawn

Figure 9. Representative Sample of Core Power Map

results. The accuracy of the calculated results will be confirmed by calculation and comparison of the maximum and nominal temperatures for the points on the instrumented fuel elements, where thermocouples are located.

D. INSTRUMENTED FUEL ELEMENT TEMPERATURE SURVEILLANCE PROGRAM

To facilitate surveillance of the instrumented fuel element (IFE) temperatures and to effect an early recognition of possible fuel fouling conditions, a computer program was developed to accept operating data and normalize indicated fuel temperatures to full power conditions. Input data to this program include the date, reactor inlet temperature, power level, reactor organic flow, and indicated cladding surface temperatures for each of the four thermocouple locations on each of the three instrumented fuel elements (Figure 10). Output data include the normalized full power temperatures for each of the four thermocouple locations in each of the three instrumented fuel elements (Table III). In addition, cathode ray tube (CRT) plots are obtained for normalized temperatures vs date for each of the three instrumented fuel elements. For further cognizance, a CRT plot showing the reactor power level is provided.

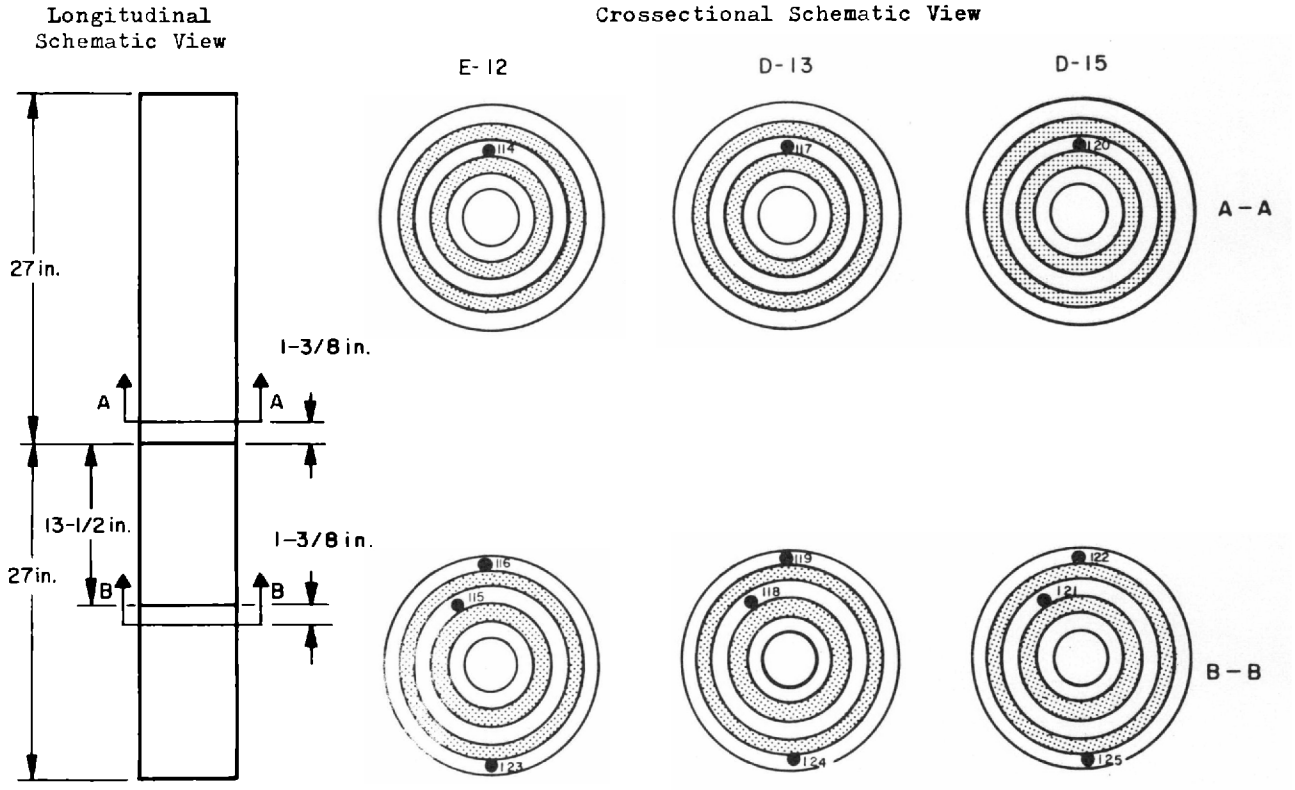

Figure 10. Thermocouple Locations in Fuel Elements in Positions E-12, D-13 and D-15

TABLE III

IFE SERIAL P-1098, CORE POSITION E-12

APR	FLOW (GPM)	POWER (MWT)	INLET TEMP (F)	T/C 114 IND TEMP (F)	T/C 114 NORM TEMP (F)	T/C 115 IND TEMP (F)	T/C 115 NORM TEMP (F)	T/C 116 IND TEMP (F)	T/C 116 NORM TEMP (F)	T/C 123 IND TEMP (F)	T/C 123 NORM TEMP (F)
1	13680.0	33.2	537.	608.	614.	596.	598.	588.	588.	620.	629.
2	13760.0	33.1	534.	609.	620.	598.	606.	589.	594.	621.	636.
3	13696.0	33.0	534.	610.	621.	599.	607.	590.	595.	621.	635.
4	13648.0	33.9	535.	611.	618.	599.	603.	590.	592.	623.	633.
5	13680.0	26.9	553.	604.	604.	596.	591.	587.	577.	616.	622.
6					SHUTDOWN						
7	13552.0	43.0	524.	622.	619.	602.	599.	587.	585.	632.	629.
8	13520.0	43.0	525.	620.	616.	603.	599.	592.	589.	630.	626.
9	13520.0	38.6	527.	615.	619.	598.	600.	591.	593.	625.	630.
10	13600.0	38.9	525.	617.	623.	602.	607.	592.	596.	629.	636.
11	13680.0	25.8	542.	602.	622.	595.	610.	585.	594.	613.	640.
12	13680.0	16.7	551.	590.	622.	588.	617.	578.	592.	602.	653.
13	13600.0	41.8	524.	622.	622.	599.	599.	588.	588.	631.	631.
14	13600.0	39.9	528.	625.	625.	598.	598.	592.	591.	625.	627.
15	13648.0	41.4	525.	608.	608.	602.	602.	592.	592.	628.	629.
16	13600.0	38.8	527.	615.	619.	598.	600.	587.	588.	620.	624.
17	13600.0	37.6	529.	620.	625.	600.	603.	590.	592.	624.	630.
18	13680.0	24.2	543.	605.	632.	590.	606.	583.	593.	608.	637.
19	13680.0	21.9	544.	602.	636.	589.	611.	579.	591.	605.	642.
20	13570.0	38.4	528.	615.	619.	599.	601.	582.	582.	625.	630.
21	13570.0	38.0	528.	617.	622.	601.	604.	588.	590.	624.	630.
22	13568.0	37.6	529.	617.	622.	600.	603.	586.	587.	622.	627.
23	13600.0	38.1	530.	617.	620.	598.	598.	585.	584.	623.	626.
24	13520.0	39.0	526.	619.	623.	600.	603.	585.	587.	625.	630.
25	13600.0	31.6	537.	611.	622.	596.	602.	584.	586.	616.	629.
26	13680.0	24.0	546.	601.	621.	590.	601.	577.	578.	605.	628.
27	13520.0	38.9	528.	617.	619.	600.	601.	582.	581.	628.	631.
28	13520.0	38.5	530.	600.	600.	602.	602.	588.	586.	626.	628.
29	13520.0	39.4	528.	605.	605.	602.	602.	587.	586.	627.	629.
30	13600.0	36.6	533.	601.	601.	601.	601.	587.	585.	624.	628.

Fuel element surface temperature data have been collected and programmed to cover the operating period from the initial operation at full power in February to the plant shutdown on May 18.

Figures 11 and 12 are composite plots of the power level and normalized temperatures for February, March, and April 1964. These plots indicate that no fouling occurred during this period, since no upward trends in cladding temperatures were observed. The May data continued to show no indication of fouling, as shown in Figures 13 through 16.

E. FUEL MANAGEMENT

In line with the fuel management program set forth in NAA-SR-TDR 8837* and the requirement of a minimum shutdown margin of 4% Δk, the first fuel shuffle was made following the May 21 shutdown. The program executed was as follows (see also Figure 17):

1) The evaluation element was removed from D-9; the element from B-11 was moved to D-9, and the special dummy from F-7 was moved to B-11.

2) The element from D-5 was moved to F-7, the element from D-3 to D-5, and the special dummy from F-15 to D-3.

3) The element from H-17 was moved to F-15, the element from H-19 to H-17, the special dummy from B-11 to H-19 (step 1) and a fresh element was placed in B-11.

As a result, the special dummies remain in the core in the outermost ring (D-3 and H-19), while the elements moved from these two core locations have had their orifices adjusted to conform to the unorificed region in which they are located. The elements were shuffled in this manner to achieve a more uniform core burnup, and at the same time, not to introduce large burnup differences between neighboring elements which could conceivably produce power peaking.

---

*D. E. Lew, "Piqua Fuel Management Program," NAA-SR-TDR 8837, August 1, 1963.

Preceding the fuel shuffle and removal of dummy elements, the shutdown margin for the compact 61-element core was estimated using available data and previous calculations. This analysis was performed as follows:

1) The measured shutdown margin at beginning of core life (with the two dummies) was 4.32% Δk.

2) In calculating the reactivity loss due to core burnup, values of 3239 Mwd and 4.88 MTU were used with a burnup rate of 1.328% Δk/1000 Mwt/MTU. The loss of ρ_{ex} was 0.88% Δk.

3) The reactivity loss due to samarium buildup was taken as 0.63% Δk. It was assumed that the xenon would decay to a negligible concentration during the shutdown.

4) The increase of ρ_{ex} due to replacement of the dummies with partially burned-up fuel was calculated to be 2.74% Δk; the measured value of 2.78% Δk for dummies replaced with fresh fuel was modified due to burnup and samarium buildup in the fuel.

5) With removal of the two fuel elements from D-3 and H-19 there was an estimated ρ_{ex} loss of 0.13% Δk.

6) The increase in control rod worth resulting from replacement of dummies with fuel had been previously determined as 1.32% Δk.

7) Not included in the 2.78% Δk figure of 4) is the increase in worth of the 17 elements added to the outside ring after placement of the dummies when these dummies are replaced with fuel. This increase amounts to 3¢ per element or 51¢ (0.36% Δk) overall.

The resultant value for shutdown margin is 4.18% Δk, approximately 0.2% Δk greater than the specified minimum.

The evaluation element removed (P-1071) had been in the core for one year. The average and peak element burnup were estimated as 920 and 1400 Mwd/MTU respectively; a relative power factor of 1.39 and an average value of axial peak-to-average flux of 1.5 were assumed for the calculations. At full power, its peak heat flux was 105,000 Btu/hr-ft^2 with a maximum cladding temperature of close to 720°F; at the February-May average power of 25.3 Mwt the corresponding values were 58,500 Btu/hr-ft^2 and 665°F.

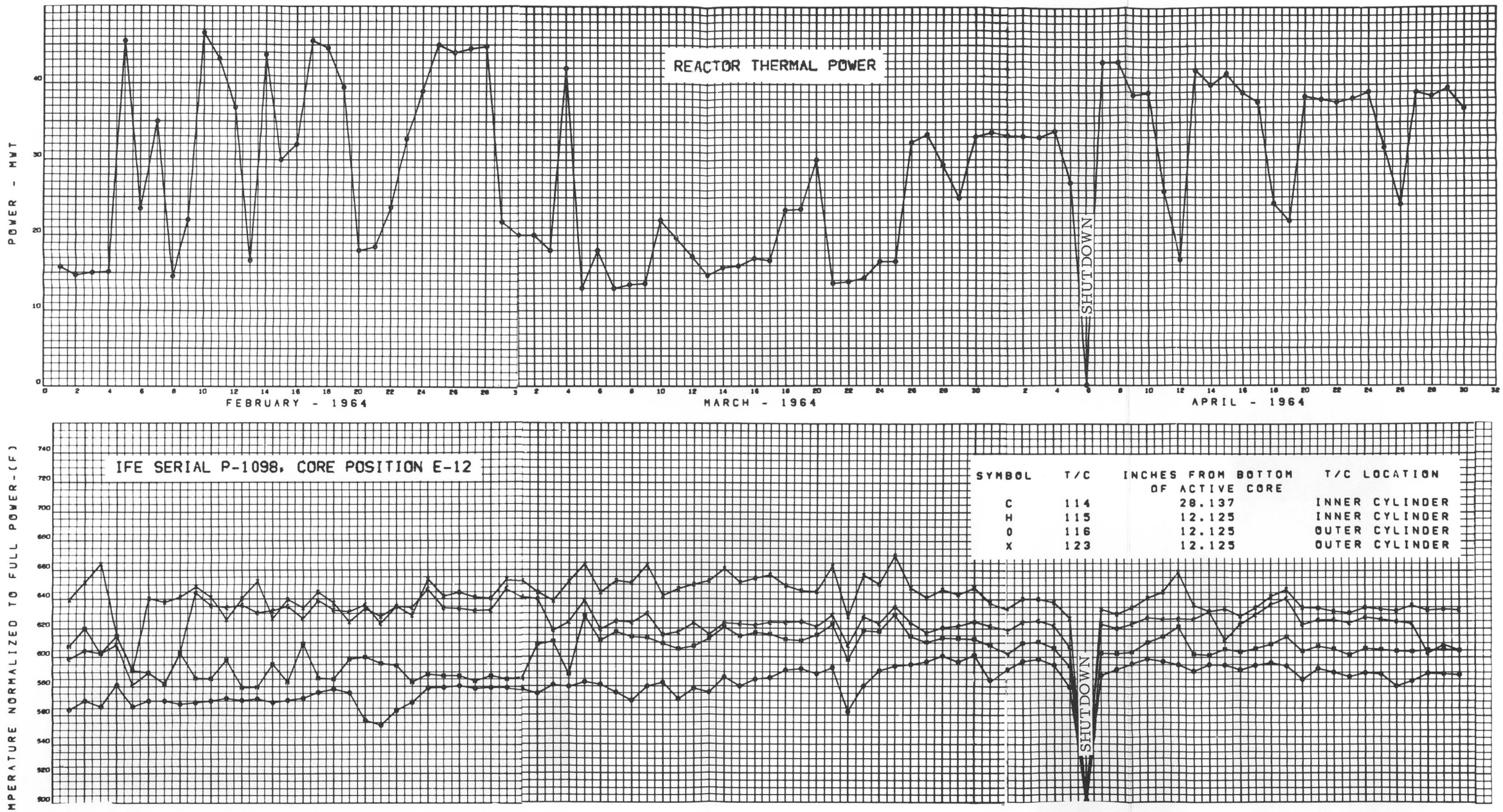

Figure 11. Normalized Cladding Surface Temperatures and Reactor Thermal Power

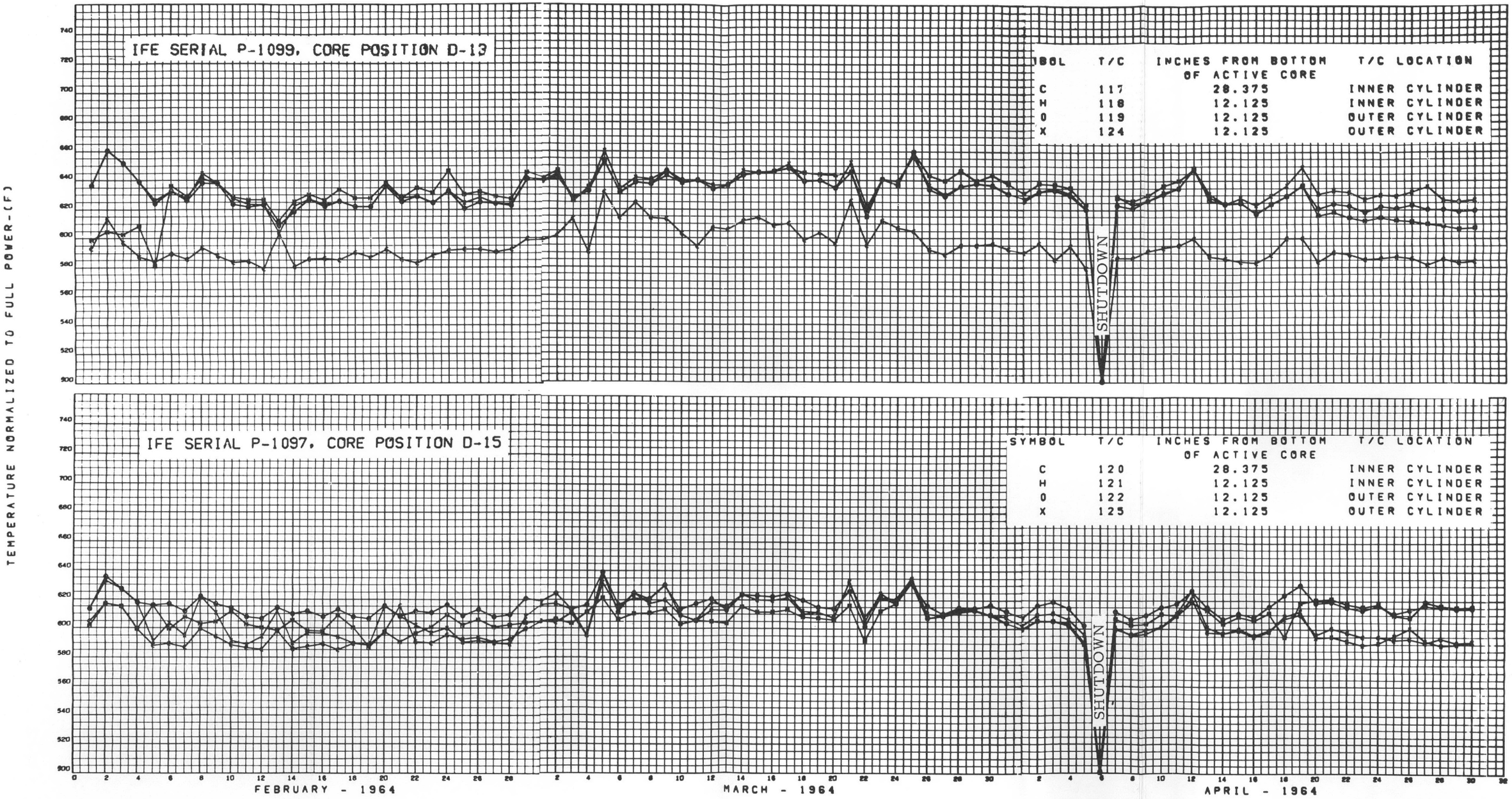

Figure 12. Normalized Cladding Surface Temperatures

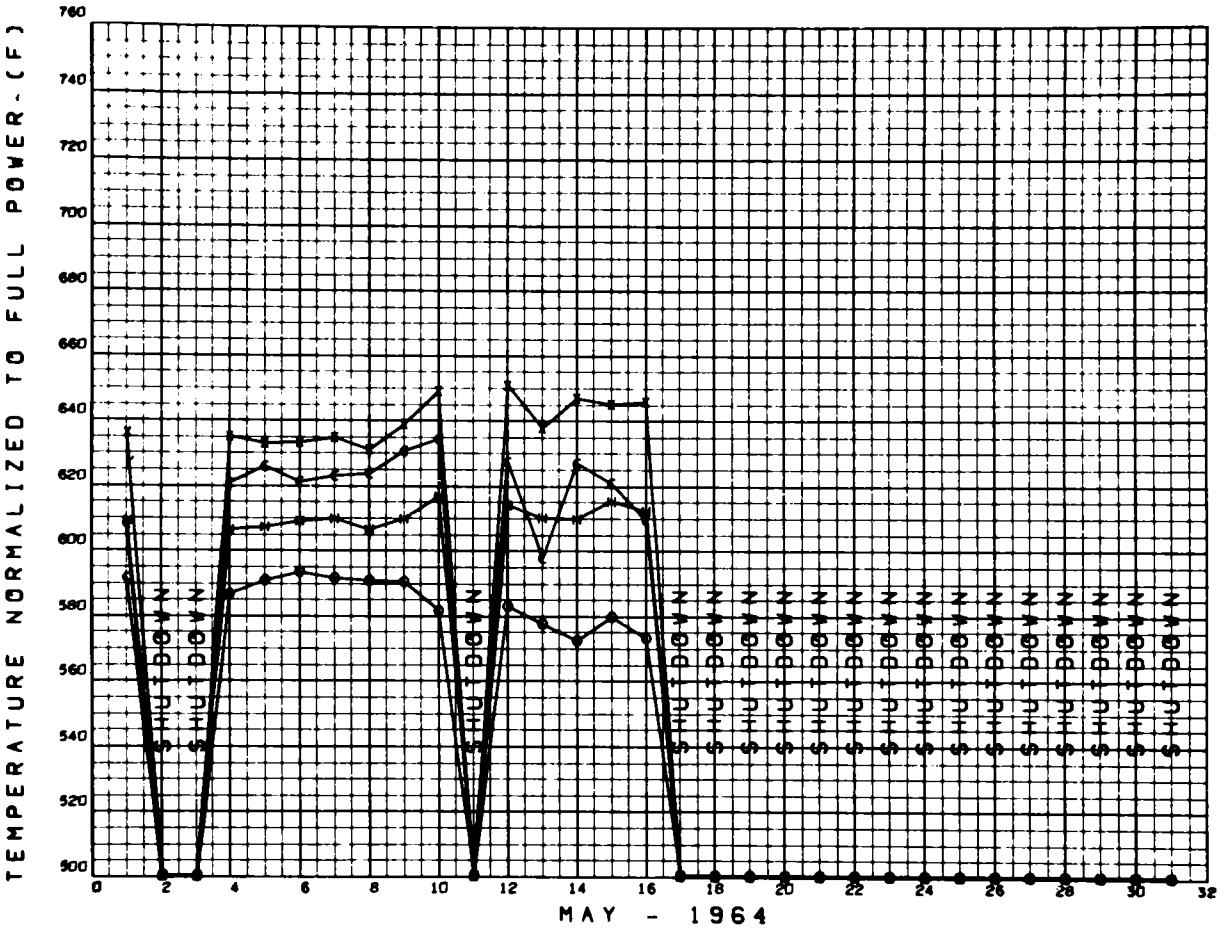

SYMBOL	T/C	INCHES FROM BOTTOM OF ACTIVE CORE	T/C LOCATION
C	114	28.137	INNER CYLINDER
H	115	12.125	INNER CYLINDER
O	116	12.125	OUTER CYLINDER
X	123	12.125	OUTER CYLINDER

Figure 13. Normalized Cladding Surface Temperatures

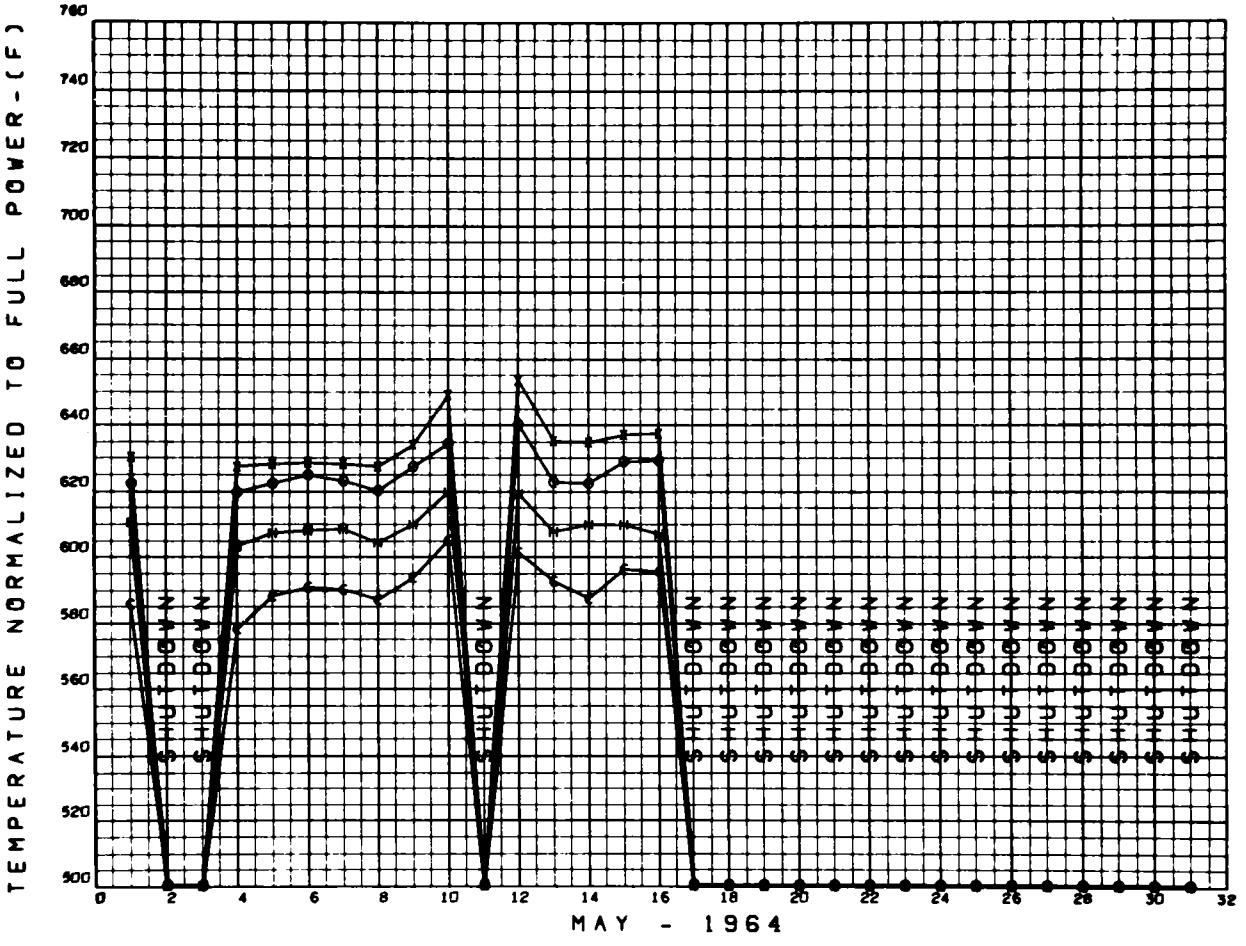

SYMBOL	T/C	INCHES FROM BOTTOM OF ACTIVE CORE	T/C LOCATION
C	117	28.375	INNER CYLINDER
H	118	12.125	INNER CYLINDER
O	119	12.125	OUTER CYLINDER
X	124	12.125	OUTER CYLINDER

Figure 14. Normalized Cladding Surface Temperatures

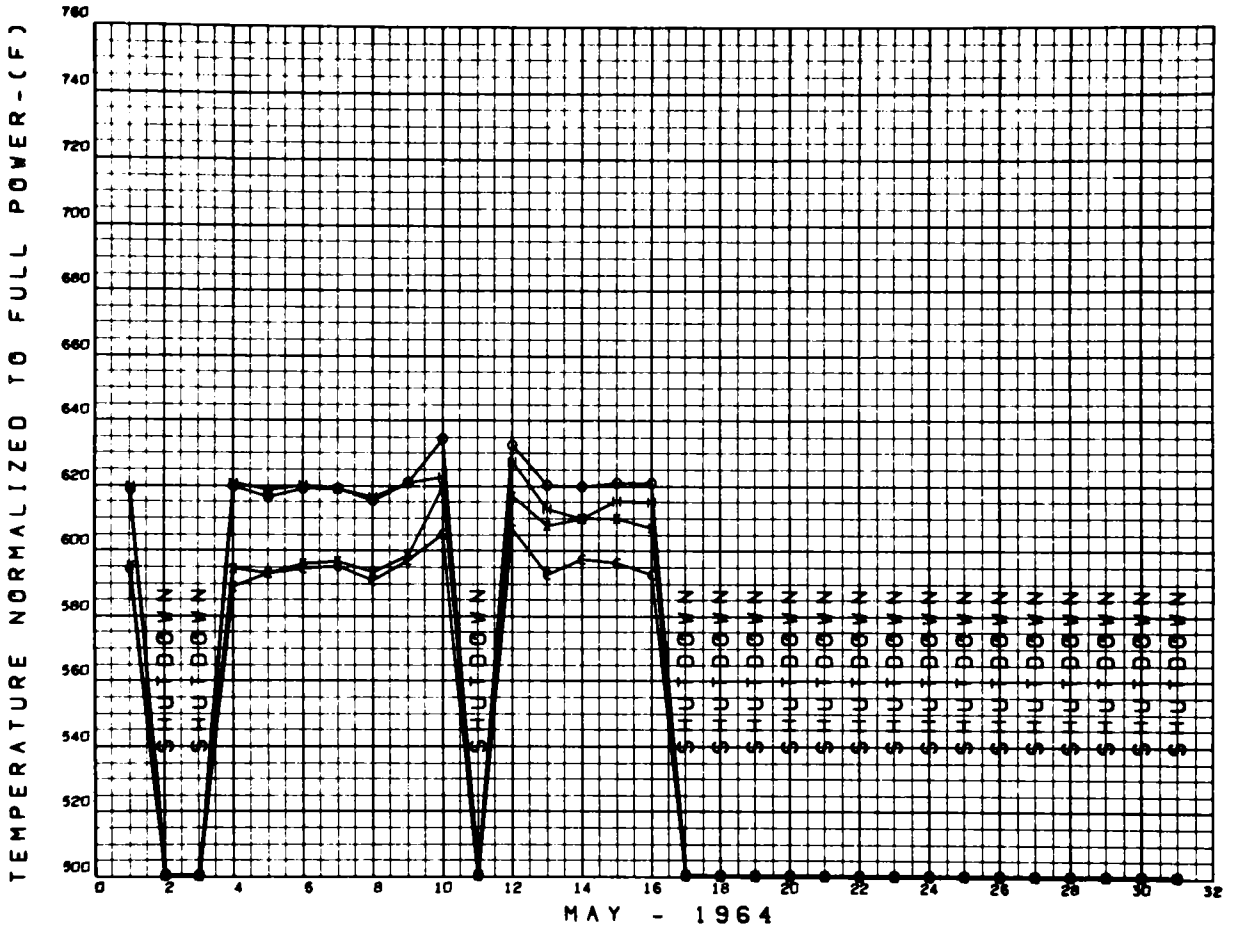

SYMBOL	T/C	INCHES FROM BOTTOM OF ACTIVE CORE	T/C LOCATION
C	120	28.375	INNER CYLINDER
H	121	12.125	INNER CYLINDER
O	122	12.125	OUTER CYLINDER
X	125	12.125	OUTER CYLINDER

Figure 15. Normalized Cladding Surface Temperatures

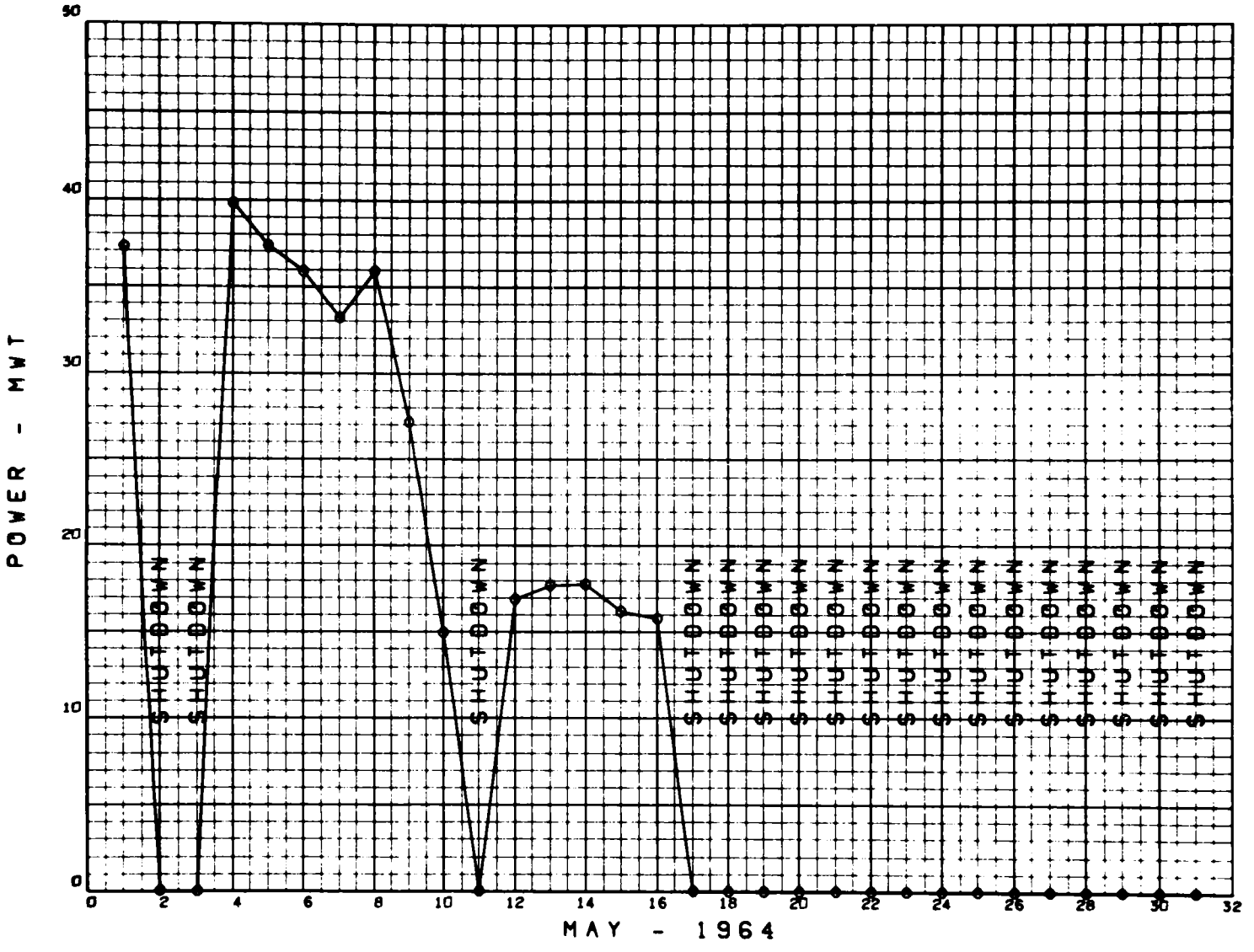

Figure 16. Normalized Cladding Surface Temperatures

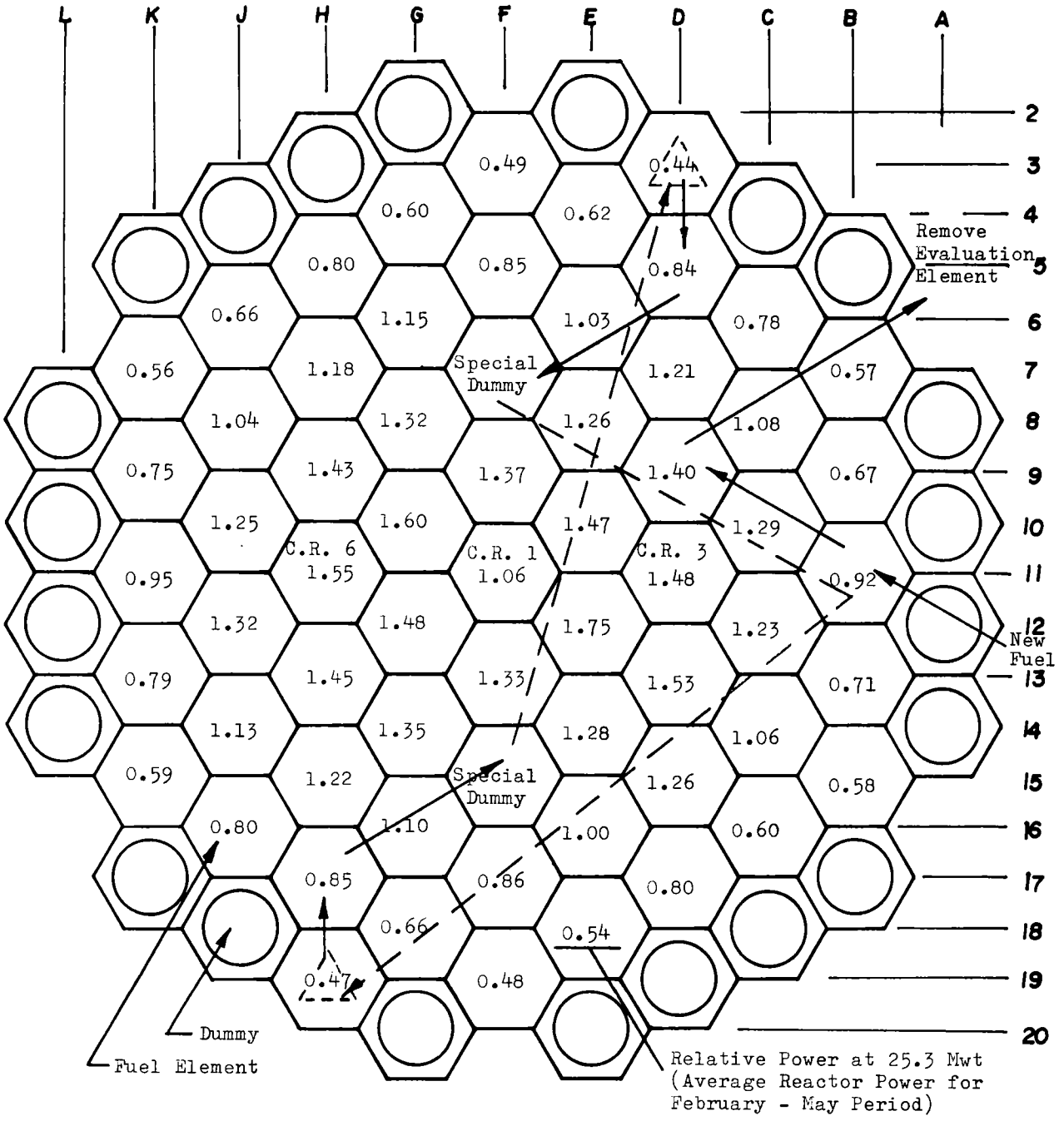

Figure 17. First Fuel Shuffle, May, 1964

III. FIRST FUEL ELEMENT EXAMINATION

Fuel element No. 1071 (core position D-9) was removed from the core on June 5, 1964 for examination in the hot cell at Santa Susana, California. This element received an estimated peak burnup of 1400 Mwd/MTU (920 Mwd/MTU average). The peak heat flux during operation for this element was 105,000 Btu/hr-ft^2, with a calculated peak surface temperature of 720°F (Table IV).

TABLE IV

PNPF FUEL ELEMENT EXAMINATION

OPERATING DATA			
Fuel Element No.		1071	
Core Location		D-9	
Estimated Burn-up Maximum		1400 Mwd/MTU	
Estimated Burn-up Average		920 Mwd/MTU	
Cladding Hot Spot Temperature		720°F	
Maximum Heat Flux		105,000 Btu/ft^{2}hr	
HOT CELL EXAMINATION RESULTS			
Successful Control of Fouling			
Very Thin Black Film < 0.1 Mil Thick			
Absence of Particulates in Valleys Between Fins and On Inlet Screen			
Fuel Swelling			
Maximum Dimensional Changes:	OD	0.28%	Within Acceptable Limits
	ID	0.52%	
	Length	0.18%	

A. PHYSICAL EXAMINATION

The element has been examined visually, photographed, and disassembled. As-received the fuel element had a very thin black film covering the outside of the process tube in the fueled portion of the element. Disassembly of the element was accomplished without difficulty. The fuel cylinders had a very thin grey-black surface-film. This film was lighter at the top of the element and appeared

to get slightly darker near the center. There was no particulate matter accumulation any place in the element and the inlet screen was completely clean.

The fuel cylinders were measured on the outside diameter, inside diameter, and length at the same stations as measured prior to irradiation. A pi-tape was used in performing the outside diameter measurements; the inside measurements were made with three-probe internal micrometer and a trimike; a special jig with dial indicators was used in measuring the length. The pre-irradiation measurements, post-irradiation measurements, and the changes from pre- to post- are presented in Table V. The post-irradiation measurements have been corrected to a temperature of 70°F. The maximum measured change in the outside diameter of the large cylinders was 0.27% at the middle of cylinder No. 3. Measurements of the inside diameter of the fuel cylinders have shown changes of up to 0.52%; these measurements, however, are subject to greater uncertainties than those of the outside diameter as a result of difficulties encountered in the measuring techniques used. The maximum length change, 0.18%, also occurred on cylinder No. 3.

Figures 18 through 21 show photographs of the fuel element in the hot cell, including a view of the element after removal of the outer process tube, a view of the individual cylinders, as well as the inlet screen and details of the fins.

In all respects, the hot cell examination confirmed the lack of fouling of the element indicated by the temperature performance during reactor operation. Fuel swelling appeared to be less than anticipated and well within acceptable limits.

B. CHEMICAL EXAMINATION

Fuel element No. P-1071 was removed from core position D-9 (June 5, 1964) and placed in the single fuel element loading thimble which was filled with HB-40 (hydrogenated Santowax OMP). On June 6, prior to loading the element into the shipping cask, a sample of the HB-40 was taken from the loading thimble for pulse height analysis. Analysis of the sample showed very low levels of gamma activity. An 80-min count gave photopeaks at 0.32, 0.52, 0.82, 1.13, and 1.34 Mev which indicated the presence of Cr^{51}, Co^{58}, Mn^{54}, Fe^{59}, Zn^{65}, and Co^{60}.

TABLE V

DIMENSIONAL CHANGES, FUEL ELEMENT NO. P-1071

A. Outer Cylinders

		Outside Diameter			Inside Diameter				Length		
Cyl. No.	Position	Post	Pre	% Chg	Post	Pre	% Chg	Position	Post	Pre	% Chg
1	Top	5.1215	5.119	.05	4.1423	4.1420	.01	0°	13.604	13.607	-.02
	Middle	5.1225	5.119	.07	4.1410	4.1430	-.05	120°	13.603	13.607	-.03
	Bottom	5.1222	5.119	.06	4.1499	4.143	.17	240°	13.604	13.607	-.02
	Ave	5.1221	5.119	.06	4.1444	4.1427	.04	Ave	13.6037	13.6070	-.02
2	T	5.1192	5.120	-.02	4.1565	4.153	.08	0	13.613	13.608	.04
	M	5.1229	5.119	.08	4.1642	4.150	.34	120	13.611	13.608	.02
	B	5.1239	5.120	.08	4.1628	4.151	.28	240	13.611	13.608	.02
	A	5.1220	5.1197	.04	4.1612	4.1513	.24	Ave	13.6123	13.6080	.03
3	T	5.1228	5.116	.13	4.1612	4.145	.39	0	13.627	13.605	.16
	M	5.1308	5.117	.27	4.1662	4.148	.44	120	13.629	13.605	.18
	B	5.1305	5.118	.24	4.1572	4.152	.12	240	13.625	13.605	.15
	A	5.1280	5.1170	.21	4.1615	4.1483	.32	Ave	13.6270	13.6050	.16
4	T	5.1277	5.119	.17	4.1638	4.142	.52	0	13.620	13.608	.09
	M	5.1304	5.120	.20	4.1527	4.143	.23	120	13.619	13.608	.08
	B	5.1224	5.120	.05	4.1480	4.143	.12	240	13.621	13.608	.10
	A	5.1268	5.1197	.14	4.1548	4.1427	.29	Ave	13.6200	13.6080	.09

TABLE V (Continued)

DIMENSIONAL CHANGES, FUEL ELEMENT NO. P-1071

B. Inner Cylinders

		Outside Diameter			Inside Diameter				Length		
Cyl. No.	Position	Post	Pre	% Chg	Post	Pre	% Chg	Position	Post	Pre	% Chg
5	T	4.0777	4.084	-.15	3.1083	3.108	.01	0	13.608	13.607	.01
	M	4.0824	4.083	-.01	3.1120	3.109	.10	120	13.609	13.607	.01
	B	4.0854	4.081	.11	3.1123	3.108	.14	240	13.611	13.607	.03
	A	4.0818	4.0827	-.02	3.1109	3.1087	.07	Ave	13.6093	13.6070	.02
6	T	4.0921	4.088	.10	3.1230	3.116	.22	0	13.622	13.606	.12
	M	4.0918	4.086	.14	3.1245	3.115	.30	120	13.620	13.606	.10
	B	4.0946	4.085	.23	3.1291	3.113	.52	240	13.623	13.606	.12
	A	4.0928	4.0863	.16	3.1255	3.1147	.35	Ave	13.6217	13.6060	.11
7	T	4.0947	4.089	.14	3.1189	3.107	.38	0	13.625	13.607	.13
	M	4.0954	4.090	.13	3.1217	3.108	.44	120	13.628	13.607	.15
	B	4.0954	4.090	.13	3.1154	3.110	.17	240	13.626	13.607	.14
	A	4.0952	4.0897	.13	3.1187	3.1083	.33	Ave	13.6263	13.6070	.14
8	T	4.0994	4.088	.28	3.1149	3.108	.22	0	13.616	13.606	.07
	M	4.0984	4.095	.08	3.1217	3.115	.22	120	13.616	13.606	.07
	B	4.0904	4.095	-.11	3.1180	3.113	.16	240	13.615	13.606	.07
	A	4.0961	4.0927	.08	3.1182	3.1120	.20	Ave	13.6157	13.606	.07

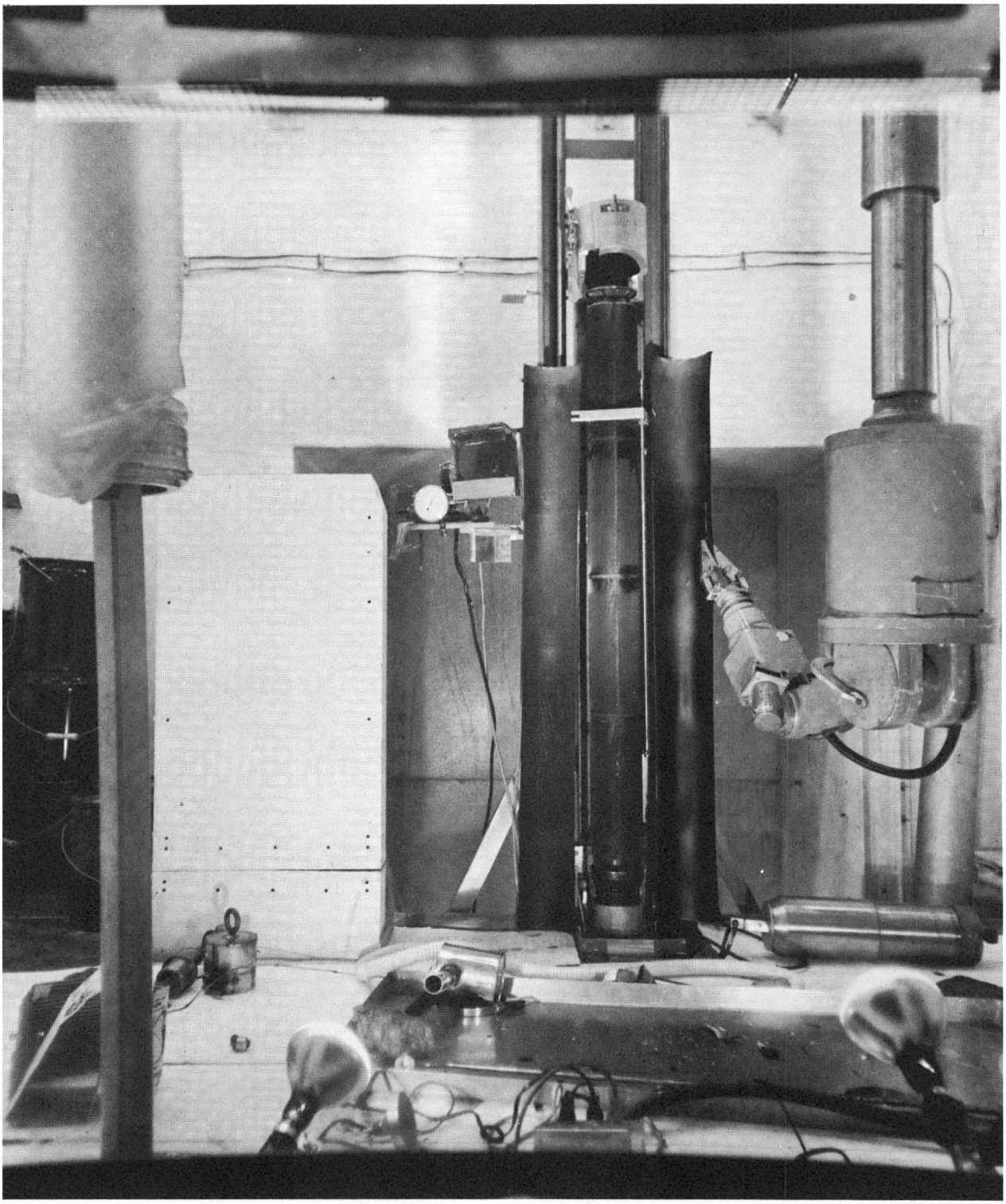

Figure 18. Overall View of Fuel Assembly Following Removal of Outer Process Tube

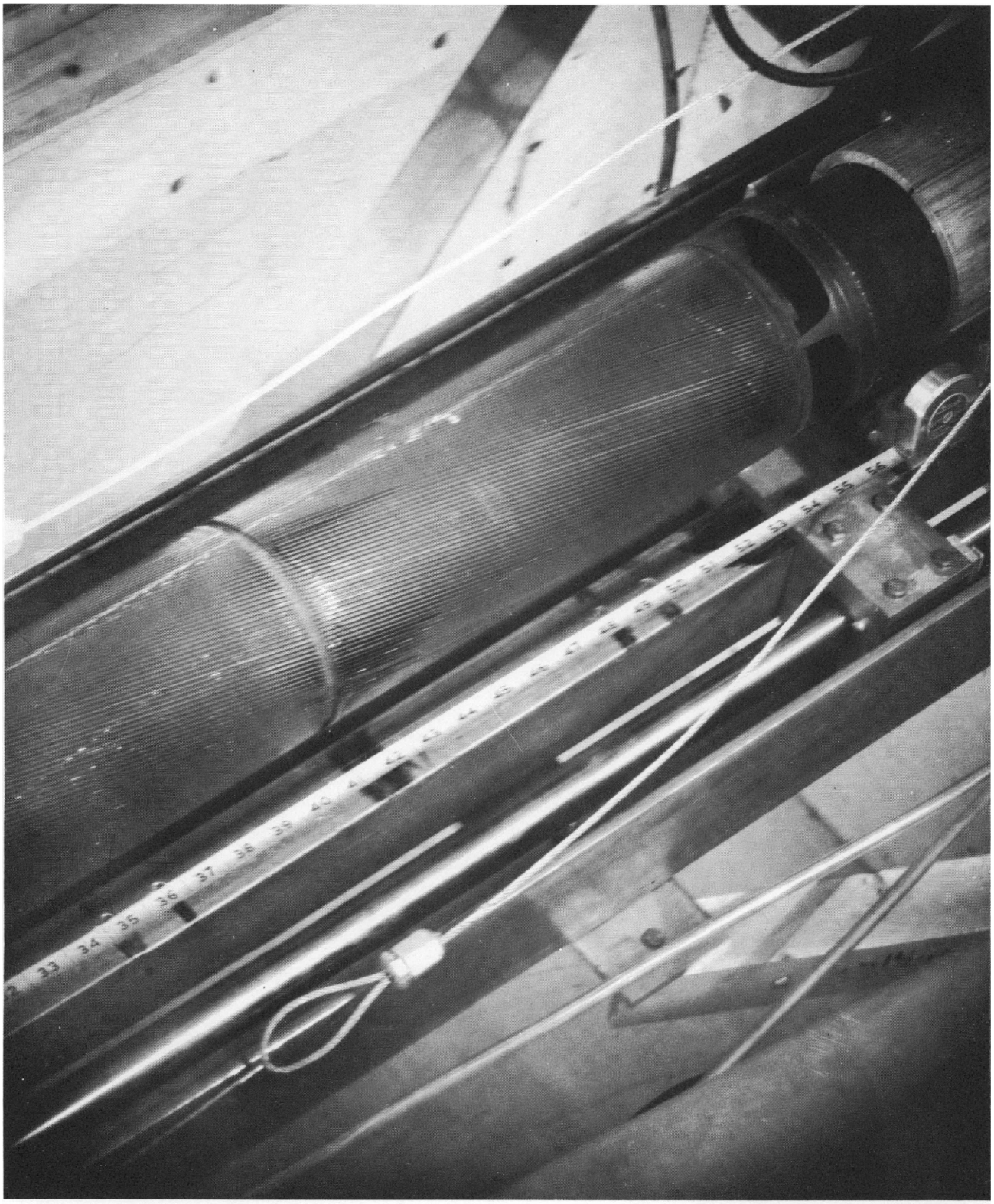

Figure 19. View of the Two Lower Outer Fuel Cylinders
(The Second Cylinder was Exposed to the Highest Flux)

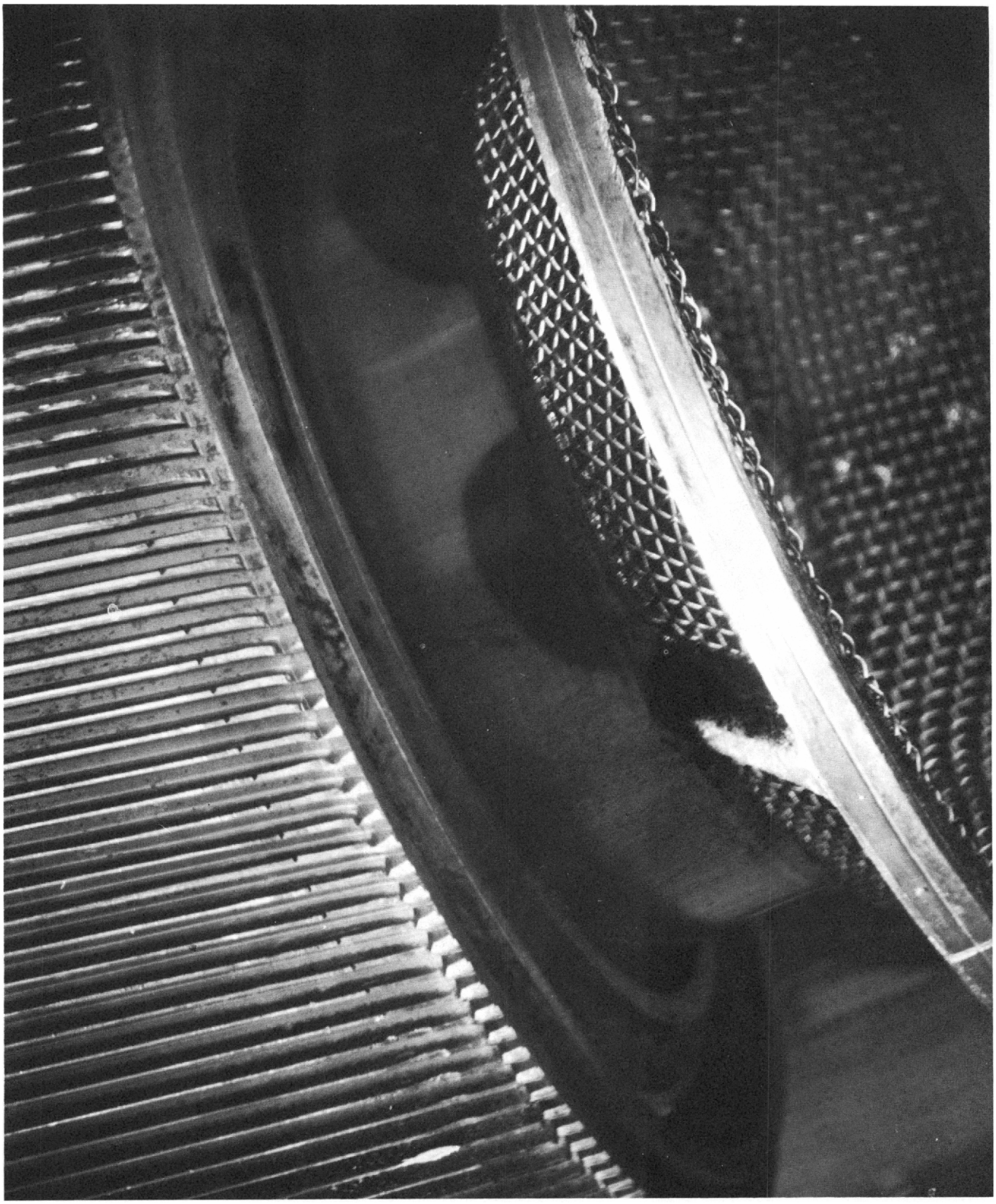

Figure 20. Close-up of the Inlet Screen and the Top of the Upper Outer and Inner Fuel Cylinders

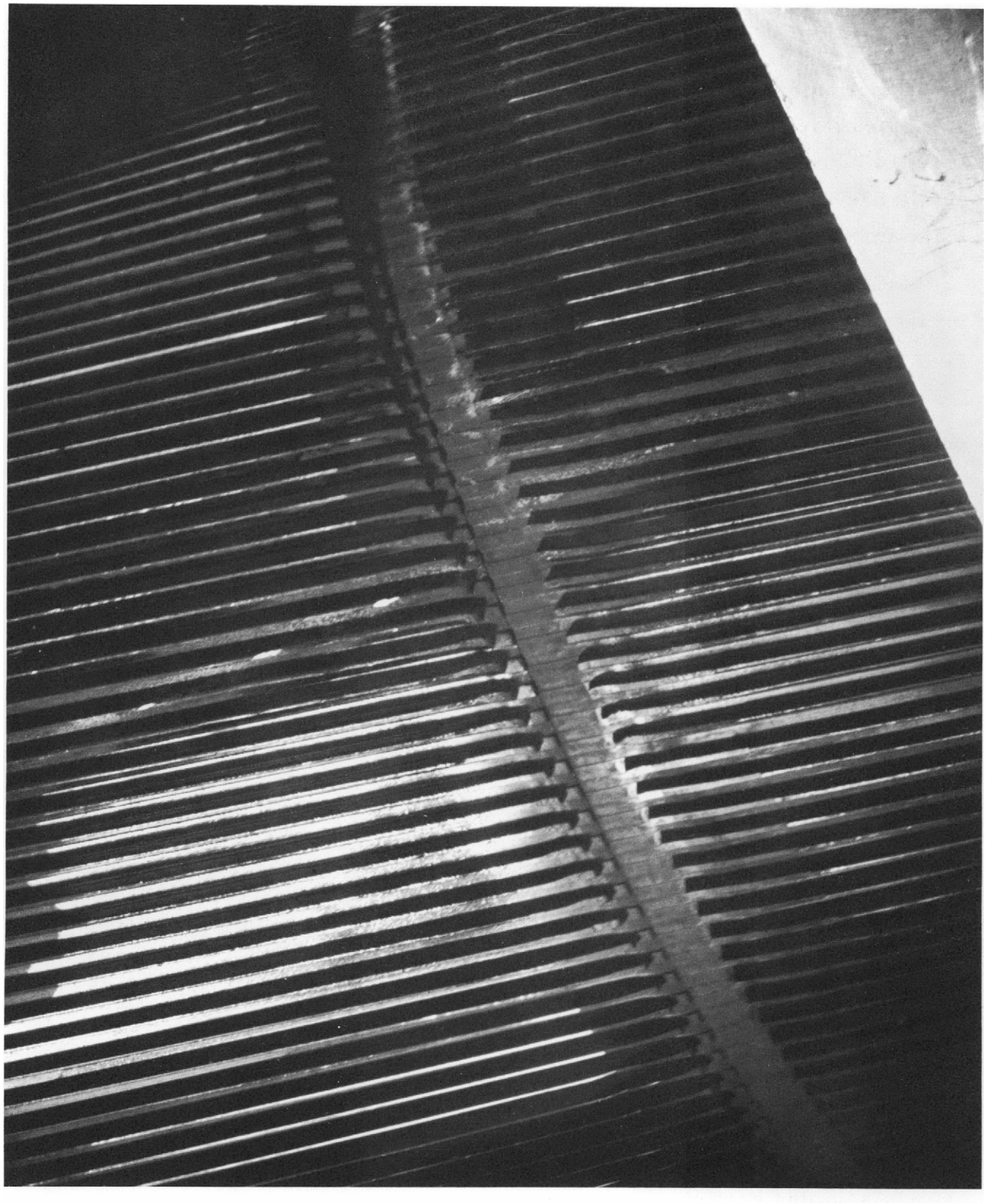

Figure 21. Close-up of the Junction Region Between Two of the Outer Fuel Cylinders

A calculation of the specific activity from the major peak at 0.82 Mev., which is attributed to Co^{58} and Mn^{54}, showed only 9.5 dpm/g. This is the equivalent of 4.3×10^{-6} microcuries per gram, as either Co^{58} or Mn^{54}. The very low activity levels found in the fluid indicates that the HB-40 did not dissolve significant amounts of coolant or film from fuel element surfaces.

After receipt at the hot cell on June 11, examination of the fuel element was initiated. In general, the exposed heat transfer surfaces of the as- received element looked cleaner than any of the previously examined OMRE elements.

The evaluation of the film on this element is to include analysis of the physical and chemical properties of the deposited material and also the film thickness. A wire brush was used with reasonable success for removal of the very thin film from two of the highest burn-up fuel cylinders (No. 3 and 7). To improve this technique, the brush was attached to a vacuum source and a Millipore filter housing in order to minimize film losses, particularly the very small film particles. In general, the film had a fine powdery texture in contrast to some fairly large flakes which had been removed from OMRE fuel elements. The film removed from the two fuel cylinders was weighed in the laboratory, and the results, including the estimated film thicknesses are shown in Table VI.

TABLE VI

FOULING FILM DATA FOR PNPF FUEL ELEMENT NO. P-1071

(Cylinders No. 3 and No. 7)

Component	Weight of Film Recovered (gm)**	Surface Area (cm^2)	Estimated* Film Thickness (mils)
Outer surface of large fuel cylinder (No. 3)	0.8172	3840	0.07
Outer surface of small fuel cylinder (No. 7)	0.4126	2860	0.05

*Assuming particle density of 1.5 gm/cm^3 and correction for unrecovered film.

**Includes aluminum cladding material scraped from the fuel cylinder.

Subsequent analysis of the film samples by emission spectroscopy showed aluminum to be a major constituent. The aluminum in the sample is probably the result of abrasion of the cladding with the wire brush. On this basis, the film thickness values shown in Table VI are too high.

Film thickness will also be obtained by encapsulation of fuel specimen cross-sections and measurement of the thickness of the film interface microscopically.

The results obtained to date are highly favorable both as regards the thickness of film present, and also the notable absence of any film aggregates which could have obstructed coolant flow in any of the channels through the element.

The results of the hot cell and chemical examination of fuel element No. P-1071 obtained thus far have confirmed the successful control of fouling achieved through careful control and monitoring of coolant quality during the first operational period ending May 21.

IV. SYSTEMS AND COMPONENTS ANALYSIS

A. MAIN HEAT TRANSFER SYSTEM ANALYSIS

1. Computer Program

A digital computer program has been formulated and employed to routinely calculate the efficiency of the main heat transfer and pressurizing pumps, and the overall heat transfer coefficient of the boiler and superheater. A description of the original computer program is detailed in NAA-SR-TDR 9475*. Input data for the program are obtained from normal plant instrumentation during periods of stable (equilibrium) plant operation. The output from the program first lists the input data for reference purposes, followed by a printout of the desired pump efficiencies, heat transfer coefficients, and other parameters calculated by the program for use in subsequent calculations. A sample of the output from this program is included in Table VII.

2. Steam Generator Performance

The steam generator part-load heat transfer performance characteristics were checked from 20 to 100% full load utilizing routine plant operating data.

The measured overall heat transfer coefficients for boiler and superheater are plotted vs percent full load in Figure 22. For comparison purposes, the design coefficients predicted by the steam generator manufacturer are also plotted. These design coefficients do not include any fouling factors and are, therefore, the clean coefficients.

As can be seen in Figure 22 initially both the boiler and superheater measured coefficients were considerably higher than the manufacturer's predicted clean values. The measured boiler coefficient was approximately 50% higher than the design value in the 20 to 50% full power range. For the superheater in this same power range, the measured coefficient was about 20% higher than predicted.

---

*J. J. Auleta Jr., "Piqua Main Heat Transfer System Component Analysis Program," NAA-SR-TDR 9475, January 28, 1964.

TABLE VII

MAIN HEAT TRANSFER SYSTEM ANALYSIS - PNPF

A. INPUT DATA	
Feedwater Temp (F)	272.0
Boiler Pressure (PSIG)	432.0
Power Plant Steam Flow (LB/HR)	130,000.0
Utility Steam Flow (LB/HR)	4700.0
Boiler Organic Inlet Temp (F)	567.0
Boiler Organic Outlet Temp (F)	474.0
Boiler Organic Flow (GPM)	5550.0
Superheated Steam Temp (F)	560.0
Superheated Steam Pres (PSIG)	430.0
Superheater Organic Inlet Temp	570.0
Total Organic Flow (GPM)	13,760.0
Organic Temp at Pump (F)	570.0
Reactor Inlet Temp (F)	525.0
Pump Suction Pressure (PSIG)	64.5
Pump Discharge Pressure (PSIG)	119.0
No. Of Pumps Operating	2.0
Static Pressure Difference (PSI)	0
Pump Motor Current (AMP)	34.7
Pump Motor Voltage (VOLTS)	4310.0
HB Content of Coolant (PCT)	10.0
Blowdown (LB/HR)	2400.0
B. HEAT TRANSFER OUTPUT SECTION	
Saturated Steam Temp (F)	455.5
Saturated Water Enthalpy (BTU/LB)	436.3
Saturated Steam Enthalpy (BTU/LB)	1204.6
Superheated Steam Enthalpy (BTU/LB)	1278.9
Boiler Heat Duty-Organic Side (MBTU/HR)	122,053.4
Boiler Heat Duty-Steam Side (MBTU/HR)	130,281.3
Average Boiler Heat Duty (MBTU/HR)	126,167.3
Boiler Heat Transfer Coefficient	240.6
Superheater Heat Duty (MBTU/HR)	10,014.1

TABLE VII (Continued)

B. HEAT TRANSFER OUTPUT SECTION	
Superheater Heat Transfer Coefficient	121.7
Boiler Pct Full Load	86.8
Superheater Pct Full Load	97.2
C. PUMP OUTPUT SECTION	
Corrected Pump Delta P (PSI)	57.5
Pump Hydraulic Horsepower	236.1
Pump Brake Horsepower (PCT)	74.1
Pump Efficiency (PCT)	79.6

The organic heat transfer film coefficient equation used by the steam generator manufacturer was compared with the present recommended heat transfer expression for organic coolants. The manufacturer computed the organic heat transfer film coefficient based on the following expression:

$$Nu = 0.015\ Re^{0.85}\ Pr^{0.3}$$

where

Nu = Nusselt number = $\frac{hD}{k}$

Re = Reynolds number = $\frac{DVe}{\mu}$

Pr = Prandtl number = $\frac{c\mu}{k}$

and

h = Organic-side heat transfer coefficient

D = diameter of fluid stream

V = velocity

ρ = density

c = specific heat at constant pressure

k = thermal conductivity

μ = viscosity

However, the presently recommended heat transfer expression is the Dittus-Boelter equation as follows:

$$Nu = 0.0243\ Re^{0.8}\ Pr^{0.4}$$

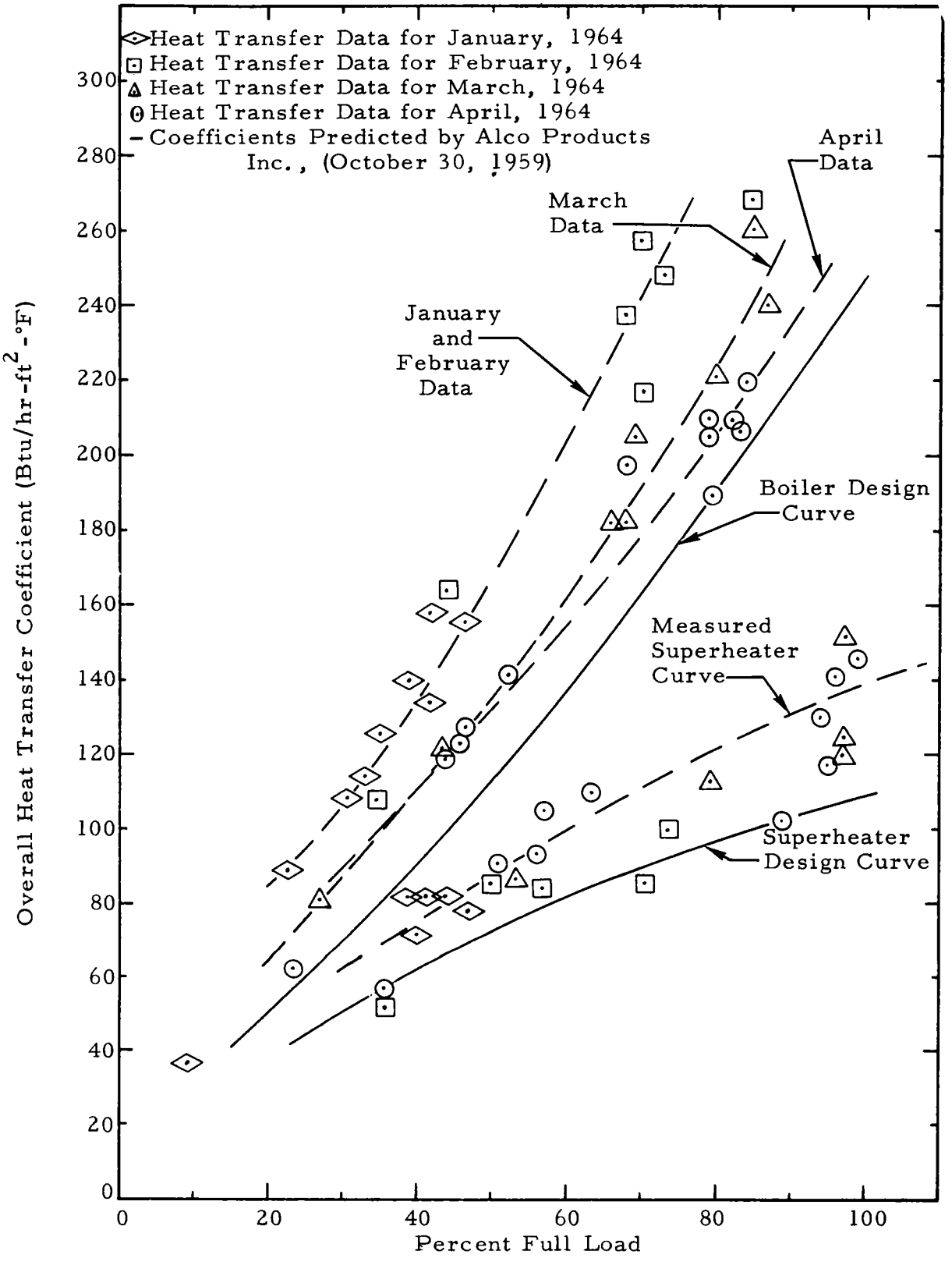

Figure 22. Steam Generator Heat Transfer Performance Characteristics

The present equation indicates an organic film coefficient approximately 28% higher than the film coefficient used by the manufacturer for design calculations. Also, the physical property values of the organic coolant, used by the steam generator manufacturer for sizing the equipment, were slightly different from the actual physical properties* of the Piqua coolant.

Because the actual value of the boiler heat transfer coefficient is higher than the design value, the design heat duty can be obtained at less than design flow through the boiler. The design flow rate at full power was specified at 12,000 gpm with coolant at 30% HB. An organic flow of ~5900 gpm through the boiler was found to be sufficient to obtain 100% full power with coolant containing 6-10% HB.

It has been estimated that with an HB content of 30% the boiler flow at full power would have to be 6300 gpm or 52.5% of the original design flow rate.

A gradual decrease in the measured boiler heat transfer coefficient was initially noted in the data reported for March and continued through the close of this report period. During this period there was no significant change in the superheater coefficient. This decrease is shown by the data in Figure 22. Several alternate methods of correlation were employed to determine if the change in coefficient was real, or due to a possible error in one or more of the instrument readings employed in the calculation. Regardless of the correlation employed, over the last several months there appears to have been a real decrease in the boiler coefficient with no associated change in the superheater coefficient. This decrease may be the result of fouling of the water side of the boiler tubes or errors in thermocouple readings. If the deviation is caused by fouling of the boiler tubes, it would be expected that the calculated overall heat transfer coefficient would show a decrease mostly at or near full load. This is the result of the excess heat transfer area available during part load operation, and the masking of the fouling resistance by the higher organic resistance at low organic flows.

The decrease in coefficient over this period corresponds to a fouling resistance of 0.0009 hr-ft^2-°F/Btu which, assuming all fouling to be on the water side, is equivalent to a scale film coefficient of approximately 1100

---

*K. Adler et. al "Organic Reactor Heat Transfer Manual," NAA-SR-MEMO 7343 December 1, 1962.

Btu/hr-ft^2-°F. The presence of a scale deposit has been verified by visual inspection of the water side of the boiler tubes during the plant shutdown. The condition of the organic side of the tubes was not determined.

The calculated scale coefficient of 1100 Btu/hr-ft^2-°F is slightly higher than values reported in the "Chemical Engineers' Handbook" (Fourth Edition, p 464) which shows a film coefficient of 500 - 1000 Btu/hr-ft^2-°F for treated boiler feedwater. However, the calculated resistance is essentially equal to the design steam side fouling resistance of 0.001 hr-ft^2-°F/Btu. Any tendency for the fouling resistance to increase will be closely monitored following return of the plant to power operation.

3. Main Coolant Pump Performance

The pump impellers in the main organic coolant pumps, P-1A and P-1B, were replaced with smaller diameter impellers during the first week of this report period. This was done to reduce the total flow rate in the main heat transfer loop and avoid possible damage to the superheater tubes from the higher than design flow rate*. Previously, an orifice had been installed in the main piping loop as a temporary measure to reduce flow. However, this method proved unsuccessful since piping vibrations resulted during subsequent plant operation at coolant flows above 9000 gpm.

The newly installed pump impellers are 15-1/4 inches in diameter; the impellers which were removed were 16-3/4 inches in diameter. On January 6, an informal test was conducted to obtain pump operating characteristic data with the smaller impellers. The two pumps were tested separately as well as in parallel operation.

Based on these test data, pump characteristic data points were computed for one and two pump operation. The pump characteristics are plotted in Figure 23, which shows the head-capacity and brake horsepower curves. A summary of the pertinent data and calculation results are presented in Tables VIII, IX, and X. Tables VIII and IX present the data and results for single pump operation with P-1A or P-1B, respectively. Information for two-pump operation is shown in Table X. It should be noted that there is no significant difference between operation with either P-1A or P-1B.

---

*PNPF Reactor Operations Analysis Monthly Report No. 15, November 1963

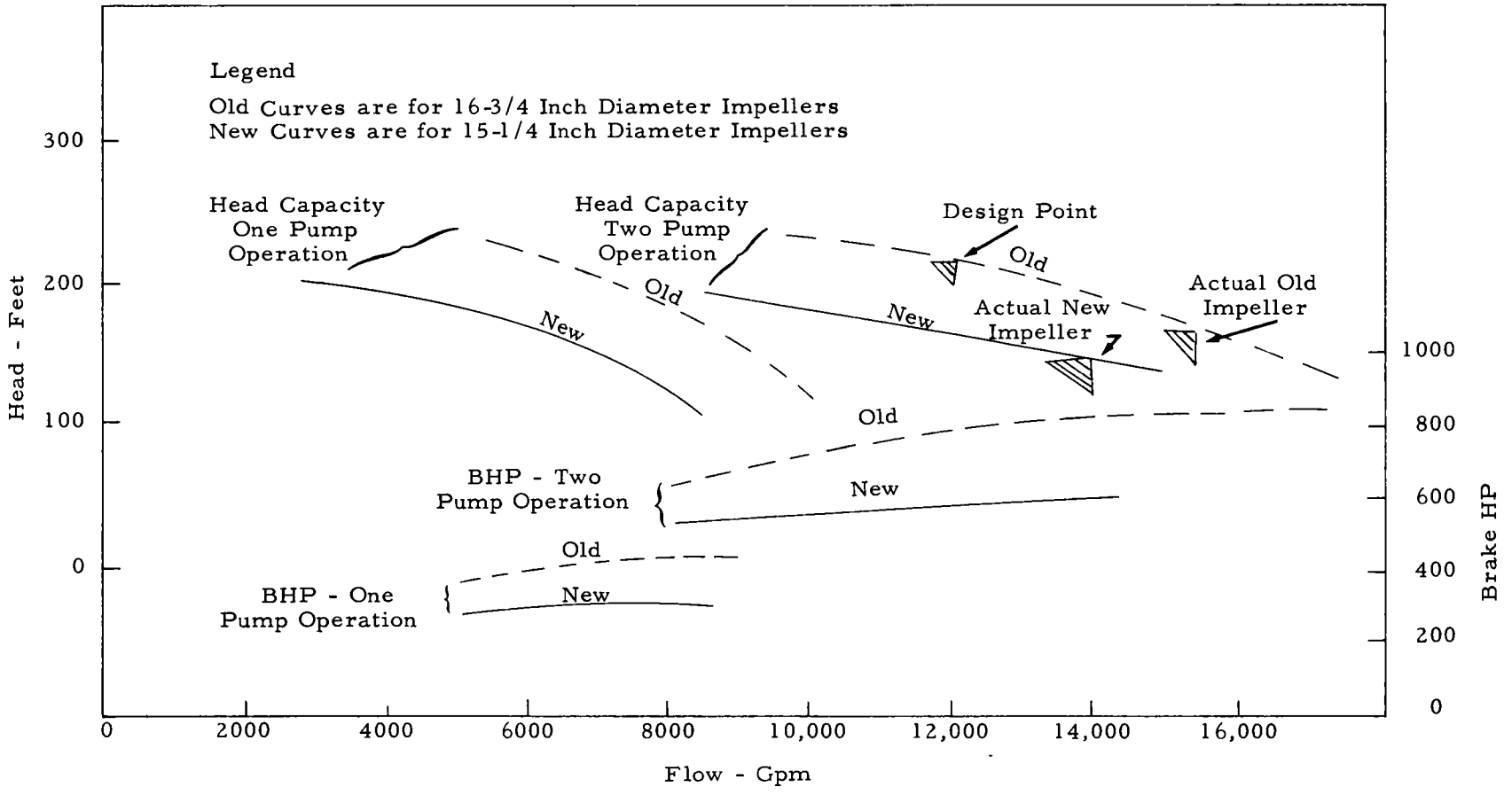

Figure 23. Effect of Impeller Replacement on Pump Performance Characteristic Curves

TABLE VIII

SINGLE PUMP OPERATION - P-1A

Parameter	Unit	Test Data					
Flow Rate	gpm	8240.0	7500.0	7000.0	6200.0	5600.0	5070.0
Disch. Press. Gage Rdg.	psig	126.0	138.0	146.0	155.0	158.0	161.0
Suction Press. Gage Rdg.	psig	84.0	88.0	89.0	91.0	92.0	93.0
Gage Correction-Elev.	psi	0.0	0.0	0.0	0.0	0.0	0.0
Line Loss-Suct. Gage to Suction	psi	4.0	3.3	3.0	2.4	2.1	1.9
Total Pump Head	psi	46.0	53.3	60.0	66.4	68.1	69.9
(S.G. = 0.9)	ft	118.0	137.0	154.0	170.0	175.0	179.0
Hydraulic Horsepower	hhp	221.0	233.0	245.0	240.0	223.0	206.0
Motor Current	amp	34.7	34.5	34.2	33.5	32.5	32.0
Motor Output*	kw	227.0	226.0	224.0	219.0	212.0	209.0
Brake Horsepower	bhp	304.0	303.0	300.0	294.0	284.0	280.0
Pump Efficiency - $\frac{hhp}{bhp}$	%	72.8	77.0	81.8	81.8	78.6	73.6

*Motor Voltage 2.52 Kv, Power Factor 0.89, Motor Efficiency 97%

TABLE IX

SINGLE PUMP OPERATION - P-1B

Parameter	Unit	Test Data						
Flow Rate	gpm	8490.0	7920.0	7400.0	6900.0	6240.0	5600.0	4960.0
Disch. Press. Gage Rdg.	psig	127.5	137.0	145.0	153.0	160.0	164.0	168.0
Suction Press. Gage Rdg.	psig	85.0	87.0	88.5	90.0	91.0	93.0	94.0
Gage Correction-Elev.	psi	4.0	4.0	4.0	4.0	4.0	4.0	4.0
Line Loss-Suct. Gage to Suction	psi	4.3	3.8	3.2	2.8	2.5	2.1	1.8
Total Pump Head	psi	42.8	49.8	55.7	61.8	67.5	69.1	71.8
(S.G. = 0.9)	ft	110.0	128.0	143.0	158.0	173.0	177.0	184.0
Hydraulic Horsepower	hhp	212.0	230.0	240.0	248.0	246.0	226.0	207.0
Motor Current	amp	35.2	35.5	35.0	34.5	34.0	33.0	32.5
Motor Output*	kw	230.0	232.0	229.0	226.0	222.0	216.0	213.0
Brake Horsepower	bhp	308.0	311.0	307.0	303.0	298.0	290.0	286.0
Pump Efficiency - $\frac{\text{hhp}}{\text{bhp}}$	%	69.0	74.0	78.1	81.8	82.6	78.0	72.5

*Motor Voltage 2.52 Kv, Power Factor 0.89, Motor Efficiency 97%

TABLE X

PUMPS P-1A AND P-1B IN PARALLEL OPERATION

Parameters	Unit	Test Data								
Total Flow Rate (Two Pumps)	gpm	5000.0	5960.0	7000.0	7950.0	8960.0	9920.0	10,900.0	12,300.0	14,240.0
Disch. Press. Gage Rdg. Avg.	psig	175.0	172.0	168.0	164.0	159.0	152.0	147.0	136.0	119.0
Suction Press. Gage Rdg. Avg.	psig	94.0	92.0	90.0	88.0	86.5	83.0	80.0	74.0	67.0
Gage Correction-Elev.	psi	0	0	0	0	0	0	0	0	0
Line Loss-Suct. Gage to Suction	psi	1.0	1.0	1.2	1.4	1.6	1.8	2.0	2.0	3.0
Total Pump Head	psi	82.0	81.0	79.2	77.4	74.1	70.8	69.0	64.0	55.0
(S. G. = 0.9)	ft	210.0	208.0	203.0	198.0	191.0	182.0	176.0	164.0	142.0
Total Hydraulic Horsepower (Two Pumps)	hhp	239.0	282.0	323.0	359.0	387.0	411.0	436.0	458.0	453.0
Motor Current Avg.	amp	28.7	29.8	30.5	31.3	31.5	32.3	32.6	34.2	34.5
Total Motor Output (Two Motors)*	kw	362.0	376.0	386.0	396.0	398.0	408.0	412.0	432.0	456.0
Total Brake Horsepower (Two Pumps)	bhp	486.0	504.0	518.0	532.0	534.0	548.0	552.0	580.0	610.0
Pump Efficiency- $\frac{hhp}{bhp}$	%	49.2	56.0	62.4	67.4	72.5	75.0	79.0	79.0	74.5

*Motor Voltage 2.5 Kv, Power Factor 0.89, Motor Efficiency 97%

Also plotted in Figure 23 for comparison purposes are the pump head-capacity curves for single and dual operation with the old 16-3/4-inch impellers. Changing the diameter of the impellers from 16-3/4 inches to 15-1/4 inches reduced the total pump head for the same flow rate by approximately 20 to 30%; this is in good agreement with the pump affinity laws relating to centrifugal pumps. These are theoretical laws or rules which apply to the change in pump performance as a result of a change in the speed of rotation or a change in impeller diameter. For a change in impeller diameter the affinity laws for constant speed are stated as follows:

$$\frac{Q_1}{Q_2} = \frac{D_1}{D_2} \quad ; \quad \frac{H_1}{H_2} = \left(\frac{D_1}{D_2}\right)^2 \quad ; \quad \frac{HP_1}{HP_2} = \left(\frac{D_1}{D_2}\right)^3$$

D = Impeller Diameter

Q = Flow Rate

HP = Pump Power

Based on these laws, trimming the impeller should have reduced the flow rate ~10% the total pump head ~17%, and the horsepower by ~25%. Later test data show that the pump capacity was reduced by ~9%, the head by ~12%, and horsepower by ~27%.

Heat transfer tests conducted on the steam generator, just prior to replacing the pump impellers, resulted in a readjustment of the boiler butterfly control valve which is used for varying the flow rate through the boiler during load-following operation. This valve adjustment reduced the frictional flow resistance in the main coolant system. Therefore, although the flow rate in the main loop was reduced due to the installation of the smaller impellers, this flow reduction was not as great as anticipated.

Following the modifications and testing of the pumps the system was operated (generally) at flow rates of 13,000 - 14,000 gpm, with the two pumps operating in parallel. The pump head, hydraulic horsepower, brake horsepower and efficiency were calculated utilizing the main heat transfer system analysis computer program. No significant deviation is observed between current and test results. This, plus the internal consistency of the current data, is indicative of satisfactory pump performance.

4. Main Coolant Pump Coastdown Test

Pump coastdown data, taken on April 6, 1964 following interruption of power to the main coolant pumps, were analyzed and compared with data presented in the PNPF Safeguards Report* and the PNPF transient study.† The fraction of full initial main loop flow is plotted vs time after pump shutoff in Figure 24. The total core flow however is the main loop flow plus the flow from the pressurizing pumps, P-3A and P-3B, which deliver a constant flow of 500 gpm through the pressurization loop following a scram. Since the original data reflected only the main loop flow, these data were corrected by adding on the fraction of total core flow due to the pressurization system. The corrected curve is also shown in Figure 24, along with the predicted flow decay curve. Very good agreement between predicted and measured data is observed for the first five seconds after loss of pump power. After this length of time, however, the predicted flow is higher than the measured flow. This deviation may be due in part to an inherent inaccuracy of the main loop flow meter in the low flow (less than 20% of full flow) region.

The major concern, following loss of pump power, is the possibility of the fuel surface temperatures rising to unacceptable levels due to low coolant flow. This problem was investigated; reactor power (the summation of decay heat power and neutron kinetics) and fuel element heat transfer coefficient, both normalized to the initial value at the time of loss of pump power, are plotted in Figure 24. Reactor power continues at approximately the initial value, for slightly over one second following loss of pump power before the reactor is scrammed by the power-flow comparator, after which it decays rapidly. Due to the time lag between initiation of flow decay and power decay, the fuel element hot spot temperature is expected to peak within one second following the scram, and then begin to decrease because the normalized core flow and heat transfer coefficient is greater than that required to remove the heat generated.

Following the initial temperature peak a second temperature peak could occur as the flow decays. However, as seen in Figure 24, up to 20 seconds

---

*"Final Safeguards Summary Report for the Piqua Nuclear Power Facility," NAA-SR-5608, August 1, 1961.

†R. E. George and W. W. Scott, "Piqua OMR Uncontrolled Core Transient and Frequency Response," NAA-SR-TDR 5521, April 27, 1960.

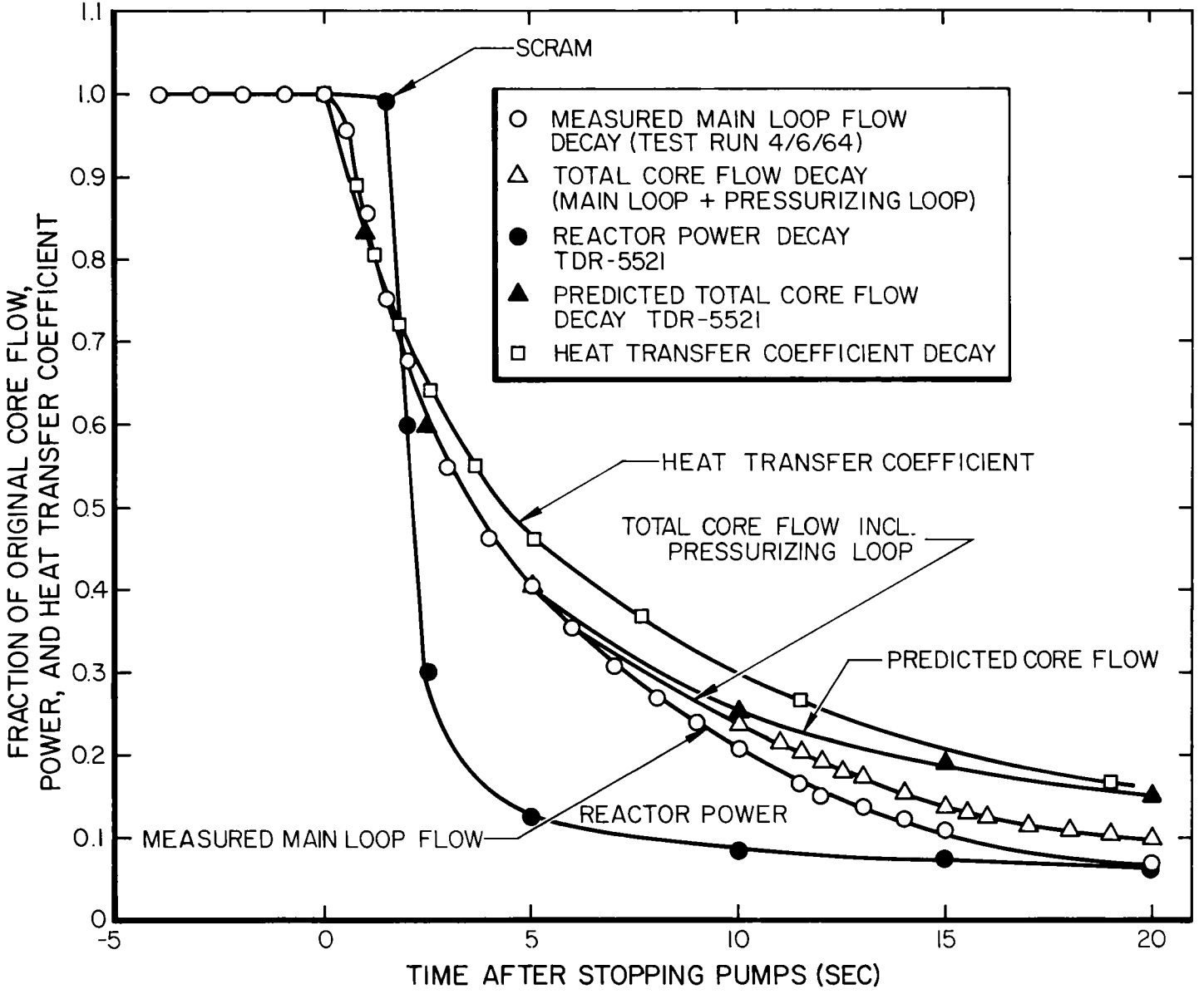

Figure 24. PNPF Transient Response Following Loss of Main Pump Power

after loss of power, there should be no second temperature peak, because the power decreases more rapidly than the heat transfer coefficient and total core flow.

B. FLOW RATE AND PRESSURE DROP FOR MAIN HEAT TRANSFER SYSTEM AND DEGASIFICATION SYSTEM

1. Introduction

To aid in maintaining coolant purity, two sets of glass spool filters are included in the reactor coolant system. One set of filters, 25μ pore size, is located within the reactor vessel with one filter above each fuel element position, with the exception of the three instrumented elements. A second set of filters, F-2A and F-2B containing 1μ and 3μ glass spools, respectively, is located in the degasification system supply line. The units located within the reactor vessel filter the full core flow before the coolant enters the fuel elements, and the degasification filters process a side stream of coolant at a lower flow rate, but finer porosity filtration.

2. Analysis

A plot of the daily flow rate and filter pressure drops for both the full flow and degasification system filters was maintained for the period of power operation from mid-January to mid-May. The pressure drop across both sets of filters increased gradually, but steadily with operating time, indicating the gradual deposition of material on the filters. At a total flow rate of approximately 14,000 gpm, the pressure drop across the full-flow filters increased from approximately 5 psi on January 15 to a high of 10 psi prior to plant shutdown. Over a similar period of time the degasification filter pressure drop, though more erratic in day-to-day readings, showed a general increase from approximately 6 to 10-11 psi at a constant flow rate of 320 gpm. The flow ΔP data are summarized in Figure 25.

C. PRESSURIZING PUMP PERFORMANCE

A description of the pressurizing pumps and the results of the pump test program has been reported previously*. Throughout this report period, operating data were processed to check the performance of the pumps by comparing

*Piqua Nuclear Power Facility, Operations Analysis Program Progress Report No. 3, July 1, 1963 - December 31, 1963.

measured head and efficiency with values obtained from manufacturer's data. The manufacturer's performance curves are shown in Figure 26. A sample of the pertinent performance data and calculated pump efficiencies is tabulated in Table XI. Also presented are the expected performance parameters from the test data.

The calculated pump efficiencies are in excellent agreement with the values obtained from the manufacturer's data (38-39% calculated vs 39% expected), as well as with previous data, indicating satisfactory pump performance.

D. COOLANT DISTILLATION SYSTEM PERFORMANCE

During the first two weeks of January, the HB content of the main loop coolant was maintained at approximately 3-4%. Beginning about January 16, the HB content slowly increased to approximately 10% by the end of the month. Figure 27 presents the HB content vs time. Review of operating data for the purification system indicated that starting approximately January 14, considerable quantities of material from the HB decay tanks were being processed through the purification system to recover the terphenyls present in this waste material. As a result of this procedure, a smaller quantity of main loop coolant was processed, thus resulting in an increase in the HB concentration. During this same time, the terphenyl content of the bottoms stream from the column was approximately 20-25%, rather than the design value of 2-3%.

Review of column performance data indicated that the high terphenyl content (20-25%) in the bottoms stream was due to poor vapor-liquid contact in the packed section of the column, and/or insufficient reboil heat due to excessive heat loss. Plant operations personnel subsequently determined that the liquid level in the bottom of the column was above the vapor return line from the reboiler. As a result, the majority of the vapor returning to the column from the reboiler was condensed in the liquid layer rather than passing up the column as stripping vapor. The liquid level was subsequently lowered to a position below the reboiler return line. Following this change, the composition of the bottoms stream increased to 97-98% HB and the bottoms temperature increased to 650°F at a feed rate of approximately 500 lb/hr. These data indicate

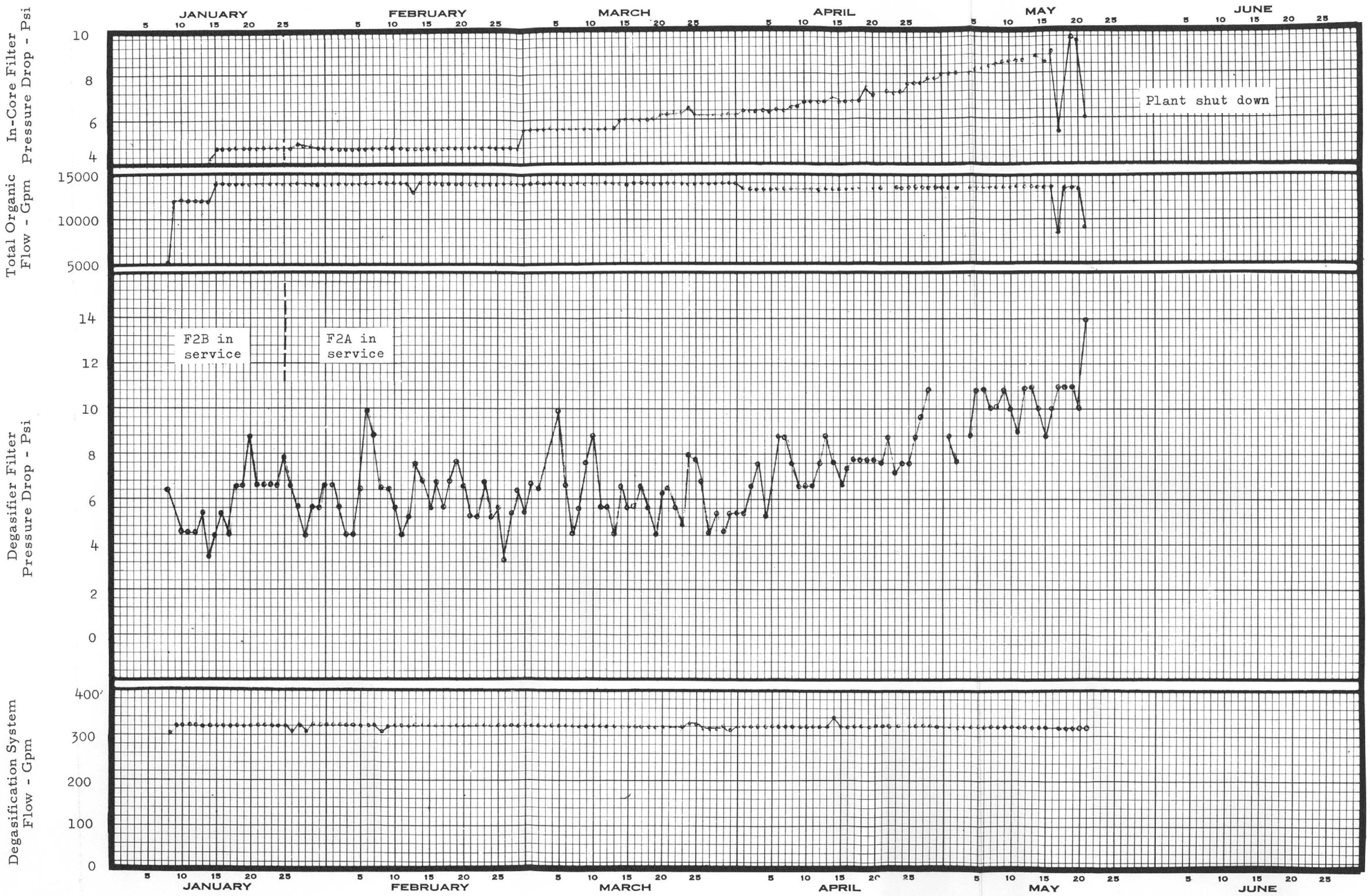

Figure 25. Flow and Pressure Drop for MHTS and Degasifier System

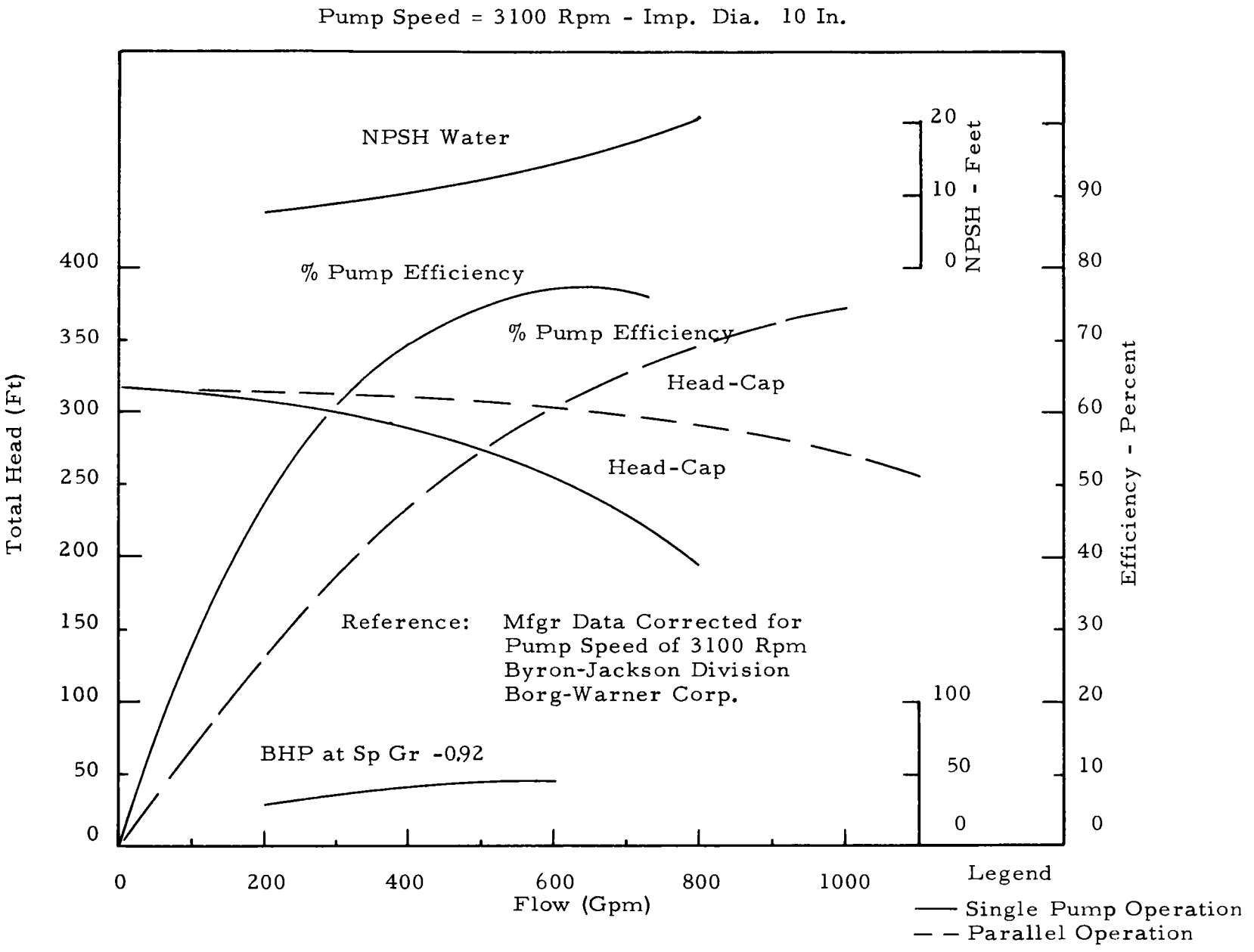

Figure 26. Performance Curves - Pressurizing Pumps P-3A and P-3B

TABLE XI

SUMMARY OF PRESSURIZING PUMP PERFORMANCE DATA

(P-3A and P-3B Operating in Parallel)

Date	1-10-64	1-17-64	1-26-64	1-30-64	4-2-64	4-4-64	4-10-64	4-22-64	5-9-64	5-13-64	5-15-64
Total Flow Rate (gpm)	320.0	320.0	315.0	320.0	320.0	320.0	320.0	320.0	320.0	320.0	320.0
Pump Total Head (ft)	290.0	296.0	300.0	297.0	297.0	295.0	301.0	298.0	294.0	300.0	300.0
Pump Total ΔP (psi)	112.7	115.7	116.6	115.3	115.9	114.9	117.4	115.9	113.2	115.7	115.7
Hydraulic HP per Pump (hp)	10.6	10.8	10.7	10.7	10.8	10.7	10.9	10.8	10.6	10.8	10.8
Average Motor Current (amp)	100.0	102.0	97.0	97.0	96.5	96.0	99.0	98.0	93.5	94.0	96.0
Average Motor Voltage (volt)	247.0	250.0	252.0	250.0	249.0	250.0	249.5	249.5	251.5	248.0	249.0
Brake Horsepower (hp)	28.5	29.4	28.1	27.9	27.8	27.7	28.5	28.2	26.8	26.6	27.6
Calculated Pump Efficiency (%)	37.2	36.9	38.0	38.4	38.9	38.7	38.3	38.3	39.4	40.0	39.2
Predicted Efficiency (Mfgr Data)	39.0	39.0	39.0	39.0	39.0	39.0	39.0	39.0	39.0	39.0	39.0
Predicted Total Head (ft) (Mfgr Data)	310.0	310.0	310.0	310.0	310.0	310.0	310.0	310.0	310.0	310.0	310.0

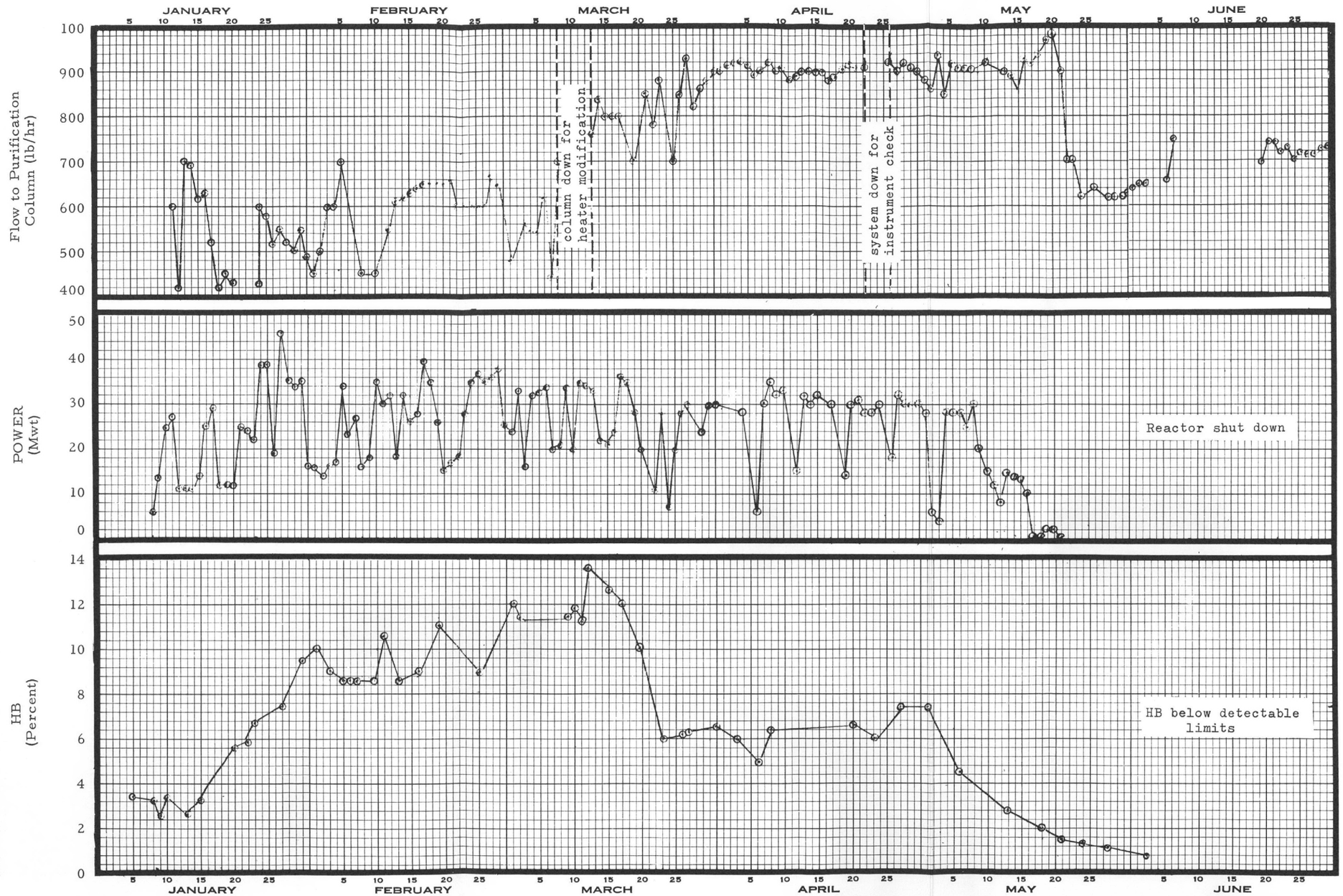

Figure 27. Relation of PNPF HB Content, Distillation Column Feed Rate, and Thermal Power

satisfactory performance of the column at this feed rate. Further testing by plant operating personnel indicated that additional reboil heat was required to enable the column to operate at the desired flow rate of 1000 lb/hr.

From March 9 to 12 the purification column, C-2, was shutdown for modification of the power supply to the reboil heater, H-4. Auto transformers were installed to increase the allowable heater voltage from 480 V to 600 V and the operating power from 8 kw to approximately 13 kw. During this period the HB content of the coolant increased from approximately 10% to 13.5%. When the column was returned to service on March 13, the maximum total feed rate (irradiated plus makeup coolant) was increased to approximately 960 lb/hr with the column bottoms temperature maintained at 720°F. The effect of the higher purification rate, although somewhat masked by two days of low power operation on March 22 and 24, can be seen in Figure 27. During the period of March 13 through 23, with the flow of irradiated coolant material between 700 and 850 lb/hr, the coolant HB content was steadily reduced from a maximum of 13.5% to approximately 6%, where it was maintained until about two weeks prior to the reactor shutdown on May 21. This HB content was in good agreement with previous calculations which indicated that at 75% power (34 Mwt) a purification rate of 1000 lb/hr would result in a steady-state HB content of 6.5%. Due to the decreased power operation for several days prior to plant shutdown, the HB content was reduced to 3.1% on May 18. Following the reactor shutdown, the distillation system was employed to further reduce the coolant HB content prior to removing the reactor cover and potentially exposing the coolant to the atmosphere. Previous experience has shown the HB fraction of the coolant to be more reactive with air than the terphenyl fraction, possibly due to the high concentration of free radicals and olefins. Coolant from the main loop and reactor vessel continues to be processed through the column during a major part of the shutdown period, and the HB content has been reduced to below detectable levels.

E. HIGH BOILER BURNING

Operation of the waste-fired boiler (B-2) for the disposal of high boilers was initiated on February 17. Initial attempts to bring the unit on-stream were unsuccessful due to poor control of the HB flowrate and pressure at the burner. Following slight modifications to the HB piping system, the unit was successfully

operated on HB on February 26 and 27 when it was again shutdown and restarted for purposes of operator training. During this period the HB burning rates were varied from 60 to 100 lb/hr as determined by the decrease in level in the HB decay tank, T-9. The total HB burned during this period was ~1935 lb. Steam production rates varied from ~500 lb/hr to a maximum of 1400 lb/hr.

The exhaust gas filtration system was checked by monitoring gas samples taken from before and after each filter. System performance was excellent as evidenced by the extremely low activity in the gas stream leaving the absolute filter and entering the base of the plant stack. The activity data are summarized in Table XII.

TABLE XII

WASTE-FIRED BOILER EFFLUENT ACTIVITY

	Particulate Activity (μc/cc Mixed Beta-Gamma) Sample Location			
Date	Boiler Discharge	After Cooling Air Addition	After First Dust Collector	After Absolute Filter (Before dilution in stack)
2-25-64	-	-	1×10^{-9}	Background
			2.9×10^{-9}	Background
2-26-64	-	-	5.3×10^{-10}	Background
2-27-64	9.9×10^{-9}	4.4×10^{-9}	1.2×10^{-10}	4×10^{-11}

During subsequent operation of the unit, difficulties were experienced with a high pressure drop across the flue gas dust collector (F-6) and with considerable quantities of unburned carbon being thrown from the flame. The latter problem was alleviated by increasing the pressure of the atomizing steam supplied to the burner. This resulted in improved atomization of the fuel and more complete combustion.

It was determined that the high pressure drop across F-6 was being caused by higher than design air flow through the system, combined with heavy dust loading during system startup. If the pressure drop built up to greater than approximately 8 in. of H_2O, the collector could not be cleaned. The manufacturer recommended that air flow through the unit be reduced to decrease the

ΔP across the filter media and thus enable the cleaning mechanism to operate against a lower back-pressure.

The original system design employed Dacron filter bags in the collector, which limited the operating temperature of the unit to 250°F. To insure this temperature was not exceeded, a dilution air inlet had been provided upstream of the collector to supply room air for cooling the gas entering the collector. As the original dust collector bags had been replaced with high temperature (425°F) bags, the cooling air was no longer required and the dilution air inlet was blocked off to decrease the air flow through the unit. This reduction in air flow resulted in a ΔP decrease of approximately 5 in. H_2O and enabled the cleaning mechanism to function properly and maintain a low (3-4 in. H_2O) ΔP across the collector. Following this modification, combined with the use of increased atomizing steam pressure, successful operation of B-2 was resumed. Operation was interrupted periodically by pulsations in the firebox pressure resulting in flame-out of the unit and subsequent safety circuit shutdown. The pressure fluctuations have apparently been eliminated by the combustion of a small quantity of propane along with the HB. This method of operation is providing the required stability to the HB flame. At the end of this report period, the unit was on stream at an HB burning rate of approximately 100 lb/hr.

F. FAILED ELEMENT LOCATION SYSTEM

1. Introduction

A failed element location system (FELS) was provided to aid in determining the presence of a failed fuel element in the core, by monitoring the delayed neutron activity of the coolant at the exit of each fuel channel and of the mixed coolant. The position of a failed fuel element may be determined by selectively sampling the outlet coolant from each fuel element.

2. Analysis

Data from three FEL system surveys were reviewed and all count rate data were normalized to full power and a standard sampling flow rate of 10 gpm, and corrected for the number of BF_3 detector tubes in operation. These data are presented in Table XIII for the two mixed mean channels and for the five fuel channels which have repeatedly shown the highest activity. These data indicate very little change in the delayed neutron activity over the three months

TABLE XIII

FAILED ELEMENT LOCATION SYSTEM SURVEY

Activity (cpm)*

Location	Date	2-2-64	4-12-64	5-9-64
Mixed Mean Outlet				
MM-1		1,370	1,200	1,240
MM-2		1,390	1,235	1,142
Fuel Channels with Maximum Activity				
C-12		12,000	11,200	12,200
D-7		6,300	5,550	4,300
B-7		4,600	4,820	4,740
D-13		3,500	3,250	4,180
D-11		4,650	3,400	4,460

*Normalized to full power, sample flow of 10 gpm, and 12 detector tubes in operation

for which data were analyzed. Although the exact source of the delayed neutrons is not specifically known (possibly uranium contamination of the aluminum cladding or cladding imperfections), these data indicate that the source is not varying significantly with operating time.

3. Computer Program

A Fortran computer program was written and checked out to normalize the neutron count rate data obtained from FELS. The reported data are routinely normalized to a sampling flow rate of 10 gpm, a reactor power of 45.5 Mwt and all 12 BF_3 detector tubes operating. A further modification, to include the relative power of each element in the normalization calculation is in progress.

G. CORE COVER GAS SYSTEM

Due to the importance of preventing contact of the organic coolant with air, an inert gas atmosphere must be maintained in the space between the upper shield plate and the organic liquid level during open reactor vessel fuel handling and maintenance operations. By purging this space with nitrogen, the

possibility of diffusion of air through openings created by the removal of shield plugs is minimized. In order to purge this volume of the reactor vessel it is necessary to provide a source of N_2 under the upper shield plate. It is also necessary to utilize an existing gas line within the vessel since it is impossible to bring a gas line into the reactor from an external source with the rotating shield in place for fuel handling. This has been accomplished by connecting the existing 2 in. drain line, into which nitrogen can be introduced to a modified shield plug in a manner similar to that shown in Figure 28. Calculations to determine the required purge gas flow rate were made on the basis of preventing diffusion and thermal convection of air across the upper shield plate through an open fuel channel. The recommended flow rate was approximately 10 scfm per shield plug removed, with additional flow possibly required, depending on the amount of leakage between the shield plate and support ring.

Following removal of the reactor head, the purge gas system was placed in operation at various gas flow rates, and gas samples removed from the space between the coolant and upper shield plate, as tabulated below.

Gas Flow Rate (Scfm)	O_2 Concentration (Volume %)
4.8	5.0
5.8	1.4

These flow oxygen-concentration data show reasonable agreement with the calculated flow rate necessary to purge the reactor vessel vapor space.

H. RADIATION LEVELS

1. Plant Radiation Levels

At all power levels, radiation levels at the surface of the 20-in. primary coolant lines proved to be very low. The maximum radiation observed was (at the surface of these unshielded pipes) 15 to 20 mr/hr at full power (Figure 29). A very low neutron level was detected at the 14-in. outlet coolant lines at the point of emergence from the biological shield. Gamma radiation which penetrated the biological shield was less than 1 mr/hr. A net reading of 0.3 mr/hr

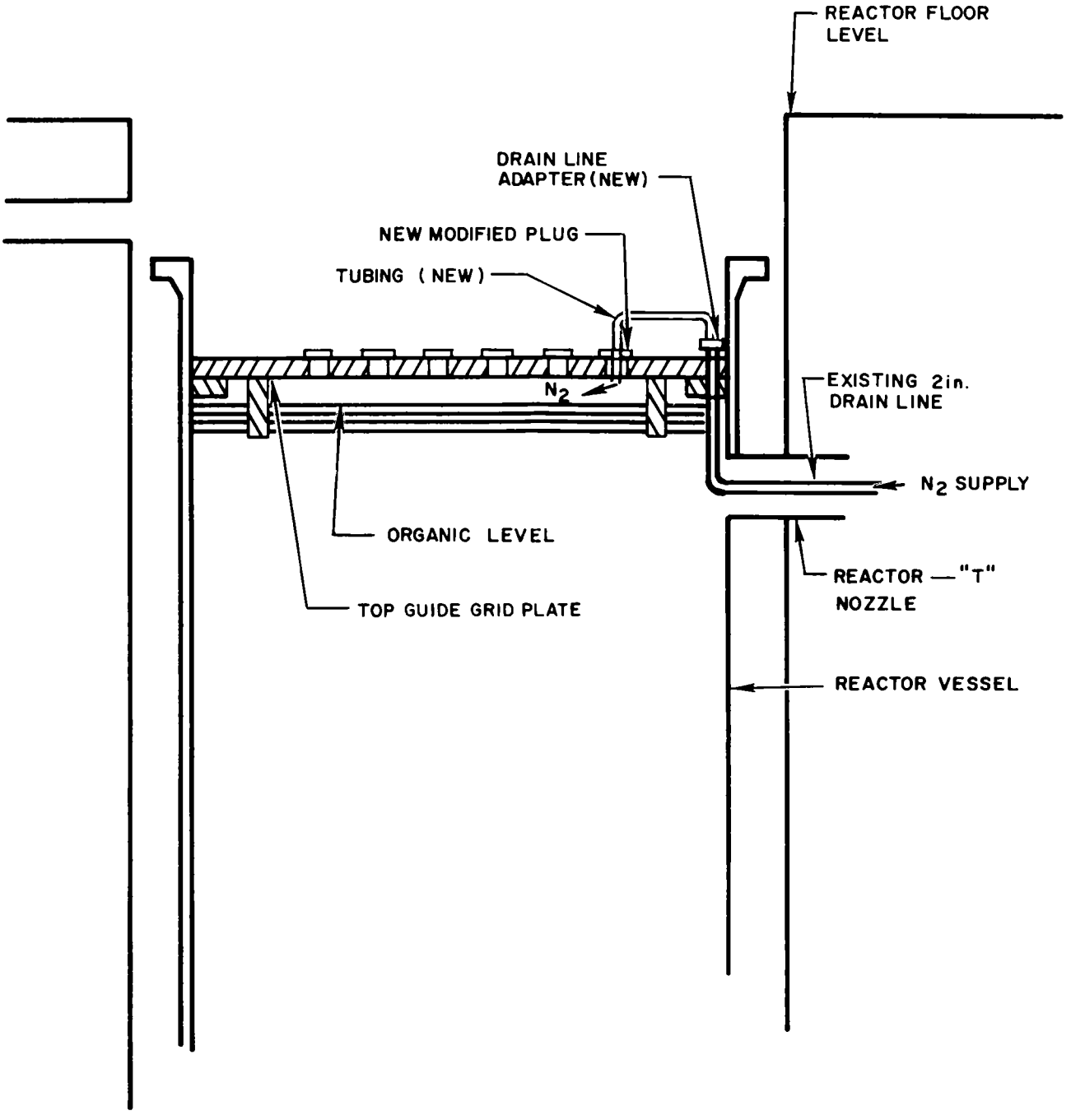

Figure 28. Core Cover Gas Piping Inside Reactor

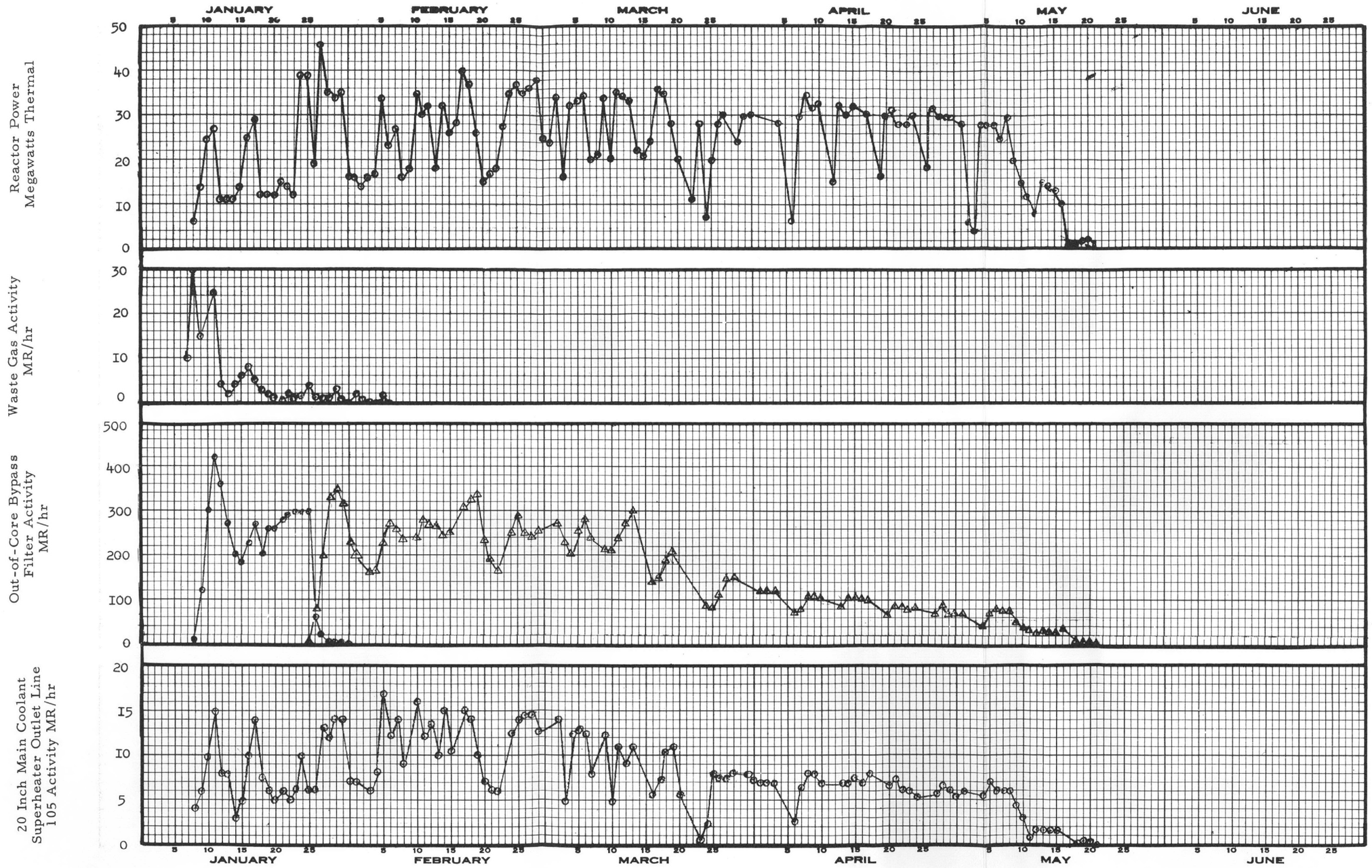

Figure 29. PNPF Radiation Levels

was obtained above the reactor plenum on the 100 ft level in the Reactor Building. No neutrons were detected from the biological shield or above the reactor at the 100 ft level.

Effluent gases and liquids have remained well below the maximum permissible limits.

Radiation levels throughout the plant have remained sufficiently low to permit operator access for contact maintenance activities on the primary coolant system during operation, without imposing time limitations (the only exception was the degasifier filter which has served as a collection point for radioactive impurities). Work in this area has not resulted in an exposure to any one person above 50 mrem per month.

Table XIV gives the results of a typical radiation survey taken at full power.

The radiation levels from the coolant lines and filters result from the activation of impurities and corrosion products in the coolant and from recoil products from the core. The gamma-emitting isotopes having about a 10-min. half-life are responsible for the majority of the radiation from the coolant lines. These isotopes are Mg^{27} and N^{13}. The Mg^{27} is a recoil product from the aluminum clad fuel elements and the N^{13} is an impurity in the coolant resulting from the nitrogen cover gas in the surge tank. The Na^{24} contribution to radiation levels of the primary coolant system has remained low as a result of continued operation of the degasifier filter. The recoil product, Na^{24}, activity is gradually being reduced with continued reactor operation. The highest radiation levels in the plant are measured at this filter.

At full power operation, the radiation level relative to reactor power was about 0.4 mr/hr per megawatt from the unshielded 20 in. primary coolant line.

Airborne activity in the containment building has not exceeded that normally observed from natural background. During the performance of coolant sampling, gas samples were taken which indicate that any gas activity which may have been released was below the maximum permissible concentration.

No detectable contamination of personnel has resulted from maintenance or operation of the reactor systems.

TABLE XIV

RADIATION SURVEY

Power 45.5 Mwt

Mr/hr at 4 inches from lines and filters

	Location	Radiation Level (Mr/hr)
1.	Reactor 100-ft. level	Bkgd, except 0.3 mr/hr > bkgd over reactor plenum. No neutrons.
2.	FELS Tank	0.1
3.	East Reactor Biological Shield at the 78-ft. level	0.6 above bkgd. No neutrons.
4.	6A-201-OC line from Degasifier Tank (T-15)	6.5
5.	6A-210-OC line to the Degasifier Tank (T-15)	7.5
6.	F-2A Degasifier Filter	250*
7.	F-2B Degasifier Filter (off line)	17
8.	East Reactor Shield at the 72-ft. level	3 including ~2.5 bkgd. No neutrons.
9.	FELS Valve at the 92-ft. level	2
10.	SH-1 at the 82-ft. level	12
11.	OC-104, 14-inch line in the P-1B Room	13.5 < 0.5 mrem/hr neutrons.
12.	OC-101, 14-inch line in the P-1A Room	< 0.5 mrem/hr neutrons. 11
13.	P-3B Pressurizing Pump line	2
14.	P-3A Pressurizing Pump line	2
15.	Surge Tank (T-2)	0.1
16.	Drain Tank (T-1)	0.2
17.	OC-106, 20-inch coolant line at the 82-ft. level	14
18.	OC-105, 20-inch coolant line at the 76-ft. level	18

*Degasifier filter activity has decreased continuously from this value to about 100 mr/hr or less during the week before shutdown. This reduction is attributed to the reduction of recoil product Na^{24} release into the main coolant stream due to a slight buildup of film on the aluminum cladding surface of the fuel element (< 0.01 mils would account for the observed decrease).

2. Waste Gas

During the report period, the waste gas flow rate from the degasifier system was reduced considerably. The maximum activity observed prior to the gas entering the waste gas hold-up tanks was 2×10^{-2} μc/cc. The maximum concentration leaving the hold-up tanks prior to entering the stack was 1.1×10^{-3} μc/cc. After dilution with heating and ventilating discharge air, the maximum activity was 4×10^{-9} μc/cc. The activity of the waste gas from the degasifier is 10% A^{41}, 28% Xe^{135}, 18% Kr^{88}, 11.5% Kr^{85}, and 0.5% Xe^{133}.

3. Aqueous Waste

The maximum beta-gamma concentration detected in the aqueous waste hold-up tanks for this report was 3.5×10^{-6} μc/cc. Arsenic-76 has been identified in small volumes of waste from the waste gas handling system which enter the aqueous waste disposal system. Liquids condensed in the waste gas system are the primary source of activity in the aqueous waste. The beta-gamma activity in the effluent to the river is calculated to be below MPC by a factor of 10.

4. Solid Waste

The solid wastes are packaged and shipped off-site for burial. This waste has consisted primarily of paper, filter material, and unusable organic material.

I. COOLANT DECOMPOSITION RATE

Coolant inventory and material balance data were routinely analyzed to determine approximate values of the terphenyl decomposition rate. The decomposition rates were calculated by a procedure similar to that presented in the October 1963 PNPF OAP Report. The values of the decomposition rates are approximate values due to inaccuracies in reading of tank levels and lack of analysis of material held in the two organic drain tanks. Since, during the period of time over which the material balances are made, the volume of material in the drain tanks changes by only a small amount, its composition is assumed to remain constant over the period without introducing any significant error.

During the period of February 27 through March 18, the plant was operated with the HB content of the main loop coolant varying between approximately 10% and 13%. This period was broken down into four sub-intervals for which material balance, coolant compostion, and exposure data were available. Following the purification system modification, HB concentration was reduced to 5-6%.

The measured decomposition rates, as well as the rate predicted based on experimental neutron and gamma absorption data are summarized in Table XV. The measured decomposition rates average 1.97 and 2.19 lb/Mwht for the 10% and 6% HB systems, respectively. These results are in excellent agreement with the predicted values of 1.92 and 2.10 lb/Mwht for the corresponding HB levels.

TABLE XV

COOLANT DECOMPOSITION RATES

Time Period	HB Content of Main Loop Coolant		HB Formed (lb)	Exposure (Mwht)	Measured Decomposition Rate (lb/Mwht)	Predicted Decomposition Rate (lb/Mwht)
	Start	Finish				
Feb. 27-March 1	10.0%	11.9%	4,412	2,383	1.85	1.92 at 10%
March 1-March 9	11.9%	10.2%	10,167	5,112	1.98	
March 3-March 9	11.4%	10.2%	7,956	3,700	2.15	
March 15-March 18	12.8%	9.4%	3,080	1,615	1.92	
April 2-April 6	5.7%	5.5%	5,560	2,611.9	2.13	2.10 at 6%
April 2-April 16	5.7%	5.6%	19,000	9,000.0	2.11	
April 16-April 23	5.6%	5.9%	10,190	4,360.0	2.33	
April 2-April 23	5.7%	5.9%	29,200	13,350.0	2.19	
April 2-April 27	5.7%	7.6%	34,650	15,700.0	2.20	

V COOLANT CHEMISTRY AND ANALYSIS

A. COOLANT QUALITY REVIEW

The Operations Analysis Project has recommended a program of coolant quality control which is being implemented at the PNPF. In addition to day-to-day surveillance and evaluation of coolant data, this project has provided laboratory support both for routine analyses (e.g. water, carbonyl content, flash point, and coolant composition of major components) as well as assistance with special investigations that have been required from time to time. The routine analyses performed on a day-by-day basis on-site include ash, membrane stain test (MST), iron, coolant radiochemistry by pulse height analyses (PHA), and on a less frequent basis, high boiler content. A summary of the ash, MST and HB data, and average daily power production, for the operating period ending May 21, 1964 is shown in Figure 30. The iron analyses performed are not shown over most of the operating period; the iron values were less than 1.0 ppm, usually less than 0.5 ppm. Some increases in iron values to 2.0 ppm maximum were observed after the shutdown in May, concurrent with increases in ash and MST values which occurred at that time. Ash values over most of the operating period were < 5.0 ppm with few exceptions. Regarding the MST results, in January and February, fairly large fluctuations in day-to-day MST results were observed. It was also observed that there were fairly large deviations within individual sets of analyses of the same coolant sample. After investigation of this problem some suggested improvements were made regarding the laboratory equipment and procedures used, and the reproducibility of the test was noticeably improved. Despite the limitations of the MST data obtained during January and February, an increasing trend was observed, concurrent with increases in high boiler and daily average power levels. The difficulty in correlating these three variables is illustrated by the analytical data obtained in April and early May (Figure 30) during which time very noticeable, and occasionally sudden, increases in MST were observed even though the HB levels were about 5% lower than during the previous two months, and the ash values were showing normal fluctuations. It was at this time also that black particles* were observed in the

*Coke-like particles first noted on April 4 in the bottom zone of solidified beaker coolant samples. The particles were separated from hot coolant by decantation and by dissolution of coolant in benzene or tetrohydrofuran, followed by filtration. The particles displayed little or no magnetic properties.

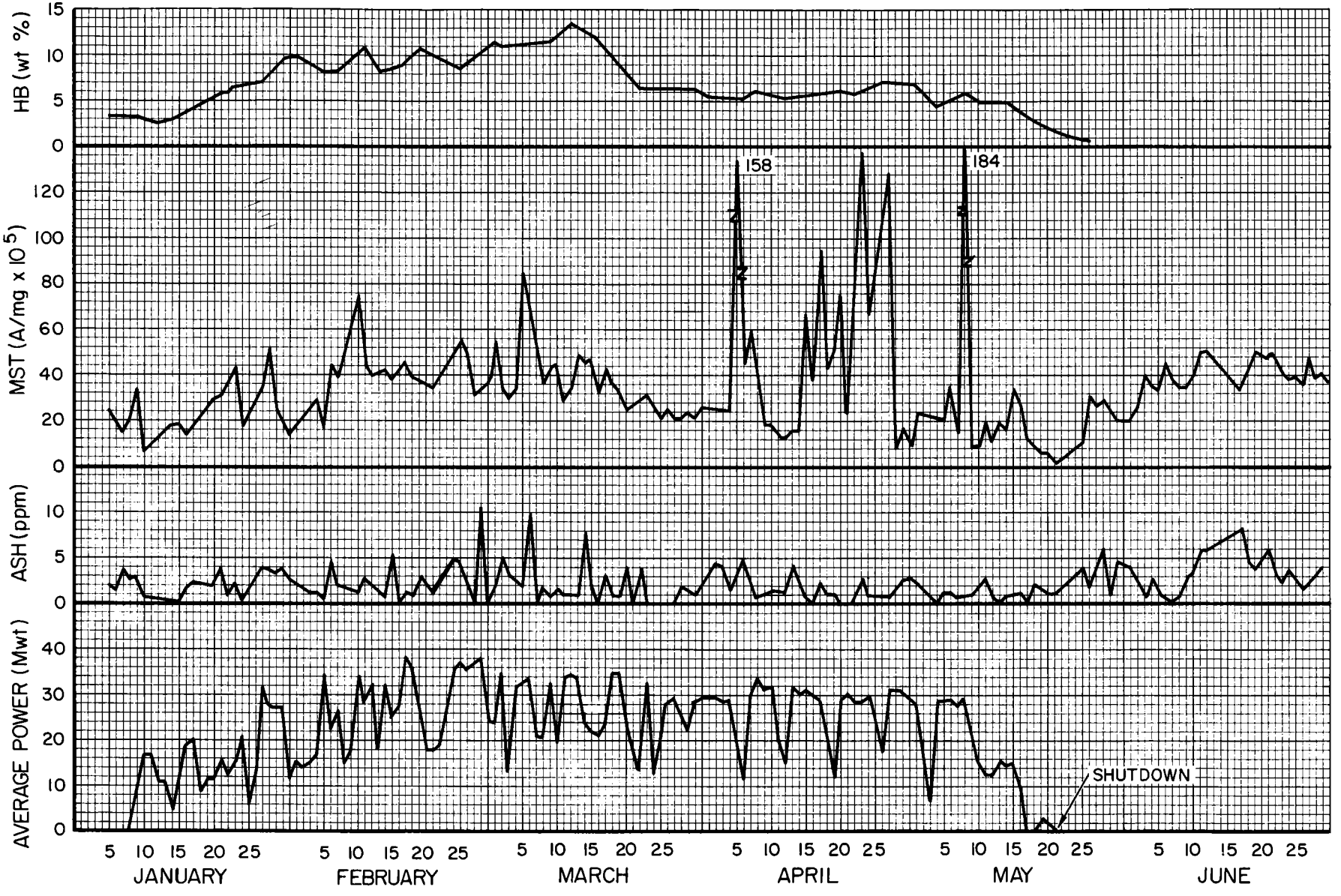

Figure 30. PNPF Coolant Analysis History

coolant samples. The presence of these particles in coolant samples taken at sample station No. 1 was established by visual observation at the site and was also observed in samples examined in A.I.'s Canoga Park laboratory. The origin of these particles has still not been definitely established, although one possible source which has been considered is the coking of the coolant by a welding operation on the sample line during modification of the coupon test station. A sample taken April 17 was found to contain 103 ppm of the black particles. The only radioisotope detected was Co^{58}. This isotope and Co^{60} are the only ones of any significance generally found in the circulating coolant after the short-lived radionuclides have decayed. By contrast, particles separated from the in-core glass filters more than a month after the May 21 shutdown have been found to contain Mn^{54}, Co^{58}, Co^{60}, Fe^{59}, Zn^{65} and Cr^{51}. There is reason to believe, therefore, that the black particles which resulted in the high MST values observed, did not originate from a release of particles or foreign material from inside the reactor vessel.

Analysis of the black particles by X-ray diffraction indicated an amorphous structure. Analysis by X-ray fluorescence indicated Fe and Hg to be the major elements, with lesser amounts of Zn, Cu, Ni, and possibly Cr. It should be noted that while Fe and Hg are the major inorganic elements, the total inorganic content was very low. The presence of mercury as a major inorganic component was also confirmed by emission spectroscopy. The origin of the mercury is still uncertain. In cleaning of the waste gas monitor with inhibited acid, analysis of the acid by PHA after washing strongly indicated the presence of the Hg^{203} isotope. More positive identification of this isotope awaits verification of its half-life which is 47 days.

The increase in ash, MST, and iron content, which occurred after the shutdown of May 21 is believed to have been caused by a number of factors. Even though a nitrogen blanket was used above the coolant during removal of the fuel element and during fuel shuffling, the cover gas contained from 1 - 5 vol % oxygen, as determined by Orsatt analysis at the site. Previous experience at the OMRE during shutdown operations and exposure of the irradiated coolant to air, has indicated adverse effects on coolant quality during subsequent reactor operation. The effects of air in-leakage and its detection during PNPF power operations are discussed in the sections that follow. In addition to the nitrogen purge used at PNPF, the coolant HB level was reduced to 1.0 wt % before the

reactor was opened. This was done to minimize oxidation effects. Another factor which may have caused the increased ash, MST, and iron values after the shutdown was the fact that the 3-micron spool filters were not used, and also the purification system was down a significant portion of the time.

B. RADIOCHEMISTRY AND RADIOACTIVITY

1. Gamma Emitters in the Coolant

The circulating coolant contains a wide variety of inorganic materials arising from recoil and corrosion products, and other contaminants which are either in the raw material or are picked up elsewhere in the system. Gamma emitting radioisotopes which have been detected in the coolant as a result of activation of these impurities include N^{13}, Na^{24}, Mg^{27}, Cl^{38}, A^{41}, Mn^{56}, and As^{76}. In addition, some fission product isotopes, including Kr^{88}, Xe^{133}, and Xe^{135} have also been detected in the waste gas. The specific activities of four of the isotopes routinely monitored in the coolant at the site are shown in Figure 31. One of the problems that arises in evaluating the results is the effect of fluctuating power levels on normalization of the data. In the case of short-lived isotopes, significant variations in power level can seriously effect the determined specific activity values.

Starting with the January 31 sample, the power level used in the calculations was as follows:

Isotope	Power Level Used
Cl^{38}, N^{13}, Mg^{27}	That existing at sampling time
A^{41}, Mn^{56}	Average power level over previous 8 hours
As^{76}, Na^{24}	Average power level over previous 24 hours.

Interpretation of the data shown in Figure 31 is also rendered difficult for other reasons. The generation and removal rates of the various contaminants and associated activation products are now known with a sufficient degree of accuracy in a number of cases. This would include removal by filtration and distillation, adsorption on core vessel and fuel element walls as well as systems piping, and addition via corrosion processes and make-up coolant contaminants.

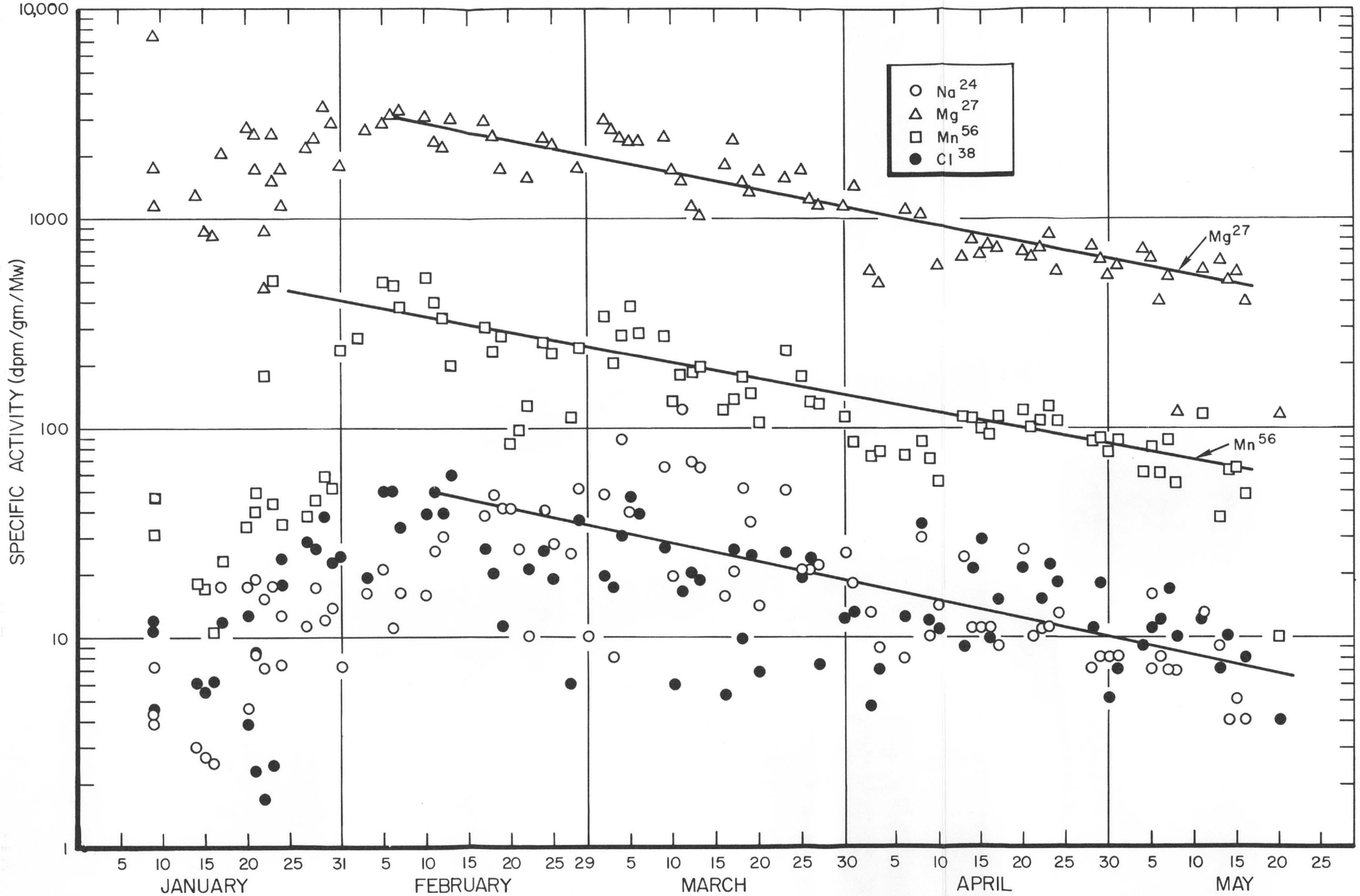

Figure 31. Specific Activity of Radioisotopes in PNPF Coolant

The results for Mg^{27} and Mn^{56} shown in Figure 31 are significant as regards the general trend shown. The overall tendency (more clearly evident for Mg^{27} and Mn^{56} than for Cl^{38} and Na^{24}) is a decrease in specific activity with operating time. In the case of Mg^{27}, the overall decrease in specific activity was about 86%. For Mn^{56}, over the same period, the apparent decrease was about 84%. Lines of best fit drawn through the data points for Mg^{27} and Mn^{56} have similar slopes.

As part of the routine coolant analysis program, the activity of two recoil products from the aluminum cladding of the fuel elements, Na^{24} and Mg^{27}, are monitored by pulse height analysis. During March, April and May, the measured Na^{24} activity in the PNPF main loop coolant fluctuated between 10 and 80 dpm/gm-Mwt. Assuming that the primary source of the Na^{24} activity is the recoil reaction, Al^{27} (n, α) Na^{24}, the predicted Na^{24} activity would be approximately 2.8×10^3 dpm/gm-Mwt*. The lower measured value (a factor of ~ 100) compared with the predicted activity may be due to removal of Na^{24} in the in-core or degasification filters and might also be indicative of the formation of an organic film over the aluminum cladding on the fuel elements. Such a film would decrease the number of Na^{24} recoil products that could escape from the Al surface and enter the coolant. This latter hypothesis is strengthened by the fact that the activity (mainly Na^{24}) measured at the degasification filters has decreased from values measured shortly after the initiation of power operation. When degasification filter F-2A was valved into the system on January 25, the activity measured 4 in. from the filter was approximately 250 mr/hr. Current activity at approximately the same reactor power is 100 mr/hr. Using a recoil length of 2.5×10^{-5} cm for Na^{24}, a factor of 2.5 reduction in the Na^{24} activity could be accounted for by a film thickness of approximately 0.006 mil. This film thickness of 0.006 mil is approximately a factor of ten lower than the film thickness of 0.070 mil determined from the first hot cell examination of a fuel element.

The measured Mg^{27} activity in the PNPF main loop coolant now tends to fluctuate at about 600-800 dpm/gm-Mwt, while earlier data showed much greater scatter and an overall tendency to decrease with reactor operating

*C.A. Goetz, "Parameter Study of Coolant Activity in the Piqua OMR and in the OMRE," NAA-SR-TDR 3800, May 1, 1959.

time. Assuming that the major source of Mg^{27} is the recoil reaction, Al^{27} (n, p) Mg^{27}, the predicted Mg^{27} activity is approximately 5.5×10^3 dpm/gm-Mwt. As in the case of the Na^{24} activity, the lower (a factor of 10) than predicted activity may be due either to removal of the isotopes in the in-core or degasification filter, or to a reduction in the amount of recoil products which can leave the fuel element surface due to the presence of an organic film on the aluminum fuel element cladding.

It should be pointed out that the use of Mg^{27} activity as an indication of coating of fuel elements with an organic film may be difficult due to the very short half-life of this isotope (9.5 min vs the 15 hr half-life of Na^{24}). Variations in sampling procedures resulting in variation in transport time from the main loop to the sample point could possibly negate the utility of this analysis. Further evaluation of the use of recoil product activity, especially Na^{24}, as an indication of fuel element film deposition will be made when the final results of the fuel element examination program are available.

It was noted than Mn^{56} showed an overall specific activity decrease similar to that of Mg^{27} (see Figure 31). On the one hand, and coincident with the recoil product and fouling film hypothesis, some of the observed decrease in the coolant Mn^{56} activity could be due to Mn^{56} concentration in the film. On the other hand the reduction in Mn^{56} activity as well as other radioisotopes in the coolant (which seemed to consistently lower after March 30) may be due to other factors such as increased filtration and distillation removal efficiencies, and the cessation of air in-leakage.

Problems have arisen in interpreting and relating coolant Cl^{38} measurements to the actual chlorine concentration in the circulating coolant inventory. Fresh coolant containing varying amounts of chlorine is added to the system in varying amounts. The raw coolant is distilled before it goes through the core, and the chlorine removal by distillation is somewhat uncertain and perhaps variable. It is fairly safe to assume that the chlorine input will not exceed 5.0 ppm, and will generally average around 2.0 ppm, since there is this limitation on the purchased material. The chlorine analysis of the circulating coolant made in A. I.'s Canoga Park laboratories using activation analysis has generally shown values in the range of 2.0 ppm. The analysis of chlorine by activation methods in the presence of contaminants such as Mn^{56} and Na^{24}, which are

almost always present in varying amounts and which interfere in the Cl^{38} photopeak region, probably has a detection limit very close to this 2.0 ppm. The absolute chlorine concentration in the coolant at these low concentrations is therefore very difficult to determine by the present activation methods.

Taking the highest Cl^{38} value obtained during the January through May operating period of 60 dpm/gm-Mwt, at full power, or 45 Mwt, this would be equivalent to about 1.2×10^{-3} μc/gm. Chlorine values (as Cl^{38}) were predicted some time ago for PNPF coolant based on constant power level of 45.5 Mwt, 195 lb/hr still throughput, a constant chlorine content in the still feed, and assuming various removal efficiencies by distillation*. On this basis, assuming a chlorine removal efficiency of 60% by distillation, the predicted Cl^{38} activity was 8.56×10^{-3} μc/cc per ppm of chlorine impurity in the feed. The still throughput at PNPF over the initial operating period was about 960 lb/hr, or about five times higher than that used in TDR-3800. Assuming the equilibrium chlorine value in the PNPF coolant to be related to this removal rate in the still, the predicted value would be lower by a factor of 5, or would be about 1.7×10^{-3} μc/cc per ppm of chlorine in the feed; this value is comparable to a maximum Cl^{38} activity of 1.2×10^{-3} μc/cc. Typical values have been from 0.2×10^{-3} to 0.7×10^{-3} μc/cc (See Figure 31). In view of some of the uncertainties involved, this may be considered fairly good agreement.

2. Radioisotopes Found in PNPF Waste Gas

Off-gas samples taken at the waste gas monitor (after light ends and water had been trapped out) were analyzed by pulse height analysis at the site for major radioisotopes present. The isotopes found and the associated activities in dpm/cc are shown in Table XVI.

At the inception of reactor operation in October 1963, the only detectable radioisotope was Argon-41. The presence of large quantities of Argon-41 was subsequently determined to be caused by air in-leakage. The air in-leakage was brought under control and the pulse height analysis of the gas on March 20 indicated a significant reduction in Argon-41 activity. Subsequent waste gas samples taken on April 1, 16 and 28 indicated that the activities of the

*C.A. Goetz, "Parameter Study of Coolant Activity in the Piqua OMR and in the OMRE," AI-TDR-3800, May 4, 1959.

TABLE XVI

RADIOISOTOPES FOUND IN PNPF WASTE GAS

Date	Isotope Activity (dpm/cc)					
	A^{41}	Kr^{85m}	Kr^{87}	Kr^{88}	Xe^{133}	Xe^{135}
1-25-64	2.5×10^{3}	8.7×10^{1}	ND	ND	1.4×10^{-2}	3.6
2-29-64	9.0×10^{4}	1.5×10^{2}	2.9×10^{2}	2.5×10^{2}	1.5×10^{1}	4.9×10^{2}
3-20-64	1.0×10^{2}	1.2×10^{2}	3.5×10^{2}	2.7×10^{2}	1.4×10^{1}	9.3×10^{2}
4-1-64	7.4×10^{1}	1.6×10^{2}	3.9×10^{2}	3.5×10^{2}	1.2×10^{1}	4.3×10^{2}
4-16-64	8.6×10^{1}	1.6×10^{2}	4.7×10^{2}	3.3×10^{2}	7.8	4.5×10^{2}
4-28-64	1.4×10^{2}	1.6×10^{2}	4.7×10^{2}	2.5×10^{2}	8.2	4.0×10^{2}
5-6-64	38.6	1.4×10^{2}	4.0×10^{2}	2.9×10^{2}	8.3	3.7×10^{2}

ND = Not Detected

radioisotopes shown were fairly constant. However, it should be noted that the data shown in Table XVI are not normalized according to power level; hence fluctuations by a factor of 2 to 3 may not be real. The total waste gas activity at PNPF decreased simultaneously with the reduced A^{41} activity and has remained fairly constant since that time. The fission gas activity has also remained relatively constant. It is possible that these gases are due to pinhole leaks in the fuel element aluminum cladding; however, there is no indication of any cladding failure. It is also possible that these gases are from "tramp" uranium in the aluminum cladding of the fuel elements.

3. Removal of Impurities by Filtration and Distillation

The effectiveness of filtration by the in-core and out-of-core glass spool filters and of continuous distillation in removing coolant impurities can be evaluated by the radioisotope data, and by gamma activity measurements made on the out-of-core filters and main heat transfer pump housings. The out-of-core filter data are admittedly meager and cover too short a time interval to establish absolute filtration efficiency. Radioisotope measurements were

obtained in January by pulse height analysis using coolant samples taken upstream (line 201) and downstream (line 208) of the 3 micron glass spool filters. The most significant reduction in activity as shown in Table XVII occurred in the case of Na^{24}, ranging from 42% to 70%. The gamma activity data shown in Figure 32 is somewhat more illuminative as regards the trend in gamma activity observed with fluctuating power levels and operating history. Note that both the spool filter and main heat transfer activity data show a decrease occurring after mid-March, even though the power levels were still in the 30 to 40 Mwt range. There are two factors which must be considered in the observed decrease of

TABLE XVII

REDUCTION OF SPECIFIC ACTIVITIES OF LONG-LIVED ISOTOPES BY GLASS SPOOL FILTERS (2μ)

Date Taken	Line Sampled	Specific Activity, dpm/gm/Mw		
		Na^{24}	As^{76}	Mn^{56}
1-20-64	Line 201*	15.5	361.0	34.2
1-20-64	Line 208**	4.6	344.0	34.4
Reduction of Activity (%)		70.3	4.7	0
1-21-64	Line 201	18.8	402.0	49.5
1-21-64	Line 208	8.3	392.0	40.1
Reduction of Activity (%)		56.0	2.5	19.0
1-22-64	Line 201	15.3	466.0	178.0
1-22-64	Line 208	7.1	437.0	168.0
Reduction of Activity (%)		53.6	6.2	5.6
1-23-64	Line 201	17.3	516.0	49.8
1-23-64	Line 208	6.9	477.0	43.0
Reduction of Activity (%)		60.0	7.6	13.7
1-24-64	Line 201	12.6	268.0	37.6
1-24-64	Line 208	7.3	268.0	34.6
Reduction of Activity (%)		42.0	0	8.0

*Upstream from filters
**Downstream from filters

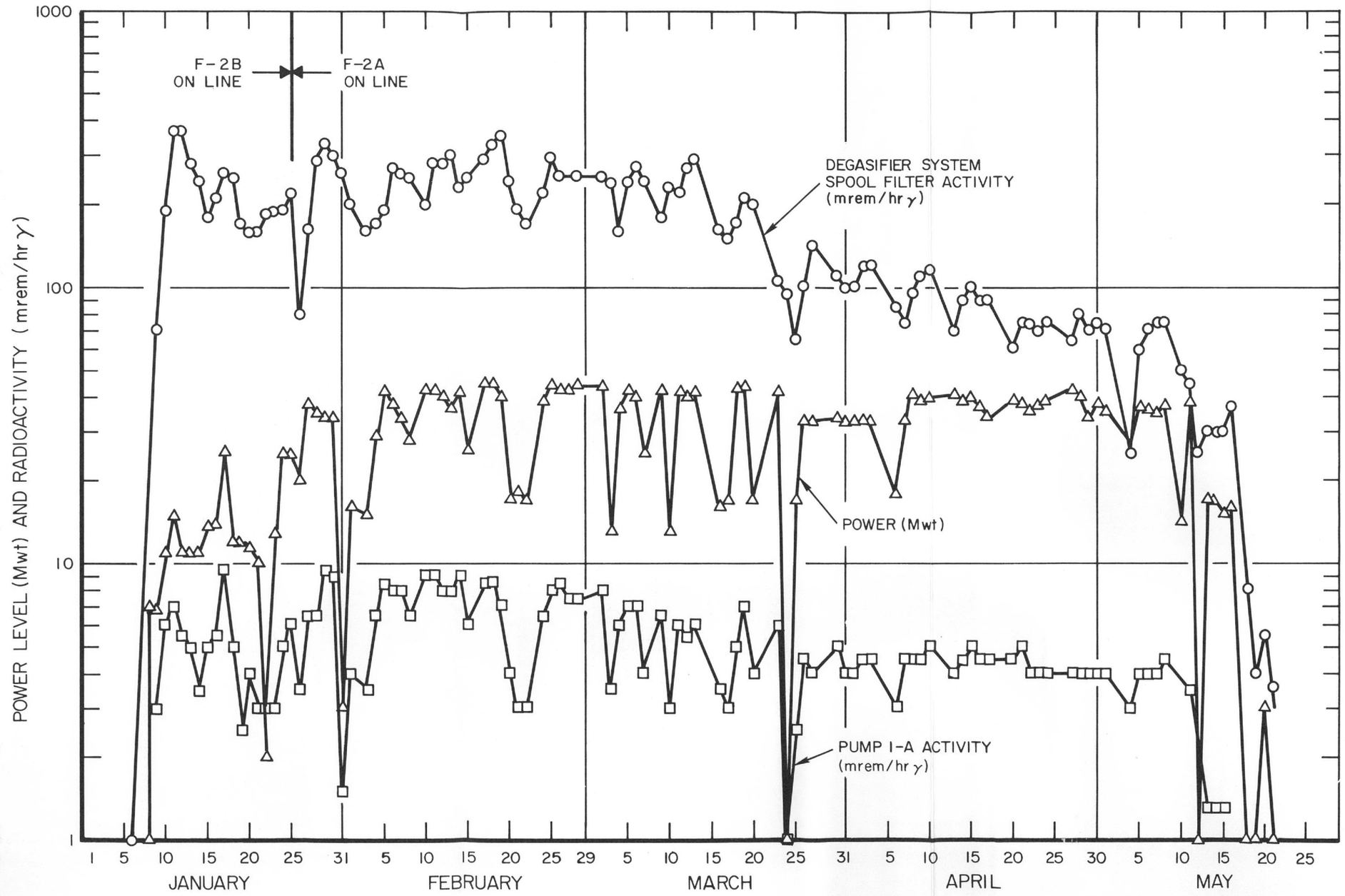

Figure 32. Power Level vs Radioactivity (mrem/hr γ) on 3 Micron Spool Filters and Pump 1-A

radioactivity. The distillation rate was gradually increased to 800 lb/hr on March 17, and to 960 lb/hr on March 20. Prior to that and through most of February the distillation rate was 600 to 650 lb/hr. By the end of March also, air in-leakage was reduced significantly as indicated by the reduction of A^{41} activity in the waste gas (see Table XVI). Both of these factors, therefore, could have caused the step-change decrease in radioactivity shown in Figure 32.

Radioisotopes in the in-core glass spool filter media removed from the core after shutdown were determined by PHA. A portion of the filter spool was refluxed in chloroform in a Soxhlet apparatus. After overnight treatment, the organic extract phase, the extracted glass fiber, and the black particles separated from the liquid phase by filtration were analyzed by PHA for the major radioisotopes present. The results are shown in Table XVIII.

TABLE XVIII

RADIOISOTOPES IN IN-CORE FILTER MEDIA

Sample	Wt. (grams)	Specific Activity (dpm/gm)				
		Co^{60}	Co^{58}	Fe^{59}	Zn^{65}	Mn^{54}
Organic* Extract	7.0862	9.82×10^{2}	6.44×10^{3}	1.30×10^{3}	1.53×10^{4}	9.71×10^{3}
Extracted Fiber	6.3579	4.44×10^{3}	7.64×10^{4}	4.50×10^{3}	1.04×10^{5}	3.14×10^{4}
Separated Black Particles	0.0529	8.87×10^{4}	8.94×10^{5}	7.54×10^{4}	8.34×10^{5}	4.22×10^{5}

*Includes organic coolant extracted with $CHCl_3$.

Note that most of the activity is associated with the black, insoluble material which was separated from the organic phase by filtration. The ash content of the particles was 21.8 w/o. On the basis of the weight of black insoluble material separated and the total weight of the spool (~1100 gm) and assuming homogeneous distribution of particles in the spool and a similar distribution of particles in each of the 10 spools per element, for a total of 61 fuel elements, the total weight of particulate material collected in all the spools would be ~6.0 lb. The total film deposited on the fuel elements with a 61 element

core, and based on the film recovered from two of the high burn-up fuel cylinders, was less than 1.5 lb. The relative ratio of film particles in the in-core filters vs film particles on the fuel elements would indicate that the filters are performing well and are significantly reducing the fouling potential of the coolant.

4. Coupon Test Data and Evaluation

An experiment to observe the equilibrium deposition of film on the out-of-pile piping in the PNPF system was conducted. Type 304 SS coupons were inserted into the sample line near Sample Station No. 1. After two and four days exposure, the coupons were removed and the amount of deposited radioactivity was measured. The results are summarized in Table XIX.

TABLE XIX

DEPOSITION OF RADIOISOTOPES ON STAINLESS STEEL COUPONS IN PNPF COOLANT (OUT-PILE)

		Deposition (dpm/cm^2 Mw) Radioisotope		
Test No.	Date	Mg^{27}	Mn^{56}	Na^{24}
1	4/6/64	0.20	0.0400	0.40
2	4/10/64	0.53	0.0075	0.29
3	4/15/64	1.20	0.1700	0.41

C. COOLANT COMPOSITION DATA

1. Major Components

Coolant composition data, obtained at A. I. 's Canoga Park laboratories by gas chromatography, for the raw material and for the circulating coolant are shown in Table XX. There are significant variations in HB (and possibly also intermediate boilers) content and ortho-meta-para ratios in the purchased raw material. The continual addition of raw coolant for make-up during power operation, coupled with the ±3 wt % variance in the accuracy of the analyses for the major components, makes an exact evaluation of trends shown by the major components during power operations difficult. Variations in distillation and/or

TABLE XX

PNPF COOLANT COMPOSITION DATA

	Sample	Biphenyl	Ortho-Terphenyl	Meta-Terphenyl	Para-Terphenyl	Total (wt %)	100%-% Major** Components	HB*** (wt %)
Virgin Coolant	Composite*	0.2	13.4	56.1	29.4	98.9	1.1	
"	1	0.2	9.6	52.4	29.6	91.6	8.4	
"	2	0.2	14.8	51.0	27.2	93.0	7.0	
Pre Critical	10/30/63	0.1	12.7	57.7	26.7	97.2	2.8	
Operating	11/13/63	-	10.9	55.0	23.7	89.6	10.4	
"	12/19/63	-	11.3	55.2	28.6	95.1	4.9	3.5
"	1/20/64	-	10.4	53.7	26.4	90.5	9.5	5.5
"	2/18/64	0.2	8.8	57.2	24.9	92.3	7.7	10.1
"	3/6/64	0.2	9.3	49.9	25.5	84.9	15.1	11.5
"	4/15/64	0.5	9.3	49.8	24.7	84.3	15.7	5.5
Post Operating	5/28/64	0.5	9.3	50.8	29.4	90.0	10.0	1.0

*Composite of five coolant lots.

**Includes intermediate boilers and low boilers.

***On-Site HB data.

degasification processes probably also exert an effect on the relative ratios of the major components, as well as HB, intermediate and low boilers in the coolant. The HB data shown in Figure 30 and Table XX were obtained by analytical distillation at the site.

2. Low Boiler Analyses

The composition and concentration of the low boilers in bomb coolant samples were determined by gas chromatography. The bomb sampler was heated and the low boiling components collected under vacuum in a cold trap at liquid nitrogen temperature. A clear liquid was visible in the cold trap after sealing and removal of the trap from the liquid nitrogen. The results from two samples are shown in Table XXI.

TABLE XXI

LOW BOILERS IN IRRADIATED PNPF COOLANT

Component	Concentration in Coolant (wt %)	
	3-24-64	4-17-64
Benzene	0.008	0.003
Toluene	0.006	0.003
Ethylbenzene	0.005	0.005
Other Low Boilers	0.004	0.002
Total	0.023	0.013

In visually examining the cold trap contents it was apparent that two immiscible liquid phases were present. The second liquid phase present is probably water. The low boiler values obtained are very low as would be expected, due to the combined effects of distillation and degasification.

3. Composition of Reactor Off-Gas

Samples of gas effluent from the degasifier were analyzed for composition by mass spectroscopy. The results are summarized in Table XXII. Samples removed on December 9 were taken in evacuated polyethylene plastic containers; the January 23 samples were taken in stainless steel bombs after

TABLE XXII

PNPF WASTE GAS ANALYSIS

	Concentration (Mole%)* Samples Taken 12/9/63				Concentration (Mole%)* Samples Taken 1/23/64***		
Component	(a)	(b)	(c)	(d)***	Air Blank	Off-Gas-I	Off Gas-II
Toluene	0.1	-	-	-	-	1.8	1.0
Benzene	0.1	-	-	-	0.9**	9.2	3.0
CO_2	0.5	0.6	0.6	0.5	-	0.9	0.9
Argon	0.8	1.0	0.9	0.8	1.0	0.04	0
Oxygen	7.2	7.5	7.2	7.5	21.5	0.4	0
Nitrogen	58.9	59.6	59.8	60.7	76.6	1.6	0
Ethylene	1.7	1.8	1.9	1.8	-	4.9	5.5
Acetylene	3.7	3.5	3.5	1.1	-	-	-
Methane	1.0	0.8	0.9	0.8	-	2.0	3.3
Hydrogen	26.1	25.2	25.3	26.7	-	67.3	79.5
Xylene or Ethylbenzene	Trace	-	-	-	-	-	-
Ortho-Xylene	-	-	-	-	-	0.2	0.1
Butene-1	-	-	-	-	-	4.0	1.5
Isopentene	-	-	-	-	-	1.7	0.5
Propene	-	-	-	-	-	1.7	1.4
Ethane	-	-	-	-	-	1.4	1.4
CO	-	-	-	-	-	2.9	1.9

*Calculated on a water-free basis. Moisture was present in all samples (air blank excepted) due to steam jet used for vacuum in degasifier.

**Benzene contamination due to benzene solvent used to rinse SS sample bombs prior to use. Off-gas samples I and II are also assumed to contain an unknown amount of this contamination.

***Taken in rapid sequence at same location.

rinsing with benzene, drying, evacuation, and purging of gas lines through the bomb sampler. The composition of the earlier set of samples indicates a large degree of air contamination. While it is not certain that the plastic containers were air-tight (the bottles were in partially collapsed condition when received), it is interesting to note that the oxygen-to-nitrogen ratio differs significantly from that found normally in air (see air blank, Table XXII), i.e., the mixture is oxygen deficient by about 50%. This deficiency could be due to previous oxygen reaction with irradiated coolant, specifically, oxygen reaction with free radicals in the coolant. This is considered undesirable from the standpoint of keeping the fouling potential of the coolant down to a minimum. Steps taken subsequently were successful in stopping the air in-leakage, as indicated by the results obtained on the January 23 samples*. The hydrogen-to-methane ratio in the January 23 samples is normal for a low HB (6.7 wt %) coolant. The benzene values of January 23 samples I and II are suspect due to possible contamination from the benzene rinse, but they could be of the right order of magnitude when compared to previous irradiated OMRE and MTR organic coolants.

4. Analysis of Aqueous Waste Tank Samples

The organic phase from two aqueous waste tank samples was analyzed for major coolant components and low boilers. The densities were measured by pipetting a known volume of the liquid into a tared beaker and recording the weight. The results of these analyses are given in Table XXIII.

The solid organic found in the water phase amounted to less than 50 ppm. Liquid organic decomposition products (such as benzene, xylene, ethyl-benzene) were not separated from the water; however, it may be noted that according to Lange's Handbook of Chemistry, benzene, and ethylbenzene are soluble in water in the range of 300 tc 700 ppm.

5. Trace Elements in Unirradiated and Irradiated PNPF Coolant

Trace elements in samples of the raw material, submitted for analysis by the vendor, and in the irradiated circulating coolant were obtained by

*Even though the gas analyses showed a significant reduction in nitrogen, the A^{41} activity indicated that the air leak was not completely controlled until the middle of March.

TABLE XXIII

ANALYSIS OF ORGANIC PHASE FROM AQUEOUS WASTE TANK SAMPLES

	Sample T14E & F (3-18-64)		Sample T14B (2-28-64)	
	Water Phase	Organic Phase*	Water Phase	Organic Phase*
Density	0.99	1.00	0.99	0.95
m-terphenyl	-	18.2%	-	5.7%
o-terphenyl	-	25.0%	-	8.9%
biphenyl	-	20.1%	-	26.7%
total major components	-	63.3%	-	41.3%
total low boilers	-	12.0%	-	27.4%
Total	-	75.3%	-	68.7%

*The low boilers contained twice as much ethylbenzene as toluene and very little benzene. The 25% and 30% material unaccounted for is probably due to water and unidentified low and intermediate boilers.

emission spectroscopy of the ashed residue. The results for a composite of five raw coolant samples and an irradiated coolant sample are shown in Table XXIV. In individual raw coolant samples, the major contaminants appeared to be Fe and Si. One of the major elements of interest in the irradiated sample was the boron content. The in-core glass fiber material contains as much as 7.0 wt % boron (as B_2O_3). It is significant that the coolant contained very low amounts of this potential neutron poison.

D. SUMMARY OF OFF-SITE COOLANT ANALYSES

A summary of the off-site analyses performed at AI Canoga Park laboratories (with the exception of composition data discussed previously) is shown in Table XXV. Flash point analyses prior to April 6 were made in open beaker samples, which means that all or most of the low boilers were absent. A sample was taken April 6, 1964 (OC-525), from a sample bomb after the low boilers had been removed by evacuation and cold trapping. The April 10 sample (OC-534) was taken from a sample bomb without removal of low boilers and gave the lowest flash point (355°F). While the difference is admittedly small and therefore inconclusive, one might expect lower flash points in samples containing the low boilers, which are much more volatile.

TABLE XXIV

TRACE ELEMENT ANALYSIS OF ASHED UNIRRADIATED AND IRRADIATED COOLANT

Element	Raw Coolant Composite (ppm)	Irradiated Coolant 3/24/64 (ppm)*
Ag	0.002	0.002
Al	0.35	>0.01
B	0.005	0.00003
Ba	0.008	0.0007
As	< 0.00008	-
Ca	0.15	0.01
Co	0.005	0.0007
Cr	0.12	> 0.01
Cu	0.05	0.0001
Fe	0.85	> 0.01
Mg	0.16	> 0.01
Mn	0.03	0.003
Mo	0.005	-
Na	0.16	-
Ni	0.15	> 0.01
Pb	0.05	0.0001
Si	0.7	> 0.01
Sn	0.05	0.0002
Ti	0.05	0.002
P	< 0.00016	-
Zn	0.12	-
Zr	0.16	0.001

*Per ppm ash in the coolant. The ash content of the irradiated sample was not obtained in the Canoga Park laboratory where the analysis was made. Ash content obtained at the site on or about 3/24/64 was $\leq$ 1.0 ppm.

The water content of the coolant, with minor exceptions varied between 25 and 50 ppm. It did not change significantly after the shutdown.

TABLE XXV

SUMMARY OF OFF-SITE ANALYTICAL DATA

Sample No.	Date	Flash Point (°F)	Water Content (ppm)	Carbon-Oxygen Content (ppm)	Chlorine Content (ppm)	PCFT (mg/250 gm)
OC-420	1-31-64	365	-	21	1.8	2.1
OC-426	2-5-64	-	-	21	-	-
OC-435	2-10-64	370	-	52	2.8	-
OC-453	2-15-64	-	-	46	-	0.7
OC-456	2-19-64	375	-	31	2.3	-
†OC-459	2-21-64	-	158	25,27	-	-
OC-476	2-29-64	385	-	-	2.1	-
OC-484	3-5-64	370	-	-	-	-
OC-486	3-6-64	-	40	20,22	2.0	-
OC-496	3-13-64	-	25	-	-	-
OC-525	4-6-64	365*	57	-	-	-
OC-534	4-10-64	355	78	-	-	-
OC-547	4-17-64	-	30	29,31	-	-
OC-579	5-1-64	360	40	21	-	-
OC-586	5-8-64	-	27	-	-	-
OC-595	5-15-64	-	37	23,25	-	-
OC-614	5-29-64	-	-	19,21	-	-
OC-630	6-9-64	-	35	58,61	-	-
OC-636	6-12-64	-	46	51,52	-	-
OC-641	6-19-64	-	40	-	-	-

†Sample taken from a stagnant line.
*Low boilers removed by evacuation and cold trapping.
**This lot was rejected and returned to the vendor due to the abnormally high chlorine content.

The carbonyl oxygen content varied between 20 and 52 ppm over the entire operating period. An increase was observed in early June after the shutdown. During the shutdown a nitrogen purge was used at the top of the reactor vessel above the coolant to minimize air-coolant contact. Oxygen analysis of the cover

gas indicated from 1.0 to 5.0 volume per cent oxygen. Whether the higher values observed in June are attributable to oxygen contact is uncertain. Note that the May 29 sample after shutdown showed a normal carbonyl oxygen value.

Chlorine values obtained by activation analysis through March 6, averaged 2.2 ppm $\pm$ 20%. Chlorine analyses were not obtained after that date because the Shield Test Reactor Facility was shutdown and other suitable neutron sources were not available.

Since only two Pyrolytic Capsule Fouling Test (PCFT) values are available (taken early in the operating period), these values cannot be correlated with operating history. The PCFT apparatus at the site developed malfunctions at start-up and was not available over the entire operating period. The MST procedure has been applied to a large number of terphenyl coolant samples for which the film-forming potential had been determined by the PCFT. A plot of MST vs PCFT for these samples indicates a general correlation of the form. *

$$\ln (PCFT) = m \ln (MST) + b$$

where:

PCFT = milligrams of film per 250 gm of coolant under standard test conditions.

and:

MST = absorbance per milligram of coolant (A/mg at 500 mμ) and m and b are constants.

On the basis of this correlation and the MST values obtained for PNPF coolant over the operating period, the PCFT values would be at, or very close to, detection limits (the precision of the PCFT is ± 2 mg at the 1-10 mg level).

---

*W. L. Orr, R. C. Shepard, and R. T. Keen, "Contamination Detection in Organic Reactor Coolants," (Atomics International Canoga Park, Calif.). Paper presented at ASTM Winter Meeting, Tulsa, Oklahoma, January 31, 1963.


ATOMICS INTERNATIONAL
A DIVISION OF NORTH AMERICAN AVIATION, INC.
AI